AN ABSTRACT OF THE THESIS OF

Hannele K. Kanerva for the degree of Doctor of Philosophy in Civil Engineering presented on June 21, 1993.

Title: Prediction of Low Temperature Cracking of Asphalt Concrete Mixtures with Thermal Stress Restrained Specimen Test Results

Abstract approved: _____

Ted S. Vinson

Low temperature cracking is attributed to tensile stresses induced in an asphalt concrete pavement that develop when the pavement is subjected to a cold temperature. Cracking results in poor ride quality and a reduction in service life of the pavement. Low temperature cracking has been predicted by regression equations, mechanistic approaches and by simulation measurements. The purpose of the study reported herein is to *(1)* evaluate the Thermal Stress Restrained Specimen Test (TSRST) as an accelerated performance test to simulate low temperature cracking of asphalt concrete mixtures and *(2)* develop a deterministic and probabilistic model to predict low temperature cracking with TSRST results.

Construction histories, cracking observations and temperature data were collected for five test roads in Alaska, Pennsylvania and Finland. A full scale and fully controlled low temperature cracking test program was conducted at the U.S. Army Cold Regions Research and Engineering Laboratory (USACRREL).

Specimens were fabricated in the laboratory with original asphalt cements and aggregates from the test roads. In addition, asphalt concrete pavement specimens were cut from the test sections. The TSRST results obtained for these samples were correlated with the field observations. Based on a statistical analysis of the data, the TSRST fracture temperature is associated with the field cracking temperature and crack frequency for the test roads where mixture properties dominated low temperature cracking. It was concluded that the TSRST can be used to simulate low temperature cracking of asphalt concrete mixtures.

A deterministic and a probabilistic model were developed to predict crack spacing as a function of time using the TSRST results, pavement thickness and bulk density, pavement restraint conditions and air temperature. The affect of aging on pavement properties was incorporated in the models by predicting the field aging with Long Term Oven Aging (LTOA) treatment in the laboratory. The calculation of the crack spacing is based on the theory that the pavement slab cracks when the pavement temperature reaches the cracking temperature of the mixture and the slab is fully restrained. The deterministic model predicts crack spacing with time whereas the probabilistic model predicts crack spacing and its variation with time and yields the reliability of the design with regard to a minimum acceptable crack spacing criterion defined by road authorities.

The models were verified by comparing the predicted crack spacings for the five test roads to the observed crack spacings. The probabilistic model is recommended for use in predicting the low temperature cracking of asphalt concrete mixtures.

Prediction of Low Temperature Cracking of Asphalt Concrete Mixtures with Thermal Stress Restrained Specimen Test Results

by

Hannele K. Kanerva

A THESIS

submitted to

Oregon State University

in partial fulfillment of
the requirements for the
degree of

Doctor of Philosophy

Completed June 21, 1993
Commencement June 1994

APPROVED:

Redacted for Privacy

Professor of Civil Engineering in charge of major

Redacted for Privacy

Head of Department of Civil Engineering

Redacted for Privacy

Dean of Graduate School

Date thesis is presented June 21, 1993

Typed by researcher for Hannele K. Kanerva

ACKNOWLEDGEMENT

The validation of the TSRST results regarding the field behavior reported herein has been conducted as a part of project A-003A of the Strategic Highway Research Program (SHRP). Without the support and encouragement of SHRP staff and R. Gary Hicks, this task would not have been accomplished. I would also like to thank my advisor, Ted S. Vinson for his advice and support throughout the project. The help of the USACRREL personnel, especially William J. Quinn and Vincent C. Janoo, and several other persons in Alaska, Pennsylvania and Finland for their help, and for providing facilities and information for the test sections is gratefully acknowledged. A special thanks also goes to Andy M. Brickman for designing and installing the instrumentation of the USACRREL test sections, Marco J. Fellin and B. Bradley Zubeck for helping in the instrumentation task and to the USACRREL employees, Jack Bayer, Chris Berrini, Robert A. Eaton, Richard Guyer, Carl Martinson and several others for their help during the project. Huayang Zeng made a substantial contribution by conducting all the TSRSTs for the study. In addition, I would like to thank my committee members, Chris A. Bell, J. R. Bell, James D. Ingle, Vincent C. Janoo and James R. Lundy for their valuable time and help, my employer, Neste Oil, for granting me a leave of absence for my studies, Neste Fund for financial support, and my parents, Eeva and Tapio, for their constant encouragement, and finally, my friends at Oregon State University, especially B. Bradley Zubeck, for making my stay a very special period of my life.

TABLE OF CONTENTS

Page

Page

LIST OF FIGURES

Figure Page

Figure Page

LIST OF TABLES

Table Page

PREDICTION OF LOW TEMPERATURE CRACKING OF ASPHALT CONCRETE MIXTURES WITH THERMAL STRESS RESTRAINED SPECIMEN TEST RESULTS

1 INTRODUCTION

1.1 Problem Definition

Low temperature cracking is attributed to tensile stresses induced in the asphalt concrete pavement that develop when the pavement is subjected to a cold temperature. As the pavement is cooled thermal stresses are induced as a result of the asphalt concrete's tendency to contract and friction between the asphalt concrete and the base layer that resists the contraction. If the thermal stresses in the pavement equal the tensile strength of the asphalt concrete mixture at that temperature, a low temperature crack will result (Jung and Vinson, 1992).

The primary pattern of low temperature or thermal contraction cracking is transverse to the direction of traffic. Cracks are regularly spaced at intervals of less than 4 to 100 m. If the transverse crack spacing is less than the width of the pavement, longitudinal cracks may develop.

With the propagation of low temperature cracks through the pavement structure, a conduit is created for the migration of water and fines into and out of the pavement. During the winter, the intrusion of deicing solutions into the base through the crack can lead to localized thawing of the base and depression at the

crack. Water entering the crack freezes, resulting in the formation of ice lenses, which can produce upward lipping at the crack edge. Pumping of the fine materials through the crack produces voids under the pavement and results in a depression at the crack upon loading. All these effects result in poor ride quality and a reduction in service life of the pavement (Jung and Vinson, 1992).

It is inevitable that low temperature cracking occurs in pavements constructed in the cold regions of the world. Esch and Franklin (1989) state that all pavements in Alaska, with the possible exception of those in the south-coastal areas, can be expected to suffer from thermal contraction cracking. In Finland, where the total length of asphalt pavements is 15,000 km, the annual maintenance costs associated with low temperature cracks were from two to three million dollars in 1984 (Ehrola 1986). Therefore, it is essential that design engineers involved in establishing the requirements for pavements in cold regions identify an asphalt concrete mixture that minimizes low temperature cracking without compromising other performance characteristics, such as resistance to rutting.

1.2 Prediction of Low Temperature Cracking

Three approaches may be employed to identify the low temperature cracking resistance of an asphalt concrete mixture: *(1)* regression equations, *(2)* mechanistic models, and *(3)* laboratory simulation tests (Kanerva et al. 1992 a).

Regression Equations Based on an analysis of data from twenty-six airfields in Canada, Haas et al. (1987) established the following regression equation to predict the average transverse crack spacing in a pavement structure:

$$TCRACK = 218+1.28\ ACTH+2.52\ MTEMP+30\ PVN-60\ COFX \quad (1.1)$$

in which,

TCRACK= Transverse crack average spacing in meters,

ACTH = Thickness of the asphalt concrete layer in centimeters,

MTEMP = Minimum temperature recorded on site in °C,

PVN = McLeod's Pen Vis Number,

COFX = Coefficient of thermal contraction in mm/1000mm/°C.

The PVN in eqn. 1.1 (determined from the penetration at 25°C and the kinematic viscosity at 135°C) is an indicator of temperature susceptibility of the asphalt cement (McLeod 1972 and 1987). As the PVN decreases, for a given grade of asphalt, the temperature susceptibility increases. Consequently, as the temperature susceptibility increases, the average crack spacing decreases. Further, crack spacing increases with minimum temperature and pavement thickness.

The twenty-six airfields used in the development of the regression equation were located below the 50° north latitude. Fifteen were "coastal associated" airports. Approximately one half of the observations were made for pavement overlays and, consequently, part of the observed cracks were due to reflection

cracking. Finally, extracted asphalt cement properties were used to develop the regression equation(s). Similar regression models for prediction of the crack frequency for roadways have been developed by Haas (1973) and by Ehrola (1986).

Mechanistic Models This approach may be visualized in Figure 1.1. Specifically, low temperature cracking occurs in the surface layer when the thermally induced tensile stress (owing to the pavement's tendency to contract with decreasing temperature) equals the tensile strength of the asphalt concrete mixture. The calculation of the thermally induced tensile stress is approximated by Hills and Brien (1966) using the following equation:

$$\sigma(\dot{T}) = \alpha \sum_{T_0}^{T_f} S(t,T) \cdot \Delta T \tag{1.2}$$

in which,

$\sigma(\dot{T})$ = accumulated, thermal stress for a particular cooling rate,

α = coefficient of thermal contraction,

T_o, T_f = initial and final temperature, respectively,

S(t,T) = asphalt mix stiffness (modulus), time (t) and temperature (T) dependent,

ΔT = temperature increment over which S(t,T) is applicable.

The approximate solution suggested by eqn. 1.2 may yield reasonable results if the coefficient of thermal contraction, and the asphalt concrete mix stiffness are

correctly measured or assumed. The tensile strength of the asphalt concrete mix is measured in the laboratory in either direct or indirect tension.

The determination of both the asphalt concrete mix stiffness and the tensile strength requires that the rate of cooling in the field (and the associated development of tensile stresses and strength) must be related to a rate of loading or deformation in the laboratory. To date, a procedure to accomplish this task has not been convincingly demonstrated to the pavement engineering community. Further, in the calculation of thermal stress the thermal contraction coefficient is generally assumed to be 2.0 to 2.5 $\times$ 10^{-5} mm/(mm°C). Recent measurements of the thermal contraction for mixes with high void contents or mixes employing modified asphalt cement suggest that this assumption could be in error by a factor of two or three (Zeng, personal communication 1993). Further, age conditioning of the specimens for the determination of the mix stiffness or tensile strength has not been considered in the application of this approach.

Simulation Measurements Monismith et al. (1965) were the first to suggest that the thermally induced stress, strength, and temperature at failure could be measured in a laboratory test that simulated the conditions to which a pavement slab was subjected in the field. The basic requirement for the test system is that it maintains the test specimen at constant length during cooling. Initial efforts to accomplish this involved the use of "fixed frames" constructed from invar steel (Monismith, et al. 1965, Fabb 1974, Janoo 1989) or from steel and aluminum

(Tuckett et al. 1970 and Kanerva 1992). A common failure mode produced by these devices is a development of micro cracks instead of sudden splitting. Arand (1987) inserted a displacement "feedback" loop into the test system, which insures constant length of the specimen by continuously correcting for the contraction that occurs during the test, and consequently totally prevents stress relaxation.

A recent version of the displacement "feedback" system is shown in Figure 1.2. The system consists of a load frame, screw jack, computer data acquisition and control system, low temperature cabinet, temperature controller, and specimen alignment stand. A beam (50 x 50 x 250 mm) or cylindrical specimen is mounted in the load frame that is enclosed by the cooling cabinet. The chamber and specimen are cooled with vaporized liquid nitrogen. As the specimen contracts, LVDTs sense the movement and a signal is sent to the computer that in turn causes the screw jack to stretch the specimen back to its original length. This closed-loop process continues as the specimen is cooled and ultimately fails. Measurements of elapsed time, temperature, deformation and tensile load are recorded with a data acquisition system. This system is called the thermal stress restrained specimen test (TSRST) (Jung and Vinson, 1992).

A typical result from a TSRST is shown in Figure 1.3. The thermally induced stress gradually increases as temperature decreases until the specimen fractures. At the break point, the stress reaches its maximum value, which is called the fracture strength, with a corresponding fracture temperature. The slope of the stress- temperature curve, dS/dT, increases until it reaches a maximum value. At

colder temperatures, dS/dT becomes constant as the stress - strain behavior of the specimen becomes elastic, and the stress-temperature curve is linear. The transition temperature divides the curve into two parts, visco-elastic and elastic. As the temperature approaches the transition temperature, the asphalt cement becomes stiffer and the thermally induced stresses are not relaxed beyond this temperature, for a specified rate of cooling.

1.3 Statement of Purpose

The purpose of the study was to evaluate the TSRST as the accelerated performance test to simulate low temperature cracking of asphalt concrete mixtures. In addition, deterministic and probabilistic models to predict the crack spacing were developed.

The scope of work includes the collection of construction histories, cracking observations, and temperature data for suitable test roads. A full scale and fully controlled low temperature cracking experiment was conducted at the U.S. Army Cold Regions Research and Engineering Laboratory (USACRREL). Specimens were fabricated in the laboratory with original asphalt cement and aggregate from the test roads. In addition, asphalt concrete pavement specimens were cut from the actual test sections. The TSRST results obtained for these samples were correlated with the field observations. The data obtained were used to verify the deterministic and probabilistic prediction models.

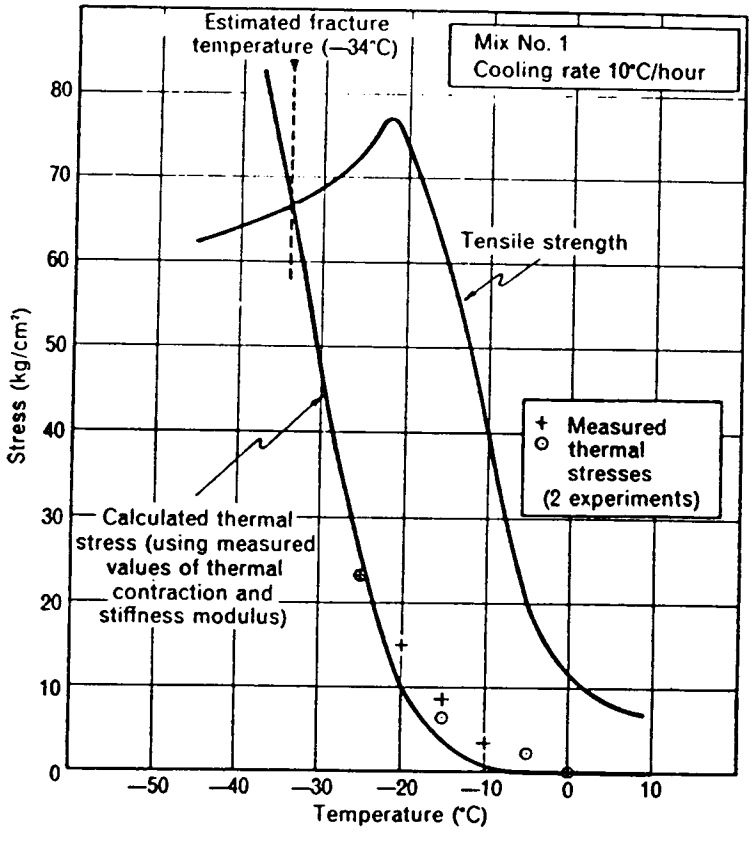

Figure 1.1 **Estimating the fracture temperature of asphalt concrete (after Hills and Brien, 1966)**

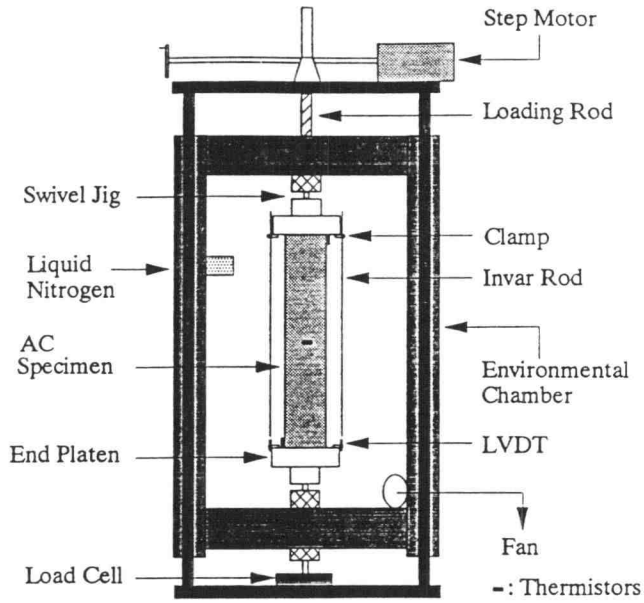

Figure 1.2 Schematic of thermal stress restrained specimen test (TSRST) system (after Jung and Vinson, 1992)

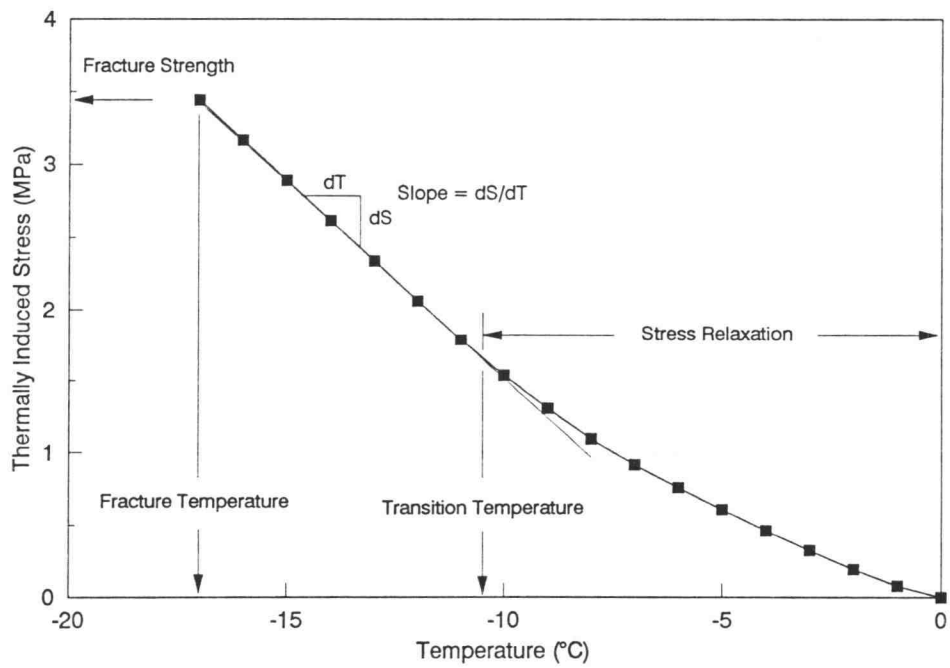

Figure 1.3 Typical TSRST results for monotonic cooling (after Jung and Vinson, 1992)

2 EXPERIMENT DESIGNS

The experiment consisted of field observations for the test roads and performing TSRST on specimens fabricated from original materials and cut from the pavement in the field. Information for each test road and the laboratory testing program is given in the following sections.

2.1 Field Experiments

Five test roads were selected to evaluate the TSRST as the accelerated performance test to simulate low temperature cracking of asphalt concrete mixtures. Two of the roads are located in Fairbanks, Alaska, one in Elk County, Pennsylvania, and one each in Peraseinajoki and Sodankyla, Finland. In addition, several test sections were constructed in the Frost Effects Research Facility (FERF) of the USACRREL in Hanover, New Hampshire.

Information for the test roads contained in the following sections was obtained from local road authorities, excluding the Pennsylvania test road and the USACRREL test sections. The information for the Pennsylvania test road was based on a report by Kandhal et al. (1984) and the information for the USACRREL test sections was obtained from a report by Kanerva et al. (1992 b and 1993).

2.1.1 Alaska

Alaska DOT pavement sections in Fairbanks were selected for the test program after they experienced exceptionally severe low temperature cracking in the first winter after paving. The first section is located on 23rd Avenue (305 m east of Peger Road intersection) under the project name "23rd Avenue Extension." The road carries primarily light traffic (average daily traffic 3175) and consists of one lane in each direction and a center turn lane. The total width of the asphalt concrete pavement is 15.8 m. The second section is located on Peger Road (30 m north of Chena River Bridge) under the project name "Geist Extension — College to Peger." This road consists of two lanes, the total width of the paved surface being 9.7 m. The average daily traffic for Peger Road is 9150. Both sections were paved in September 1988.

The pavement structure for the roads consists of (from bottom to top) 910 mm clean gravel insulation layer ($P_{200} < 6$ percent), 152 mm crushed gravel subbase and 152 mm crushed gravel base course. A 51 mm asphalt concrete wearing course was placed on 23rd Avenue and 76 mm asphalt concrete wearing course on Peger Road.

Materials used in these asphalt concrete pavements were crushed gravel from Sealand pit and AC-5 asphalt from MAPCO, North Pole Refinery. The asphalt cement properties are given in Table 2.1. Target gradations and asphalt contents were nearly identical, the only difference being the Peger Road mix design used the

75-blow Marshall procedure, whereas the mix design for 23rd Avenue used the 50-blow procedure. Mix designs for the projects are given in Appendix A. The actual aggregate gradations and asphalt contents did not meet the specifications, however, and "tender" mix characteristics and, subsequent to construction, premature raveling was observed. The actual mix proportions are given in Appendix A. For both projects, the target mixing temperature varied between 134 and 140°C and target compaction temperature between 124 and 128°C. During construction of both projects the air temperature was approximately 4°C. On Peger Road, roller "checking" was a problem and hairline cracking could be observed transverse to the rolling direction. This was at least partially due to the out of specification "tender" mix (Esch, 1990).

2.1.2 Pennsylvania

The six test sections in Pennsylvania were constructed in Elk County during September 1976 using AC-20 asphalt cements from different sources. The research was undertaken with the cooperation of the Federal Highway Administration, U.S. Department of Transportation, as a long-term durability project (Kandhal et al., 1984).

The test sections are located on Traffic Route 219 North of Wilcox, between stations 100+00 and 219+43. The average daily traffic on the two lane, 6.1 m wide highway was 3700. The sections consisted of a 38 mm resurfacing of the

existing structurally sound pavement. The pavement cross section is as follows, from bottom to top:

- 254 mm crushed aggregate base and 76 mm penetration macadam (constructed 1948)
- 76 mm binder and 25 mm coarse sand mix (constructed 1962)
- surface treatment (constructed 1974)
- 38 mm bituminous concrete wearing course (constructed 1976)

The subgrade consists of a silty soil (AASHTO Classification A-4).

A plan view of the test sections is given in Figure 2.1. Each test pavement was approximately 610 m long. Mix composition and compaction levels were held constant for all test sections. The only variable was the asphalt type or source. The mix was composed of a coarse gravel aggregate and natural sand; its composition and Marshall design data are given in Appendix A.

The mixing temperatures for each test section were adjusted to obtain a mixing viscosity of 170 $\pm$ 20 mm^2/s. The mix temperatures generally ranged from 146 to 154°C. The compaction was completed before the mix cooled down to 79°C. Cores taken after construction from each test section were analyzed for mix composition and density. The mix composition conformed to the job mix formula. The average bulk specific gravity was 2.223 and air voids content 4.4 percent. The six asphalts were supplied by five refineries. The properties of the asphalts are given in Table 2.2.

2.1.3 Peraseinajoki, Finland

The test roads in Finland are part of the Asphalt Pavement Research Program (ASTO). ASTO is funded by the government of Finland and organized by the Technical Research Center of Finland (Saarela 1991).

The test road between Peraseinajoki and Alavus is part of Highway 672. Paving of the 50 mm thick asphalt concrete surface took place in June 1990. The average daily traffic on the two lane, 7.0 m wide road is 1500.

A 200 mm thick crushed rock base course was added to the existing pavement structure before paving with the wearing course. The existing structure consists of a 350 mm thick crushed rock base course and filter sand layer of 350 mm in embankment sections and 100 mm in cut sections. The old wearing course was completely removed before reconstruction.

A plan view of the six test sections is given in Figure 2.2. Different asphalt cements were used in each section and the asphalt content varied from 5.6 to 5.8 percent. The asphalt cement properties are given in Table 2.3. The crushed rock aggregate and the mixture gradation were the same for all sections. The mix compositions are given in Appendix A.

2.1.4 Sodankyla, Finland

The test road is located 10 km south of Sodankyla on Highway 4. The construction of an additional pavement structure and an asphalt concrete wearing course took place on July 1990. The average daily traffic on this two lane, 8.5 m wide highway is 2000.

A crushed rock base course of 200 mm and a filter layer (varying thickness) was added to the existing pavement structure. The existing oil gravel wearing course was crushed and left under the new filter layer.

The test sections do not extend across the whole width of the road, but are limited to one lane only as illustrated in the plan view of the sections in Figure 2.3. The aggregate and mix gradation was the same in all sections. Nine different asphalt cements were used and the asphalt content varied from 5.4 to 5.7 percent by weight of the mix. The mix compositions are given in Appendix A. Some of the asphalt cements were same products as in the Peraseinajoki test sections. The properties of asphalt cements are given in Table 2.3.

2.1.5 USACRREL

A test program was performed in the USACRREL FERF, under SHRP Contract A-003A, Subtask C.3. The facility consists of test basins, where environmental conditions, such as temperature and moisture content, can be

controlled. A plan view of the FERF is shown in Figure 2.4. Basins TC-1 through TC-4, TB-11 and TB-12 were used in the program. A comprehensive report of USACRREL experiment is given by Kanerva et al. (1992 b).

The test program consisted of two phases. In the Phase I program, three length/width ratios and two slab thicknesses were used with one asphalt concrete mixture. In the Phase II program, four different asphalt cements were used with a fixed geometry of the test section. The same mix design and aggregate were used in both phases.

The desired geometry and thickness of the pavement slabs to evaluate low temperature cracking in newly placed asphalt concrete were not known when the layout of the test sections was developed. Therefore, a set of slabs with different dimensions was identified for the Phase I program. A 2.7 m wide, 61.0 m long and 51 mm thick section was constructed to represent field conditions as closely as possible. Two 1.2 m wide, 21.3 m long and 51 mm thick sections and two 1.2 m wide, 39.3 m long and 76 mm thick sections were constructed to analyze the effect of the geometry of the pavement slab and the thickness of the pavement on cracking. The layout of the Phase I and II are presented in Figure 2.5.

The Phase II program focused on the low-temperature performance of different asphalt cements. In this phase, four 61 m long, 1.2 m wide and 51 mm thick sections were constructed. Each section contained a different asphalt cement as illustrated in Figure 2.5.

The existing subgrade in the FERF consisted mainly of silt and partly of four concrete slabs, all at different elevations, as shown in Figure 2.6. A concrete transition block was placed at the interface of the concrete slabs and silt subgrade. A crushed gravel subbase was placed over the base, such that the uppermost concrete slab had 76 mm of aggregate cover. The subbase was placed and compacted at the northern end on plywood boards and a geotextile (to protect the existing subgrade). At the southern end, the subbase was placed directly on the concrete slabs. One layer of 51 mm thick, high bearing capacity board insulation (DOW STYROFOAM Brand Plaza Deck Insulation) was installed between the subbase and the 305 mm crushed gravel base course. The wet density of the base course was measured with a nuclear density gauge. The mean density was 2273 kg/m^3 and standard deviation 37 kg/m^3. The mean moisture content was 3.4 percent (standard deviation 0.4 percent).

The Phase I paving took place on June 12, 1991. One lift of 19 mm minus asphalt concrete mix was placed. The Marshall mix design with the actual mix composition is given in Appendix A. The aggregate used was crushed stone from Tilcon's pit, West Lebanon, New Hampshire. The natural sand came from Hartland Pit, Hartland, Vermont. The asphalt cement used was an AC-20 produced by The United Refining Company, Warren, Pennsylvania. The asphalt properties are given in Table 2.4.

The sections were constructed according to the layout presented in Figure 2.5. The mixture temperature measured on the grade varied from 152 to 154°C.

Compaction commenced when the mixture temperature reached 107°C and was completed at 46°C. The mean density determined in the laboratory for core samples was 2446 kg/m^3, Rice specific gravity of 2.600, and mean air voids content of 6.0 percent.

The Phase II sections (VI to IX) were paved on September 14, 1991. The aggregate used was from the same batch as the aggregate used for Phase I. The following asphalt cements were used as given in Figure 2.5: AC-20 and AC-10 from Viking Asphalt of Newington, New Hampshire, AC-20 from Petro Canada of Montreal, Canada and AC-20 from Cibro of Albany, New York. The physical properties of the asphalt cements are given in Table 2.4. Based on the extraction/gradation results, the mixes were not identical in Phases I and II. The actual mix compositions for each Phase are given in Appendix A. The mean specific gravities and voids contents for the core samples are given in Table 2.5 and the mixing and compaction temperatures are given in Table 2.6.

The pavement sections were cooled by cooling panels that were laid directly on the pavement surface. The section I was cooled by placing the cooling panels on the supports, so that a 20 mm air gap separated the panels from the pavement. The section I did not experience cracking and, therefore, the test was repeated. Before the testing, however, the slab was split from the middle into two 1.35 m wide sections (Ia and Ib) and the panels were placed directly on the surface of the pavement.

2.2 Laboratory Experiments

2.2.1 Tests

The laboratory test program consisted of a series of experiments using the TSRST system on laboratory prepared specimens and specimens obtained from pavement sections. The test system is described in Section 1.1. Different cooling rates were used in testing; A cooling rate of 10°C/h represents the proposed standard procedure for the TSRST whereas 1, 2 or 5°C/h represent the maximum cooling rates backcalculated for the test roads.

2.2.2 Materials

Alaska The original asphalt cement (Mapco AC-5 from North Pole Refinery) from the same year that the paving took place was used to fabricate the laboratory samples. Mapco AC-2.5 was used as a reference asphalt, since it is normally used in the Fairbanks area. Asphalt properties for the AC-2.5 are given in Table 2.1. The aggregate was sampled from the same pit (Sealand pit) as the aggregate used in the test roads pavements.

In addition, six slabs were sawed from the test sections as illustrated in Figures 2.7 and 2.8. Slabs 1A, 1B, 2A and 2B were sawed from the left turn lane of 23rd Avenue. The three lanes were placed in two strips (see Figure 2.7). Slabs

1A and 1B were from the severely cracked southbound strip of the left turn lane. The thickness of the slabs was 57 mm. Slabs 2A and 2B were from the non cracked section of the left turn lane where the thickness appeared to be 44 mm. Finally, slabs 3A and 3B were from Peger Road. The thickness of these slabs was 102 mm. The slabs were cut after the first winter and stored at ambient laboratory temperature for 10 months before testing.

Pennsylvania The original asphalt cements (given in Table 2.2) sampled during the construction of the test sections were used to fabricate the laboratory specimens. The aggregate was sampled from a similar deposit as the original aggregate in the summer of 1991. The glacial gravel in the pits, located eleven miles from each other, has a considerate variation. No field slabs were available.

Peraseinajoki, Finland The asphalt cements used in the test sections were the same asphalt products as those used in the Sodankyla test road. The six asphalts described in Table 2.3 were sampled in Sodankyla while the paving of the test road took place. Aggregate was sampled a few weeks after the construction in Peraseinajoki from the same piles as the original aggregate. The aggregate was divided into three fractions (0-6 mm, 6-12 mm, 12-20 mm) and natural sand. In addition, lime filler was sampled. Field specimens were not sampled.

Sodankyla, Finland The nine asphalts given in Table 2.3 were sampled from the truck during unloading. The aggregate consisted of one fraction and it was sampled from the pile during construction. In addition, lime filler was obtained. Field samples were compacted at the mixing plant during construction. The mixture for the slabs was collected from the truck by digging under the surface layer at several locations. A 50 mm thick, 380 × 1200 mm slab was compacted in a plywood mold using a static laboratory rolling wheel compactor. Compaction commenced when the viscosity of the asphalt was 280 mm^2/s.

USACRREL Crushed aggregate was sampled from the cold feed conveyor during plant mixing. Samples of the asphalt cements given in Section 2.1.5 were obtained after mixing from the tanks at the hot-mix plant site. In addition, 156 cores (101.6 mm in diameter) and twenty-four 343 × 457 mm asphalt concrete slabs were sawed from test the sections VI to IX as illustrated in Figure 2.9. Slabs that were taken from the sections I to V were damaged during transportation to the Oregon State University (OSU) laboratory and were not tested.

2.2.3 Sample Preparation

Using the original asphalt cements and aggregates, 140 × 140 × 406 mm beams were compacted with a California Kneading Compactor according to the procedure by Harvey (1990). The mix compositions used were as close to the actual

mix compositions in the field as possible. After the beams were compacted and cooled, four 51 × 51 mm beams were sawed, or four 57.1 mm diameter cylinders were cored from the compacted beams. Both cylinders and beams were used in the test program because the TSRST protocol was changed during the field validation program. According to Jung and Vinson (personal communication, 1993) the shape of the specimen is not a significant variable in the TSRST. The air void content was determined for each sample.

Field samples (asphalt concrete slabs) were collected from the Alaska, Sodankyla (Finland) and USACRREL test sections. Beam specimens were sawed from the Alaskan and Finnish slabs. The dimensions of the beams were 51 × 51 mm. Cylindrical specimens were prepared from the USACRREL slabs with a 38.1 mm diameter drill. The air void content was determined for the samples. The length of all the laboratory and field cylinders and beams were 254 mm.

Part of the USACRREL laboratory samples were aged before compaction at 135°C for four hours. A set of field samples from Sodankyla was aged at 80°C for eight days and another set for 85 days before testing. These aging procedures are termed Short Term Oven Aging (STOA) and Long Term Oven Aging (LTOA), respectively. They have been developed at OSU in an attempt to simulate short-term and long-term field aging (Bell et al., 1991) of asphalt concrete pavements. The aged samples were cylindrical with a diameter of 44.4 mm. A detailed information about the shape and aging treatment for each sample is given with the test results.

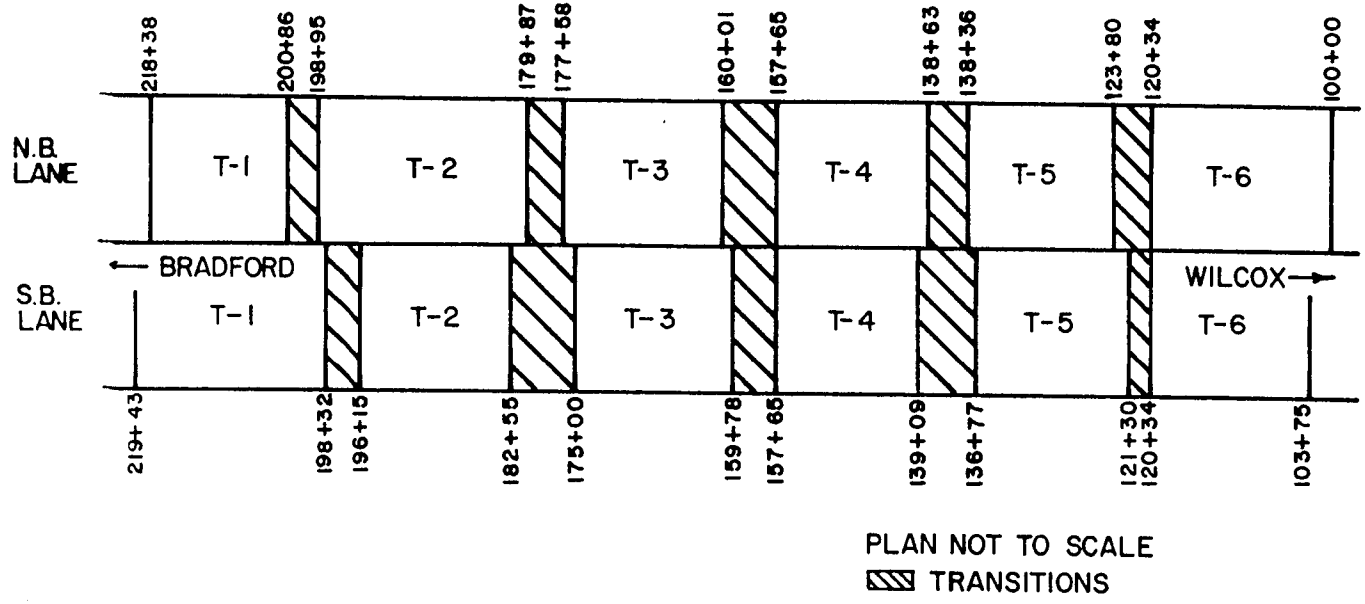

Figure 2.1 **Pennsylvania test sections (stations are given in feet)(after Kandhal et al., 1984)**

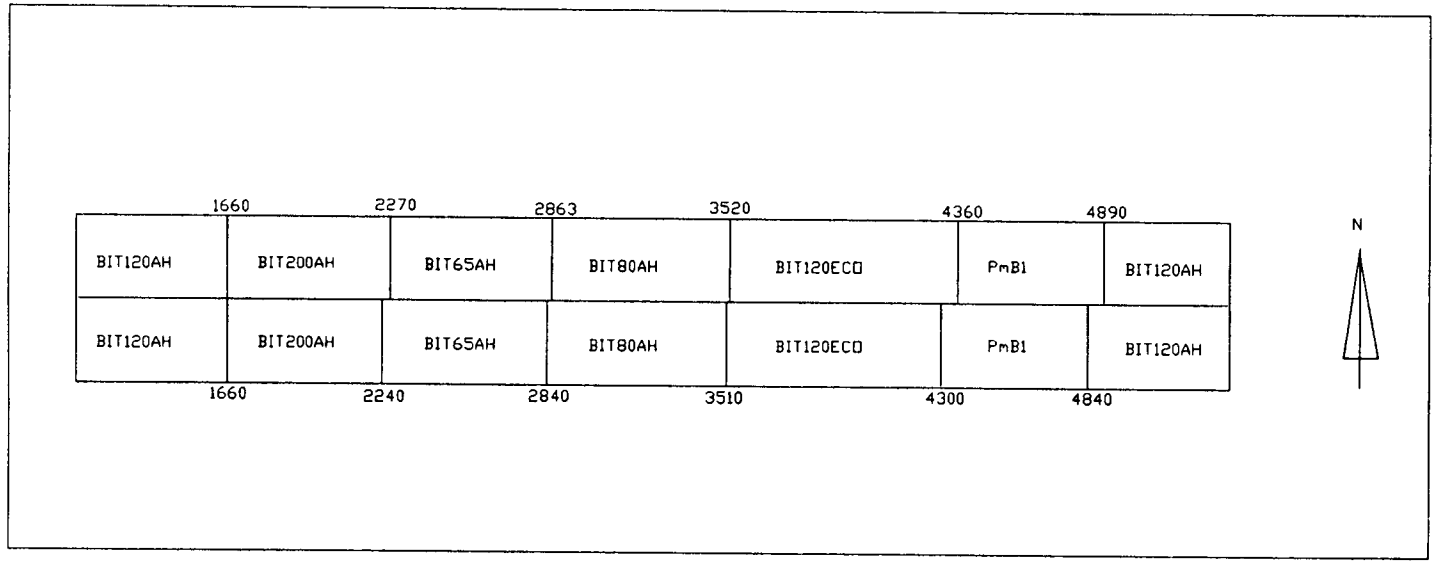

Figure 2.2 Peraseinajoki test sections

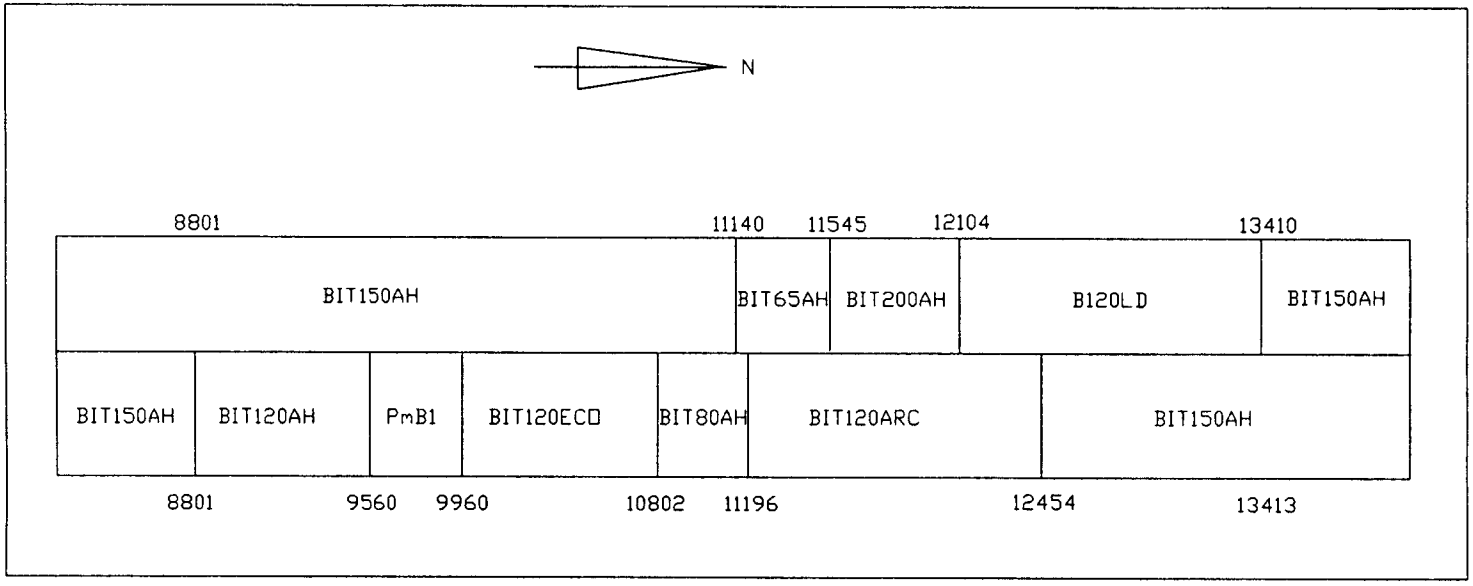

Figure 2.3 Sodankyla test sections

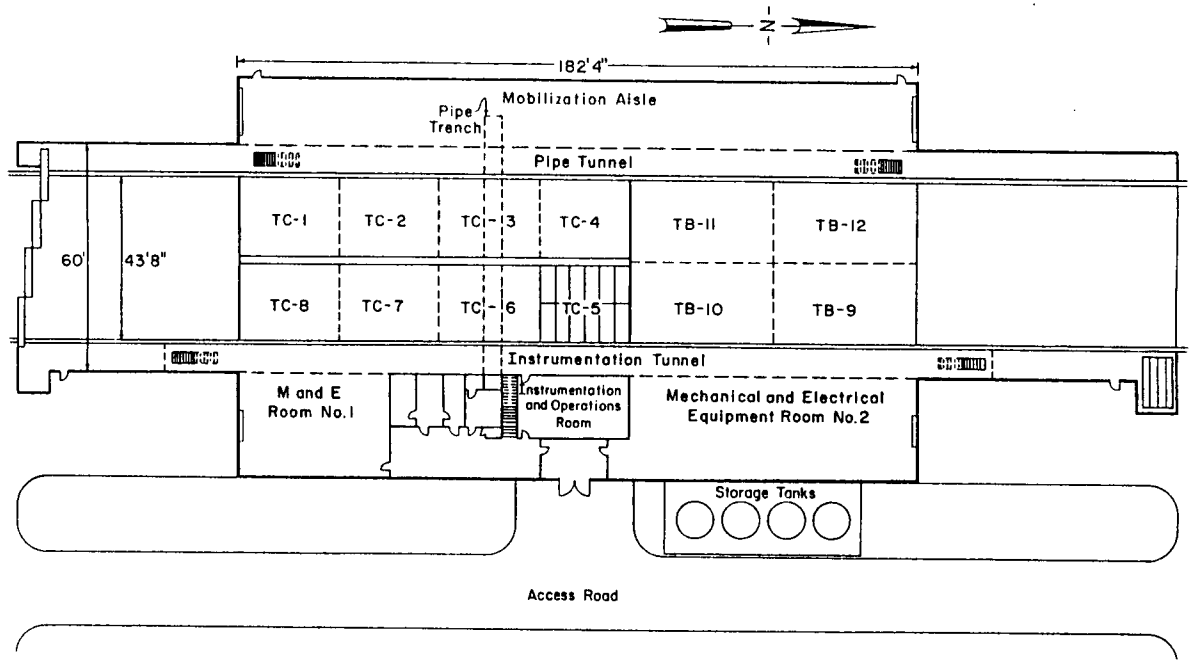

Figure 2.4 Frost Effects Research Facility at USACRREL (after Eaton, 1992)

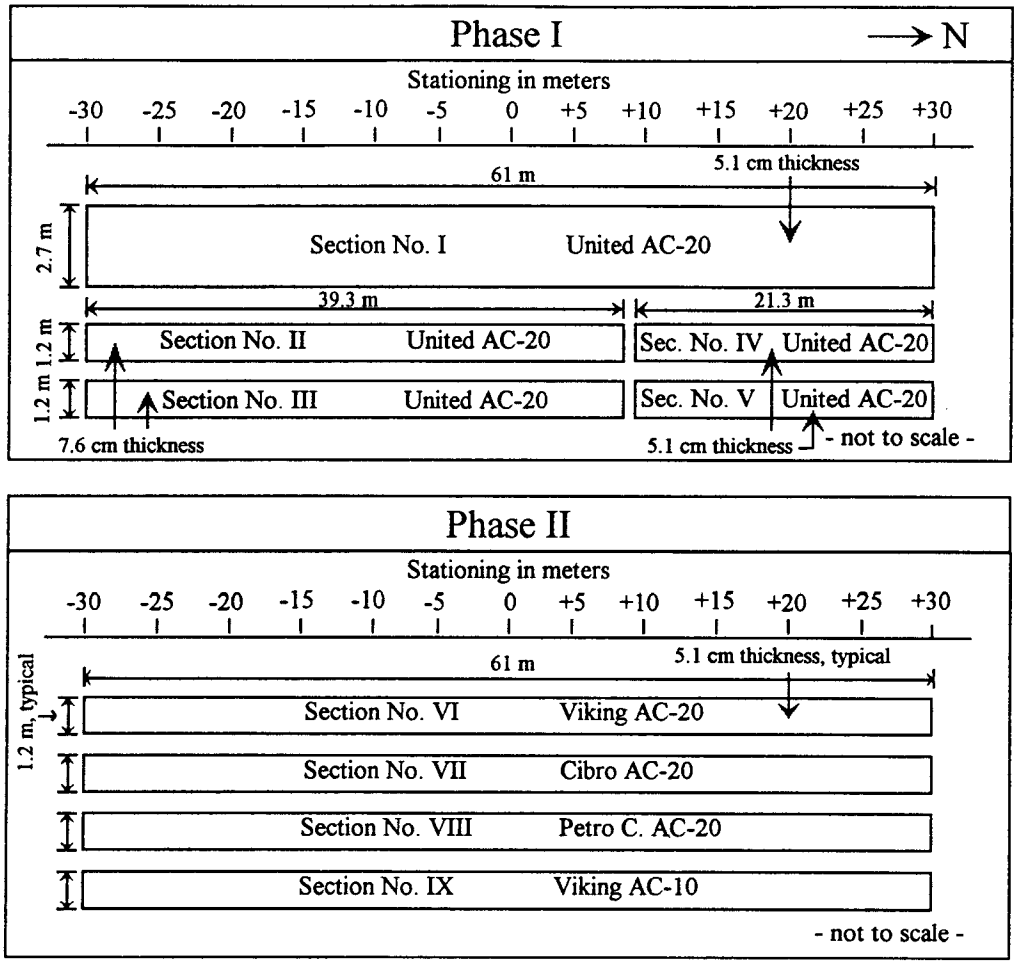

Figure 2.5 USACRREL test sections

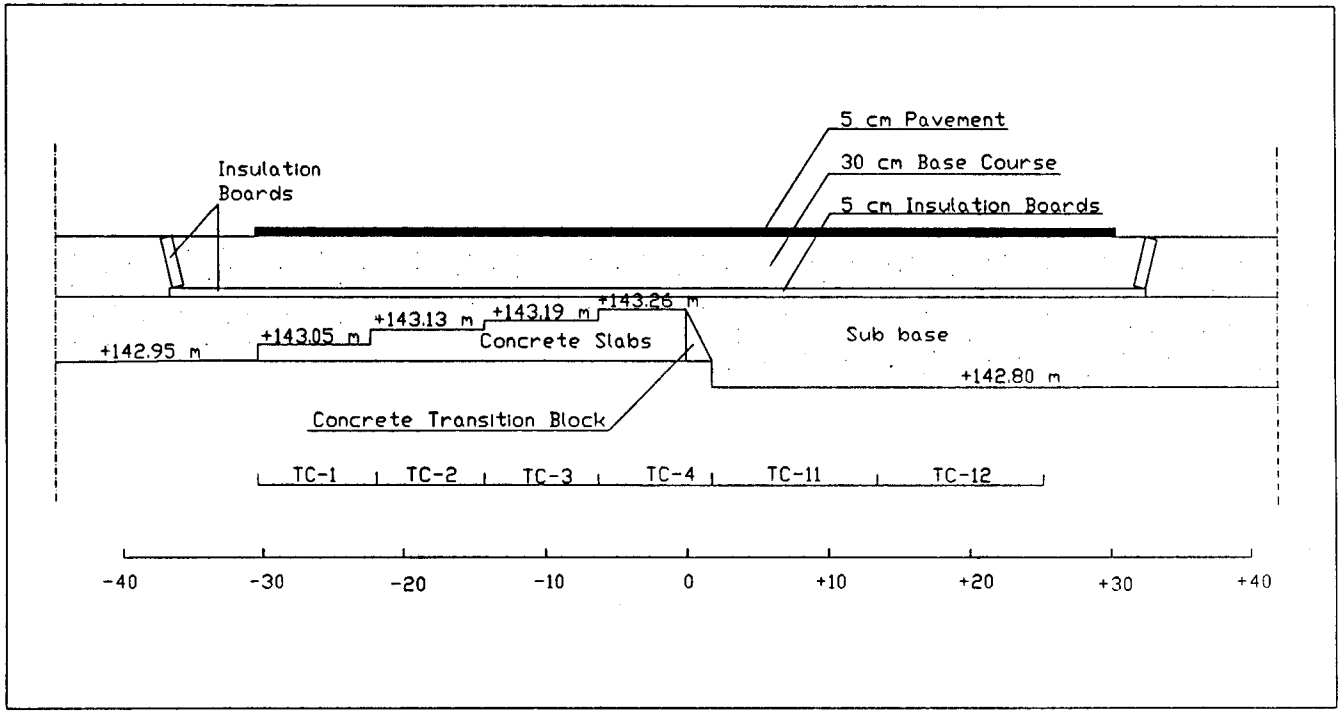

Figure 2.6 Cross section of pavement structure at USACRREL

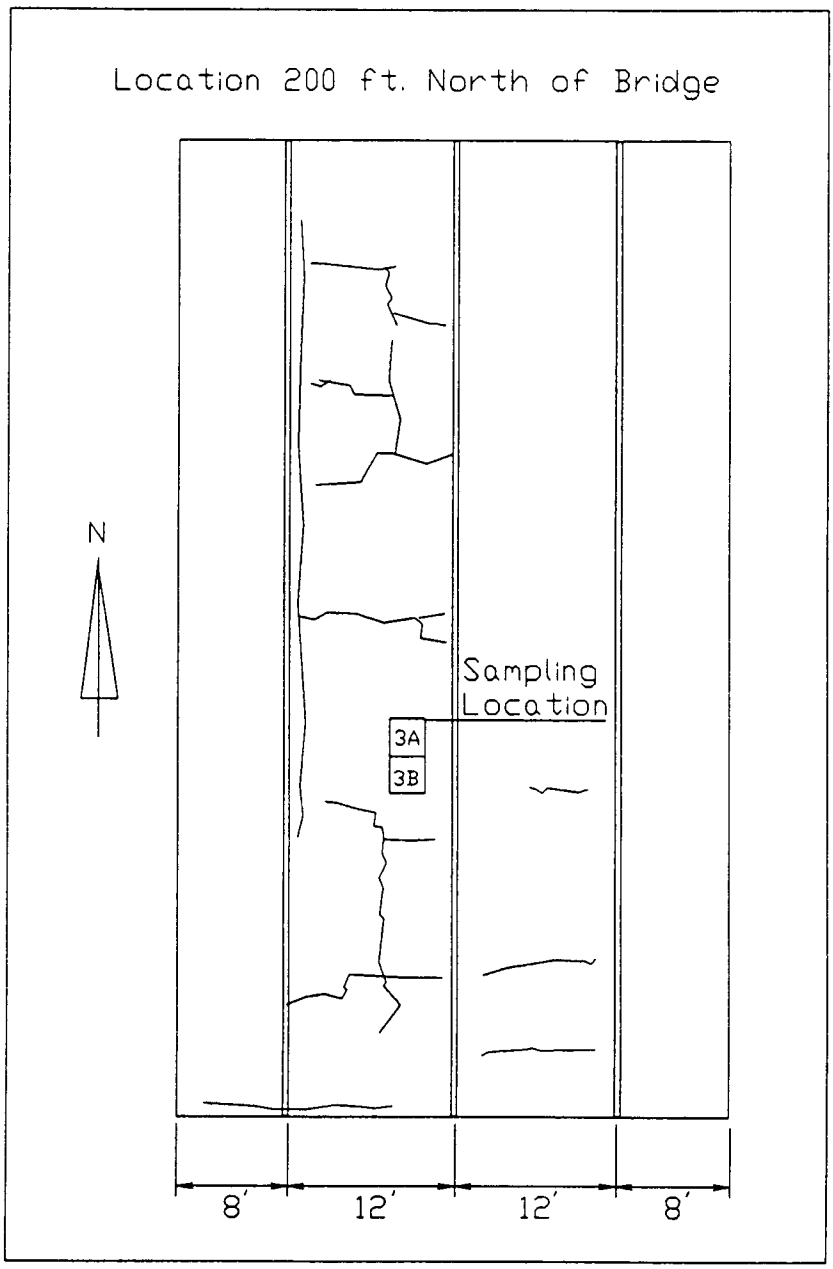

Figure 2.7 **Crack map and sample locations for 23rd Avenue, Fairbanks, Alaska (after Esch, 1990)**

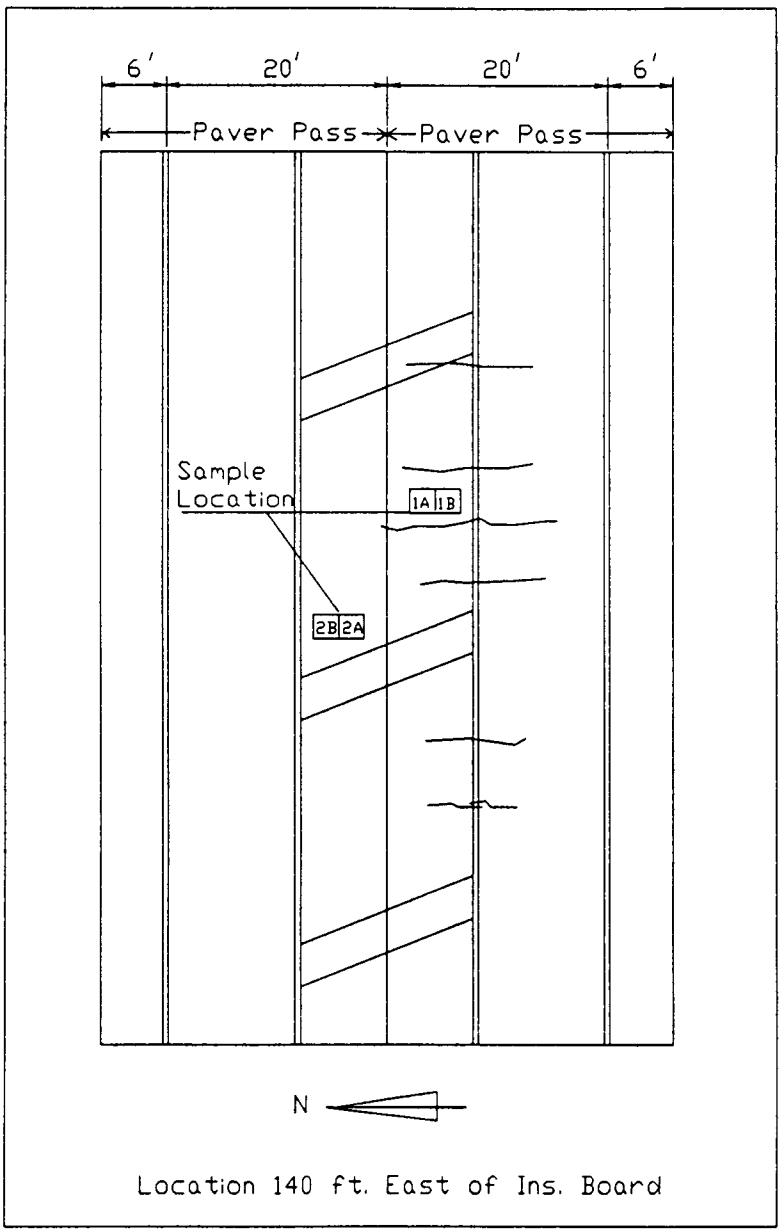

Figure 2.8 **Crack map and sample locations for Peger Road, Fairbanks, Alaska (after Esch, 1990)**

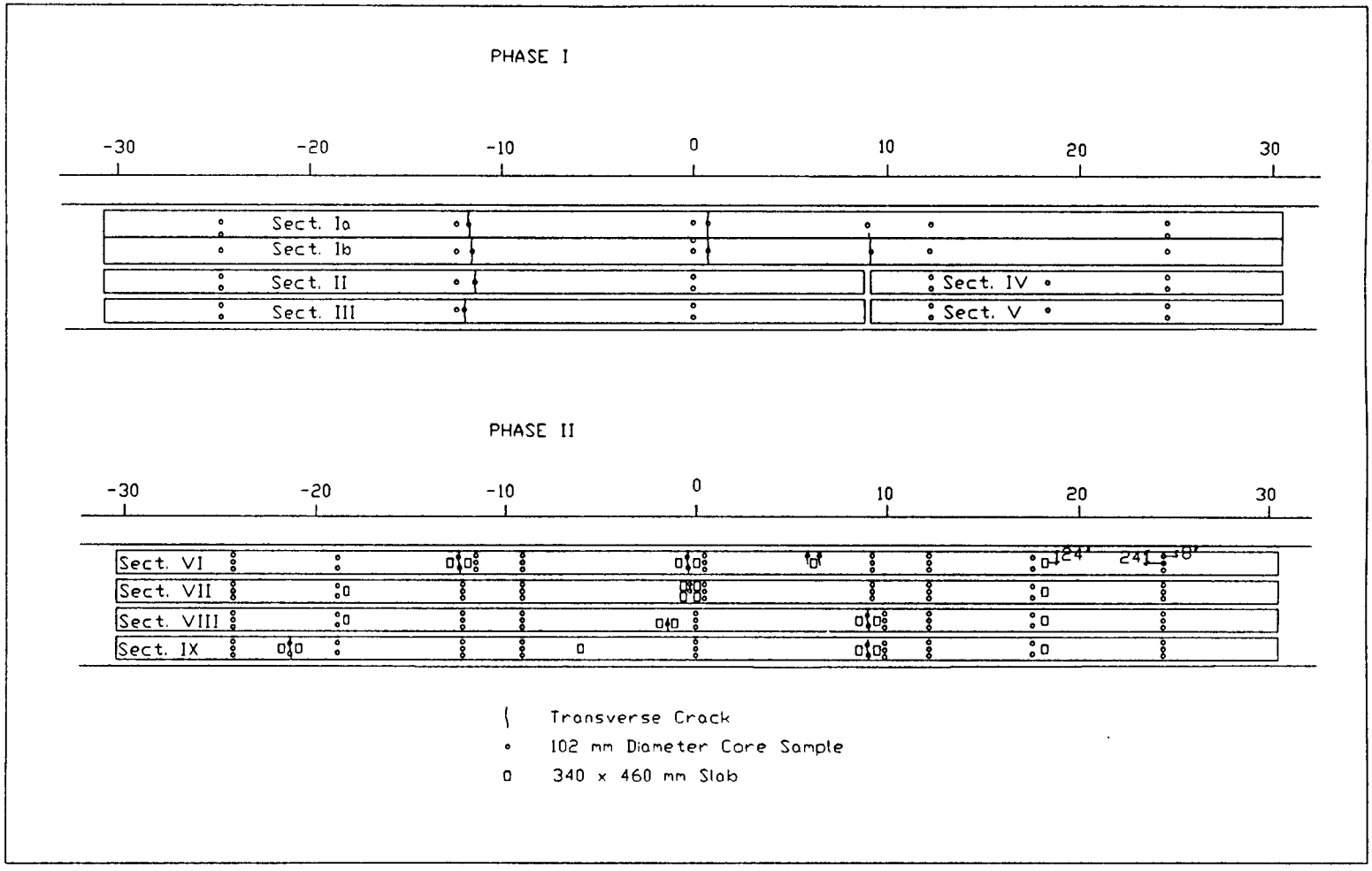

Figure 2.9 Sample locations for USACRREL test sections

Table 2.1 Asphalt properties for Alaska test sections (tested by Mapco, 1988)

Property	AC-5	AC-2.5
Original Asphalt		
Pen @ 25°C (0.1 mm)	162	249
Vis @ 60°C (Pas)	46.8	27.5
Vis @ 135°C (mm^2/s)	258	154
PVN	-0.33	-.069
TFOT Aged Residue		
Vis @ 60°C (Pas)	69.6	41.2

1 Pas = 10 Poise
1 mm^2/s = 1 cSt

Table 2.2 Asphalt properties for Pennsylvania test sections (after Kandhal et al., 1984)

Property	T-1	T-2	T-3	T-4	T-5	T-6
Original Asphalt						
Pen @ 25°C (0.1 mm)	42	64	72	65	54	80
Pen @ 4°C (100 g, 5 s)	2.0	7.4	6.2	6.7	3.4	7.5
Vis @ 60°C (Pas)	271	228	176	170	176	198
Vis @ 135°C (mm^2/s)	420	402	393	355	356	406
PI (Pen 4 & Pen 25)	-2.77	-0.71	-1.51	-1.04	-2.23	-0.14
PVN	-1.04	-0.70	-0.61	-0.86	-1.03	0.45
TFOT Aged Residue						
Pen @ 25°C (0.1 mm)	26	38	45	38	37	44
Vis @ 60°C (Pas)	550	683	398	469	325	572
Viscosity Ratio	1.34	1.42	1.41	1.48	1.30	1.42

1 Pas = 10 Poise
1 mm^2/s = 1 cSt

Table 2.3 **Asphalt properties for Peraseinajoki and Sodankyla test sections (tested by Neste Oil, Bitumen, Finland)**

Property	BIT 120AH	B 120LD	BIT 120 ECO	BIT 120 ARC	BIT 65 AH	BIT 80 AH	BIT 200AH	PmB1	BIT 150AH
Original Asphalt									
Pen @ 25°C (0.1 mm)	104	120	120	129	61	84	153	130	138
Pen @ 5°C (100 g, 5 s)	12	14	12	20	9	10	15	18	19
Vis @ 60°C (Pas)	117	114	74.2	72.7	299	203	65.2		66.2
Vis @ 135°C (mm^2/s)	363	295	226	225	573	487	278		222
Fraass Brittle Point (°C)	-25	-24	-23	-30	-20	-22	-26	-23	-30
PI (Pen 5 & Pen 25)	-1.03	-1.00	-1.43	-0.08	-0.25	-0.94	-1.48	-0.47	-0.48
PVN	-0.32	-0.48	-0.91	-0.83	-0.91	-0.13	-0.28		-0.78
TFOT Aged Residue									
Pen @ 5°C (100 g, 5 s)	9	9	9	14	7	8	13	13	14
Vis @ 60°C (Pas)	252	230	226	265	723	493	142		186
Fraass Brittle Point (°C)	-23	-22	-22	-30	-21	-22	-26	-23	-26
Viscosity Ratio	2.2	2.0	3.0	3.6	2.4	2.4	2.2		2.8

1 Pas = 10 Poise
1 mm^2/s = 1 cSt

Table 2.4 Asphalt properties for USACRREL test sections (tested for SHRP by Southwestern Laboratories, Houston, Texas)

Property	AC-20 United	AC-20 Viking	AC-20 Cibro	AC-20 Petro C.	AC-10 Viking
Original Asphalt					
Pen @ 25°C (0.1 mm)	68	76	96	69	122
Pen @ 4°C (100 g, 5 s)	6	7	11	8	12
Vis @ 60°C (Pas)	193.9	208.7	178.4	214.5	106.7
Vis @ 135°C (mm^2/s)	397	366	394	423	293
PI (Pen 4 & Pen 25)	-1.4	-1.38	-0.74	-0.66	-1.17
PVN	-0.66	-0.66	0.29	0.57	-0.47
TFOT Aged Residue					
Pen @ 25°C (0.1 mm)	---	50	61	42	77
Pen @ 4°C (100 g, 5 s)	---	5	9	7	10
Vis @ 60°C (Pas)	---	426.7	351.5	504.4	207.6
Vis @ 135°C (mm^2/s)	---	501	530	603	401
PI (Pen 4 & Pen 25)	---	-1.13	0.07	0.52	-0.36
PVN	---	-0.64	-0.36	-0.56	-0.51
Viscosity Ratio	---	2.04	1.97	2.35	1.95

1 Pas = 10 Poise
1 mm^2/s = 1 cSt

Table 2.5 Mixture properties from cores for USACRREL test sections

Section	Asphalt	Rice Specific Gravity	Specific Gravity GmbSSD	Void Content SSD (%)	Asphalt Content (% total Weight)
I . . . V	United AC-20	2.60	2.44	6.0	5.2
VI	Viking AC-20	2.59	2.44	5.6	5.2
VII	Cibro AC-20	2.61	2.44	6.7	5.5
VIII	Petro C. AC-20	2.59	2.41	6.6	5.4
IX	Viking AC-10	2.67	2.43	9.0	5.2

Table 2.6 **Field mixing and compaction temperatures for USACRREL test sections**

Section	Asphalt	Mixing Temperature (°C)	Compaction Temperature (°C)
I . . . V	United AC-20	152	107-46
VI	Viking AC-20	154	110-49
VII	Cibro AC-20	154	110-43
VIII	Petro C. AC-20	152	127-49
IX	Viking AC-10	149	121-60

3 FIELD AND LABORATORY TEST RESULTS

The field validation program results consist of temperature data and cracking observations on the test roads and TSRST results for the laboratory and field samples. The field and laboratory results for each test road are given in this chapter.

3.1 Alaska

The temperature data and the cracking observations presented herein were obtained from the Alaska DOT (Esch, 1990).

3.1.1 Temperature Data

The "critical" cooling event of the first winter (1989) was January 31. Air temperature dropped from -33 to -43°C. Pavement surface temperatures were measured at the Coldstream Valley site, 14.5 km north west of the test sections. A maximum cooling rate of 0.7°C/h was measured between January 21 and 31, during a period when pavement surface temperatures ranged from -35 to -40°C.

3.1.2 Cracking Observations

The three lanes on 23rd Avenue were placed in two strips as illustrated in Figure 2.7. The southbound strip experienced severe transverse cracking in the first winter, whereas the northbound strip was intact. The cracking interval of the southbound lane was locally as small as 1.5 m. Normal crack spacing in the Fairbanks area is from 15 m to 50 m. It is not recorded, if the northbound lane cracked within these expected limits.

The Peger Road section was placed in two phases as shown in Figure 2.8. Cracking occurred on both lanes, but was more frequent on the westbound lane and, besides transverse cracks, several longitudinal cracks were observed. The minimum cracking interval observed was 1.8 m. Crack maps in the vicinity of the sampling sites are given in Figures 2.7 and 2.8.

In addition to low temperature cracking, premature raveling of the roads was observed. Examination by Alaska DOT engineers suggested that raveling was due to the gap graded (out of specification) materials and low asphalt contents.

3.1.3 TSRST Results

The TSRST results are given in Table 3.1. The laboratory fabricated specimens made with asphalt cement AC-5 represent both 23rd Avenue and Peger Road. The specimens made with AC-2.5 represent a control section (associated with

many other roads in Fairbanks that did not exhibit severe low temperature cracking). The specimens were tested in non-aged condition.

3.1.4 Data Analysis

The TSRST fracture temperatures for the field specimens from the southbound and northbound lanes of 23rd Avenue and Peger Road, and for the laboratory fabricated specimens are given in Figure 3.1. By visual inspection, the fracture temperatures of the laboratory fabricated samples for the AC-5 and AC-2.5 mixtures do not differ appreciably from each other. Based on this finding, the low temperature cracking of the test sections is not explained by using AC-5 asphalt instead of AC-2.5. (AC-2.5 is commonly used in Fairbanks area, and severe low temperature cracking of asphalt pavements is not normally observed.) However, it is shown in Figure 3.1 that the fracture temperatures for the field samples are warmer than for the laboratory fabricated samples, which may explain the cracking of the pavements. The warmer fracture temperatures indicate a stiffer mixture, which may be due to the aging of the pavements in service and/or excessive aging of the mixture during plant mixing. Furthermore, the TSRST fracture temperature for the intact northbound lane of 23rd Avenue is colder than for the severely cracked southbound lane of the 23rd Avenue and Peger Road, which may explain the differences in performance of the pavement sections. Statistical analyses were performed to investigate if these hypothesis can be confirmed.

The fracture temperatures of the test sections were compared with each other by testing the difference between two means ($\bar{X}_1$, $\bar{X}_2$). It was assumed that the populations are normally distributed. Since the variances of the populations are unequal, an approximate procedure was used as follows (Scheaffer 1990):

The T statistic was calculated as

$$T = \frac{\bar{X}_1 - \bar{X}_2 - D_0}{\sqrt{\frac{S_1^2}{n_1} + \frac{S_2^2}{n_2}}} \tag{3.1}$$

This statistic has approximately a *t* distribution under the null hypothesis $H_0: \mu_1 - \mu_2 = D_0$, with degrees of freedom given by the integer part of

$$df = \frac{(S_1^2 + S_2^2)}{\left[\frac{S_1^2}{n_1 - 1}\right] + \left[\frac{S_2^2}{n_2 - 1}\right]} \tag{3.2}$$

in which,

S_1^2 and S_2^2 = the sample variances and

n_1 and n_2 = the numbers of observations.

For the hypothesis: fracture temperature (obtained using 10°C/h cooling rate) of the laboratory fabricated specimens containing AC-5 equals fracture temperature of laboratory specimens containing AC-2.5 (FT(AC-5) - FT(AC-2.5) = 0), the T statistic is 1.27 with three degrees of freedom (df). The p-value in the

two-sided t-test is 0.175; consequently, the hypothesis is accepted (limit for rejection of the hypothesis for 5 percent significance is: p-value < 0.025). In other words, there is no significant difference between the fracture temperatures of the mixes containing AC-5 or AC-2.5 asphalt cements. Similarly, for laboratory fabricated specimens tested using a slow cooling rate of 1°C/h, the T statistic is 0.99 with one degree of freedom. The p-value for this hypothesis is 0.25; again, the hypothesis is accepted. Thus, the use of the asphalt AC-5 instead of AC-2.5 does not explain the severe low temperature cracking of the test sections.

The same analysis was performed for the hypothesis: fracture temperature of all field samples (asphalt cement AC-5) equals fracture temperature of the laboratory specimens for the AC-5 mixture. The T statistic for the analysis is -1.39 with three degrees of freedom. The p-value is consequently 0.13 and the hypothesis is accepted. Therefore, there is no significant difference in fracture temperatures between the field specimens and laboratory fabricated specimens.

For the hypothesis: fracture temperature of southbound lane of 23rd Avenue equals fracture temperature of the northbound lane, the T statistic is 2.71, the degree of freedom is one and the p-value is 0.13. In this case, too, the hypothesis is accepted, suggesting no significant difference between the fracture temperatures.

Finally, the hypothesis that the fracture temperature for the Peger Road pavement samples that were saw cut transverse to the direction of traffic equals the fracture temperature of the samples saw cut parallel to direction of traffic was tested. This was done to investigate the affect of roller "checking" on fracture

temperature. The T statistic for the analysis is 0.21 for three degrees of freedom, and the p-value is greater than 0.4. Accordingly the hypothesis is accepted; thus, there is no evidence that the roller "checking" was associated with the fracture temperature.

Based on these findings, the TSRST ranked samples in the correct order, but there was no statistical evidence for the differences in fracture temperatures between the populations. Regarding the minimum pavement surface temperature in the field, the TSRST fracture temperatures were approximately 10°C warmer and, accordingly, cracking could be anticipated for all test sections. The severe low temperature cracking may be associated with the out of specification and consequently, "tender" mix. This assumption could not been investigated, because all samples were fabricated according to the actual, out of specification, mix design. The locally severe cracking may also be due to substantial base restraint of the pavement layer at those locations.

3.2 Pennsylvania

The temperature and cracking observations presented in the following paragraphs were reported by Kandhal et al. (1984).

3.2.1 Temperature Data

The Pennsylvania Department of Transportation had a thermocouple installation site 11.3 km north of the test road section. The system was capable of recording hourly air temperature and asphalt pavement temperature 51 mm below the surface. According to the recorded data, the critical period of rapid cooling is believed to have occurred in the first winter, on January 28 and 29, 1977. The air temperature dropped 14°C in two hours. Rapid cooling of the pavement 51 mm below the surface occurred 12 hours later, a drop of 5°C in one hour. The minimum air temperature recorded was -29°C whereas the pavement temperature reached -23°C. The 1976-1977 air freezing index was 1509 degree days. Low ambient temperatures prevailed at the site during the second (1977-1978) and third (1978-1979) winters. The minimum temperatures were -18 and -25°C respectively.

3.2.2 Cracking Observations

When constructed in September 1976, no visual differences were observed among the six test pavements. After the first winter, two test sections (T-1 and T-5) developed excessive low temperature cracking while the other sections did not have any transverse cracks. After three severe winters, the sections T-1 and T-5 developed more cracks while the other sections did not develop any significant cracking. During the fifth year, the sections T-2, T-4 and T-6 gradually developed

cracking to different degrees while the section T-3 had no transverse cracking. The cracking index (CI) with time, defined as a number of cracks per 500 ft (152.4 m) according to eqn. 3.3, is given in Table 3.2.

$$CI = FullCracks + 0.5 HalfCracks + 0.25 PartialCracks \quad (3.3)$$

3.2.3 TSRST Results

The TSRST results are given in Table 3.3. The specimens were laboratory produced beams and were tested in non-aged condition.

3.2.4 Data Analysis

The actual moments of cracking were not observed and, therefore, the cracking temperatures in the field are not known. However, the minimum air and pavement temperatures for the first and (simultaneously) the most severe winter are available. The mean TSRST fracture temperatures (cooling rate 5°C/h) for the test sections and the minimum pavement temperature in the field are given in Figure 3.2. The TSRST fracture temperatures of the field sections T-1 and T-5 (that experienced severe low temperature cracking) are warmer than the minimum pavement temperature of -23°C. The TSRST fracture temperatures for all the other sections that resisted low temperature cracking are colder than the minimum

pavement temperature. Hence, the cracking behavior of the test sections may be explained totally by the TSRST fracture temperatures.

To investigate the relationship between the CI defined in eqn. 3.3 and pavement age from 1 to 5 years in Table 3.2 and the TSRST fracture temperature, a multiple regression analysis was performed. The analysis was done with the mean TSRST fracture temperatures of the tests with a cooling rate of 5°C/h (FT5) and 10°C (FT10). According to the analysis, there is convincing evidence that the fracture temperature is associated with the CI (p-value in two-sided t-test is smaller than 0.0001). The following model was chosen to represent the CI as a function of the TSRST fracture temperature based on the smallest error of Y estimate:

$$\text{Mean}\{CI\} = -157 - 4220 / FT5 \qquad (3.4)$$

S.E. 15.5 353

p-value in two-sided t-test

<0.0001 <0.0001

$R^2 = 89\%$, Error of Y Estimate 10.95, Degrees of freedom (df) 18,

in which,

CI = cracking index (eqn. 3.3),

FT5 = fracture temperature (°C), cooling rate 5°C/h.

The predicted cracking index versus the TSRST fracture temperature is plotted in Figure 3.3.

Adding the natural logarithm of age of the pavement improves the model (p-value is smaller than 0.005 in extra sum-of-squares F-test), which is given as follows:

$$\text{Mean}\{CI\} = -163 - 4160/FT5 + 10.2 \ln(Age) \quad (3.5)$$

S.E. 12.7 286 3.13

p-value in two-sided t-test

<0.0001 <0.0001 0.0048

$R^2 = 93\%$, Error of Y Estimate 8.86, df 18

in which,

CI = cracking index (eqn. 3.3),

FT5 = fracture temperature (°C), cooling rate 5°C/h, and

Age = age of pavement (years).

Cracking indices as a function of time for the sections T-1 and T-5 are given in Figure 3.4.

3.3 Peraseinajoki, Finland

The temperature data and the cracking observations for the Peraseinajoki test road were obtained from the Technical Research Center of Finland (Kurki, 1991).

3.3.1 Temperature Data

A temperature data logger was installed at a representative location for the test sections. Temperature was measured every 30 minutes using thermocouples at the surface, at a depth of 25 mm, at the bottom of the asphalt concrete layer and in the air. The coldest recorded air temperature was -30°C and the coldest temperature in the pavement was -20°C. The maximum recorded cooling rate was 0.7°C/h. The freezing index from November 9, 1990 to March 25, 1991 was 661°C days.

3.3.2 Cracking Observations

No low temperature cracks were observed in any of the six test sections through the first two winters. In every respect, the asphalt concrete pavement was in good condition.

3.3.3 TSRST Results

Since no cracks were observed in the Peraseinajoki test road, no specimens were prepared in the laboratory. However, because the asphalt cement type is the most significant factor influencing low temperature cracking (Jung and Vinson, 1992), the laboratory test results for the Sodankyla specimens were used to represent the Peraseinajoki sections; The asphalts are the same products, both test

roads have a well-graded aggregate, and the asphalt contents are within 0.4%. A summary of the Sodankyla test results adapted for Peraseinajoki are given in Table 3.4.

3.3.4 Data Analysis

The mean TSRST fracture temperatures (cooling rate 2°C/h) for the test sections (adapted from the Sodankyla test sections) and the minimum pavement temperature in the field are given in Figure 3.5. The TSRST fracture temperatures of the field sections are all colder than the minimum pavement temperature of -20°C. Hence, the cracking behavior of the test sections could be explained by the TSRST fracture temperatures.

3.4 Sodankyla, Finland

The temperature data and the cracking observations for the Sodankyla test road were obtained from the local road authority of Sodankyla and the Technical Research Center of Finland (Kurki, 1991).

3.4.1 Temperature Data

A temperature data logger was installed at a representative location for the test sections. Temperature was measured every 30 minutes using thermocouples at the surface, at a depth of 25 mm, at the bottom of the asphalt concrete layer, and in the air. The coldest air temperature observed was -33°C and coldest temperature in the pavement -24.5°C. The recorded maximum cooling rate was 2.3°C/h. The freezing index from November 9, 1990 to March 25, 1991 was 1488°C days.

3.4.2 Cracking Observations

Visual crack observations were performed occasionally during the coldest winter months for a 300 m long segment of each test section. A complete investigation was conducted after the first winter for the entire length of the project. A total of 116 full cracks and 48 half cracks were recorded. The observations are given in Table 3.5. Because the observations were not accomplished daily, the exact cracking moment and, therefore, cracking temperature is not known. The cracking temperatures in the air and in the pavement were determined as the coldest temperatures that occurred between the observations. The temperatures given in Table 3.5 are the cracking temperatures for the first observed crack for each 300 m long test segment.

In addition to the fact that the actual moment of cracking was not recorded, the following conditions make it difficult to interpret the cracking frequencies and temperatures:

- The test sections were limited to one lane only and most of the cracks extended over the entire pavement (see Figure 2.3). Cracks may have initiated in the other lane and advanced to the section in question.

- Only 300 m long segments were observed periodically. If the first crack occurred outside that segment, the cracking moment observed would relate to the second or possibly even the third or fourth crack.

- The transverse crack pattern in the pavement before the reconstruction was given in the construction documents. Approximately half the cracks that occurred in the first winter appeared at the same locations as the existing cracks in the underlying pavements. Thus, a part of the cracks should be considered as reflection cracks.

- The cracking frequency in the preceding pavement was not constant (see Figure 3.6), although there was no variation in the materials.

Therefore, it is concluded that the conditions of test sections are not uniform.

- Ground thermal contraction may have caused many cracks in the pavement wearing course instead of contraction in the asphalt concrete.

3.4.3 TSRST Results

The TSRST results are given in Table 3.6. The specimens were produced at the mixing plant during construction. The following test program was conducted to investigate the effect of aging on the fracture temperature and fracture strength:

- Two samples of each mixture were tested after eight days of LTOA.

- Two samples of each mixture were aged for 85 days before testing (LTOA). These samples were recompacted in the laboratory, since the original cylindrical samples were disintegrated at the first day of LTOA due to the vibrations in the oven and inadequate support. The aging was continued (after refabricating the samples) on a sand bed and the vibration was eliminated. The testing of the recompacted samples was considered acceptable, because the target was to achieve

the most severe aging possible and consequently the warmest fracture temperature for each mixture.

- The results from Table 3.6 with the cooling rate of 2°C/h were used for the non-aged samples.

The aging procedure proved to be quite severe and several samples were damaged before testing. Consequently, only one or no samples were tested for some mixtures.

3.4.4 Data Analysis

A multiple regression analysis was performed to examine the relationship between the TSRST fracture temperature and cracking temperature and frequency in the field. Several prediction models for the cracking temperatures were considered but only 28 percent of the variable "air cracking temperature" could be explained with the TSRST fracture temperature and 17 percent of the variable "pavement cracking temperature." Possible reasons for the poor correlation are given in Section 3.4.2.

The TSRST fracture temperatures for each section and the minimum pavement temperature are given in Figure 3.7. According to the data, none of the pavement sections should have cracked. If compared to the conditions in

Peraseinajoki, the minimum pavement temperature was 4.5°C colder and the freezing index at the surface of the pavement was more than twice as severe. It is assumed that the cracking was partly reflective cracking through the base course and partly caused by stresses due to the ground thermal contraction instead of thermal stresses in the pavement.

The crack spacing could not be explained with the TSRST fracture temperature either. The cracking index versus TSRST fracture temperature is given in Figure 3.8. By visual inspection and assuming good low temperature behavior for the Styrene-Butadiene-Styrene (SBS) modified PmB1 asphalt cement and poor for the hard BIT65AH asphalt cement, the two data points are unreasonable. However, even if these cases are omitted, only 39% of the relationship could be explained and there is no evidence that the fracture temperature is associated with the crack spacing (p-value in two-sided t-test is 0.13). The crack spacing was most likely associated with the geometry of the test sections, possible reflection cracking through the base course, ground thermal contraction and varying restraint conditions.

A relationship between the fracture temperature and the degree of LTOA was obtained by a multiple regression analysis. From several models investigated, the following model was chosen based on the smallest standard error of Y estimate:

$$\text{Mean}\{FT(time)\} = 1.029\ FT_{orig} + 1.150(LTOA)^{0.5} \qquad (3.6)$$

S.E. 0.037 0.180

p-value in two-sided t-test

<0.00001 <0.00001

R^2 = 99%, Std. Error of Y Estimate 2.44, df 15,

in which,

FT(time) = fracture temperature with time (°C),

FT_{orig} = fracture temperature for non-aged sample (°C), and

LTOA = degree of LTOA (days).

The model with the data points is illustrated in Figure 3.9. Similarly, a multiple regression analysis was done to investigate the relationship between the fracture strength and the degree of LTOA. The following model was chosen to present the relationship based on the smallest standard error of Y estimate:

$$\text{Mean}\{FS(time)\} = 0.854\ FS_{orig} - 58.0\ (LTOA)^{0.5} \quad (3.7)$$

S.E. 0.067 39.5

p-value in two-sided t-test

<0.00001 0.163

R^2 = 97%, Std. Error of Y Estimate 553, df 15,

in which,

FS(time) = fracture strength with time (kPa),

FS_{orig} = fracture strength for non-aged sample (kPa), and

LTOA = degree of LTOA (days).

There is no statistical evidence that the fracture strength is affected by aging (p-value is > 0.1), which means that for this data set the fracture strength of the pavement will likely be constant with time.

The models presented above are based on one aggregate type and mix design only. Therefore, more data must be obtained before the model for fracture temperature and fracture strength as a function of degree of LTOA can be established.

3.5 USACRREL

The temperature and cracking observations given herein were presented by Kanerva et al. (1992 a).

3.5.1 Temperature Data

Temperatures in the pavement structure were measured using thermocouples placed at the surface and bottom of the asphalt concrete, in the midpoint of the base course, and at the top and bottom of the insulation layer. The minimum temperature achieved at the surface of the pavement was -36.7°C and at the bottom of the pavement -32.8°C. Recorded pavement temperatures, when cracking occurred, are given in Table 3.7. A typical temperature profile with detected cracking times is given in Figure 3.10. The three curves in Figure 3.10 represent the temperatures at

the surface and the bottom of the pavement and in the base course at a depth of 200 mm from the top of the pavement. The times at which cracks were detected are marked with symbols (x) on the temperature curve for the surface of the pavement.

3.5.2 Cracking Observations

The crack detection system consisted of two types of aluminum tape and hard drawn copper wire attached to the pavement surface with adhesive. Seventeen cracks were observed in the nine sections. The cracks produced are shown in Figure 3.11 and the recorded observations are summarized in Table 3.7. Note, that the section I did not experience cracking in the first cooling and, therefore, the slab was split from the middle into two sections, Ia and Ib.

Based on the recorded temperature profiles, cracking generally did not occur before the minimum possible temperature for the cooling system was achieved. Therefore, the surface temperature was constant for a period before the onset of cracking. The surface temperature does not reflect the cracking temperature, but the minimum temperature achieved by the cooling panels. The temperature at the bottom of the asphalt concrete layer decreased until cracking occurred in almost all cases. Therefore, the stress due to the distribution of temperature in the pavement layer initiated cracking instead of the stress associated with the surface temperature. Consequently, in this case, the temperature at the bottom of the asphalt pavement

would be a better indicator of the cracking temperature than the surface or average temperature. However, the surface temperature was measured at 2.44 m intervals, whereas the bottom temperature was measured only at three locations along the length of the pavement. Therefore, the surface and bottom temperatures in Table 3.7 do not necessarily relate to the same location. The surface temperature does not represent the cracking temperature and the bottom temperature may be measured as far as 10 m away from a crack, which makes the determination of the cracking temperatures very complicated. For validation purposes, the bottom temperature was termed an indicator cracking temperature. It is given with the total number of cracks and cracking index (eqn. 3.3) in Table 3.8.

3.5.3 TSRST Results

The TSRST results are given in Table 3.9. One half of the laboratory fabricated samples were tested in non-aged condition and one half after STOA to investigate which aging method best represents the field conditions. The field samples were tested without further aging.

3.5.4 Data Analysis

Indicator cracking temperatures versus TSRST fracture temperatures for the test program are shown in Figures 3.12 to 3.14. Multiple regression analysis was

performed to investigate the relationship between the indicator cracking temperature of the test sections and TSRST fracture temperature of the corresponding mixture. Results of the regression analysis are given in Table 3.10. Based on the analysis there is evidence ranging from slight to conclusive that the TSRST fracture temperature (FT) is associated with the indicator cracking temperature (CT). For non-aged laboratory samples that were tested using a cooling rate of 10°C/h, the p-value in a two-sided t-test was 0.017, and 88% of the relationship could be explained. The following model represents the relationship:

$$\text{Mean}\{CT\} = 37.2 + 2.36\,FT \qquad (3.8)$$

S.E. 13.5 0.49

p-value in two-sided t-test

0.027 0.017

$R^2 = 88\%$, Error of Y Estimate 3.24, df 3

in which,

CT = indicator cracking temperature (°C),

FT = fracture temperature (°C), non-aged samples, cooling rate 10°C/h.

Predicted cracking temperatures with measured values versus TSRST fracture temperature are shown in Figure 3.15.

To investigate the correlation between the cracking index in the FERF and the TSRST fracture temperature a multiple regression analysis was performed. The

analysis was made with the TSRST fracture temperatures for the tests with a cooling rate of 10°C/h for non-aged samples. There is slight evidence that the TSRST fracture temperature is associated with the cracking index (p-value in two-sided t-test is 0.03). The following model represents the cracking index (CI) as a function of the TSRST fracture temperature (FT):

$$\text{Mean}\{CI\} = -31.5 - 988 / FT \qquad (3.9)$$

S.E. 9.49 256

p-value in two-sided t-test

0.045 0.031

$R^2 = 83\%$ Error of Y Estimate 1.25, df 3

in which,

CI = cracking index (eqn. 3.3), and

FT = fracture temperature (°C), non-aged samples, cooling rate 10°C/h.

Predicted cracking index, with measured values, versus the TSRST fracture temperatures is given in Figure 3.16.

According to the results (see Figures 3.12 to 3.14 and Table 3.10), a slow cooling rate (1 instead of 10°C/h) or STOA does not improve the relationship between the cracking temperature in the field and the TSRST fracture temperature. The fracture temperatures for laboratory samples versus field samples are shown in Figure 3.17. The test sections were not aged in the field and, accordingly, the non-

aged laboratory samples are closer to the actual field samples regarding TSRST fracture temperatures than the short term aged samples.

Based on the USACRREL test program, where the environmental variables were closely controlled, the TSRST fracture temperature is an indicator of the pavement cracking temperature and frequency for the five mixtures considered.

3.6 Summary of Field and Laboratory Observations

Based on the data from the five test roads and the USACRREL test sections, the following conclusions are appropriate:

- Observed cracking could be explained with TSRST fracture temperatures for the test roads in Pennsylvania, Peraseinajoki and the USACRREL. In Alaska and Sodankyla, there were factors in addition to mixture properties affecting low temperature cracking. It is concluded that the TSRST can be used to predict the low temperature cracking of asphalt-aggregate mixtures.

- Preliminary models to predict cracking frequency and temperature for the test roads were developed. This experience suggests that it is possible to develop a model that would predict the development of cracking with time in all climates.

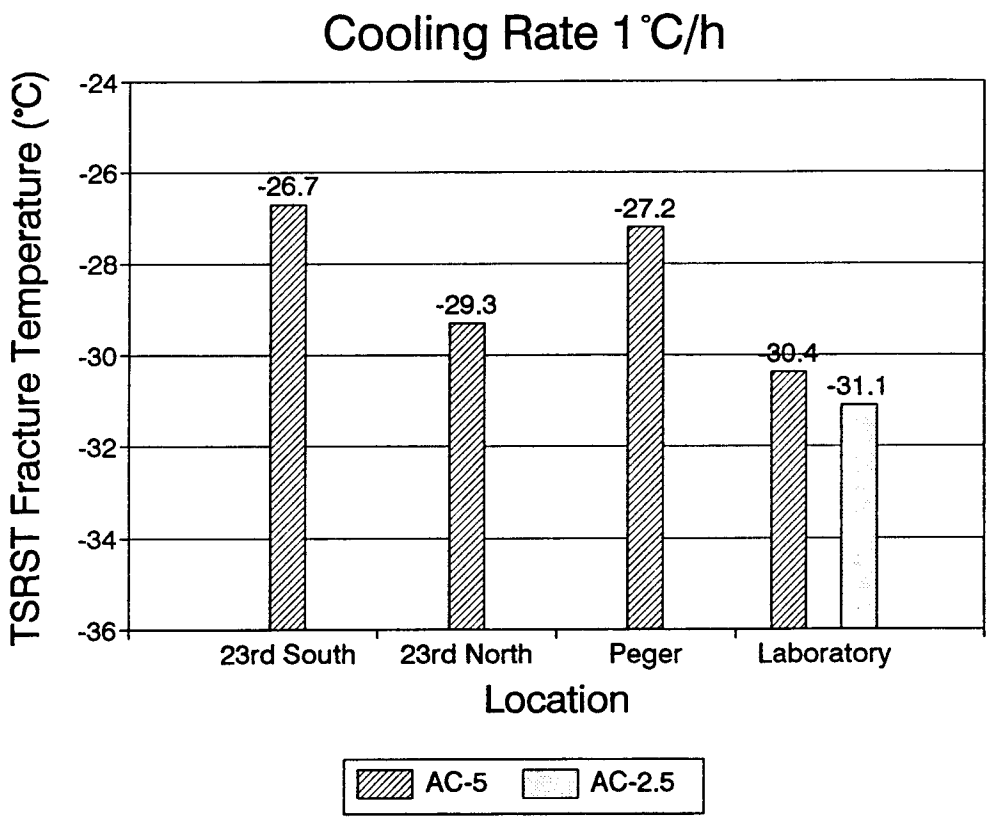

Figure 3.1 TSRST fracture temperatures for Alaska test sections

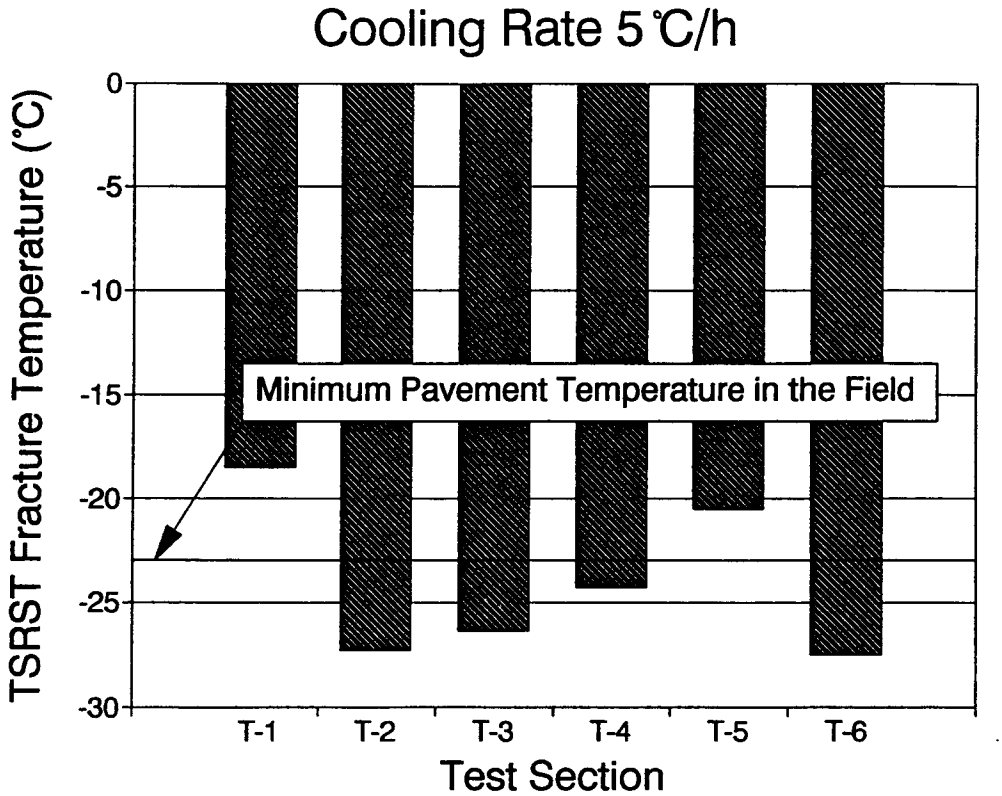

Figure 3.2 **TSRST fracture temperatures and minimum pavement temperature for Pennsylvania test sections**

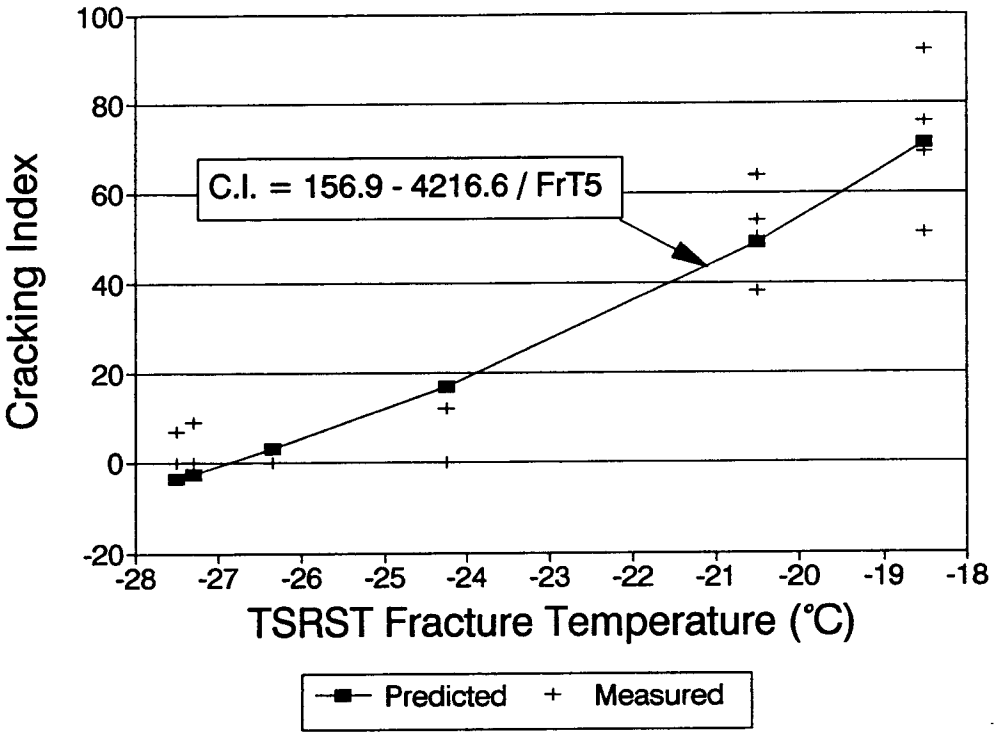

Figure 3.3 **Cracking index versus TSRST fracture temperature for Pennsylvania test sections**

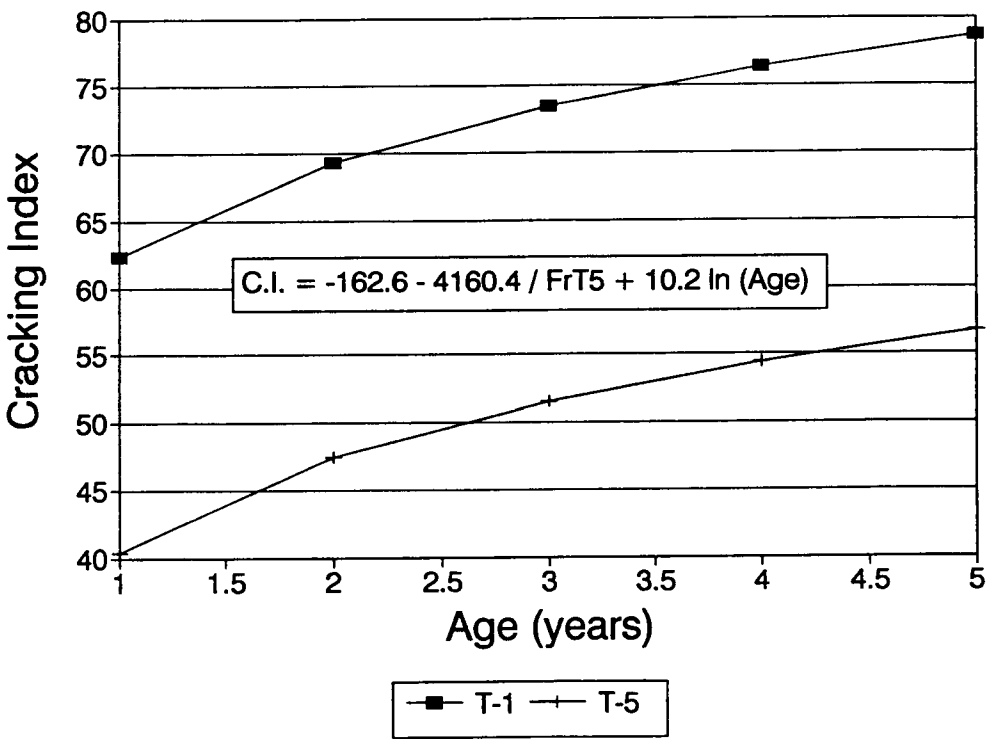

Figure 3.4 **Predicted cracking index versus time for Pennsylvania sections T-1 and T-5**

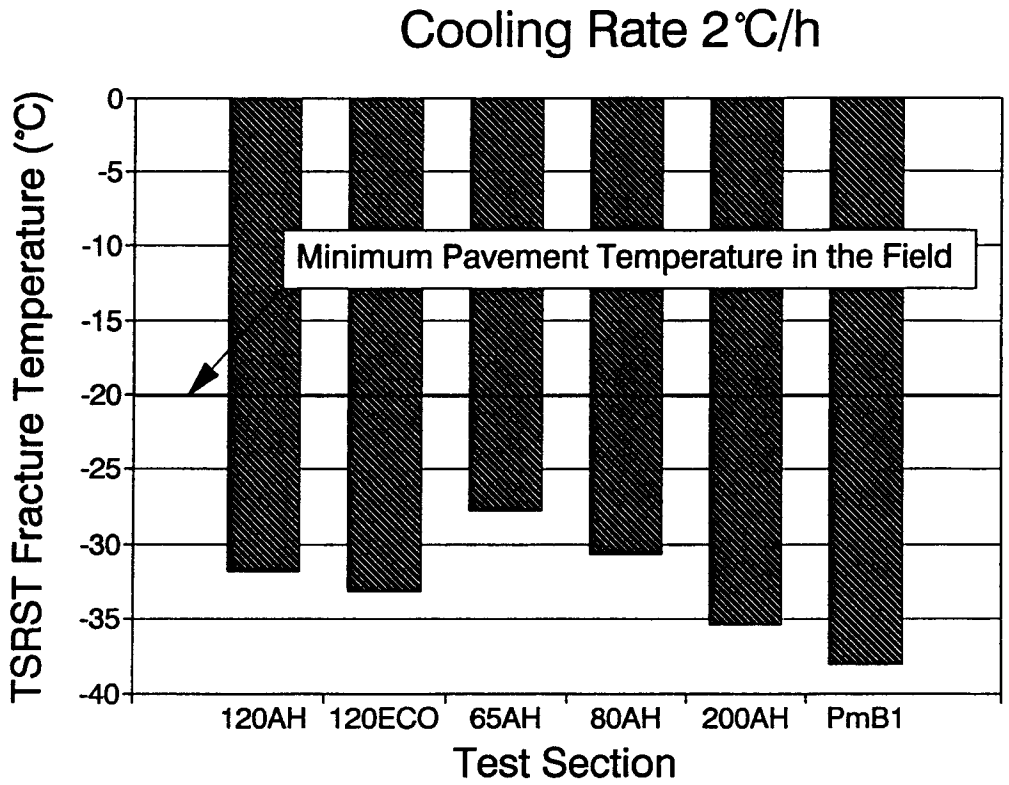

Figure 3.5 **TSRST fracture temperatures and minimum pavement temperature for Peraseinajoki test sections**

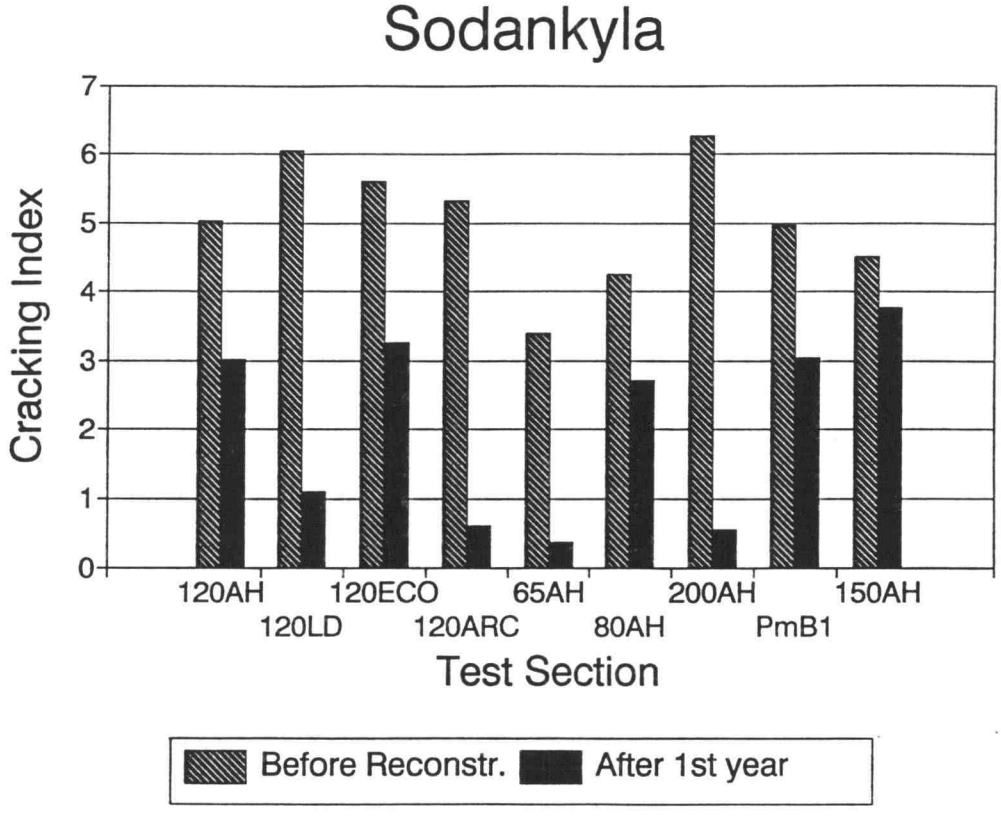

Figure 3.6 **Cracking frequency before reconstruction and after first year for Sodankyla test sections**

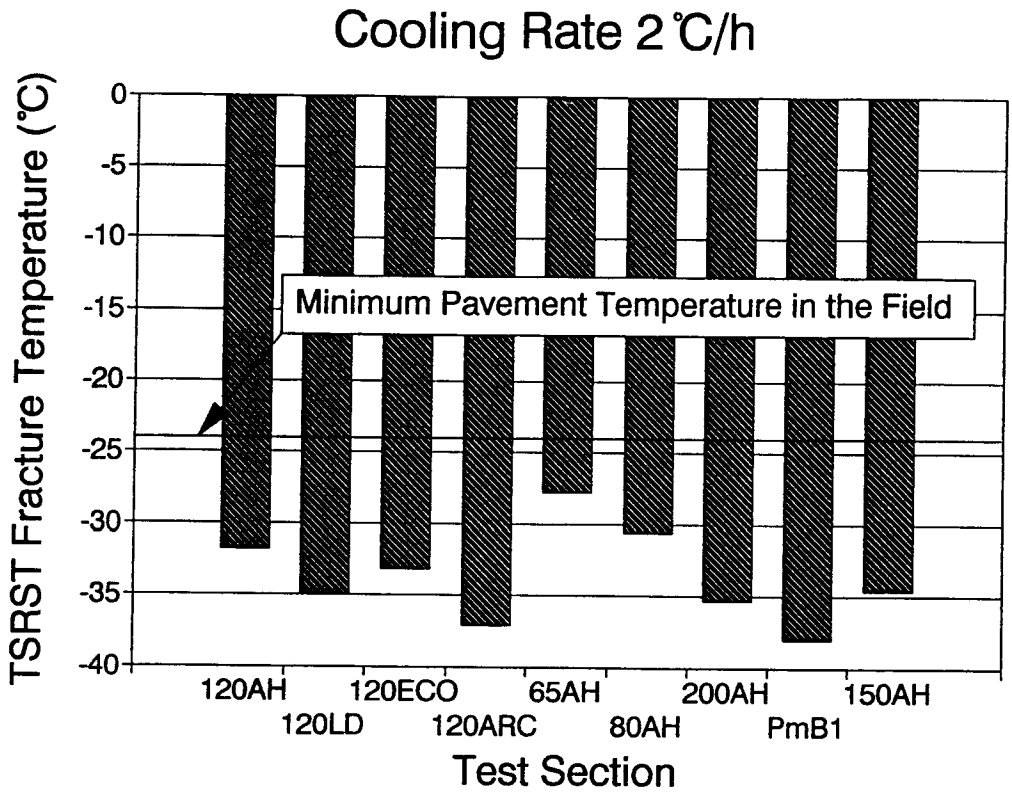

Figure 3.7 **TSRST fracture temperatures and minimum pavement temperature for Sodankyla test sections**

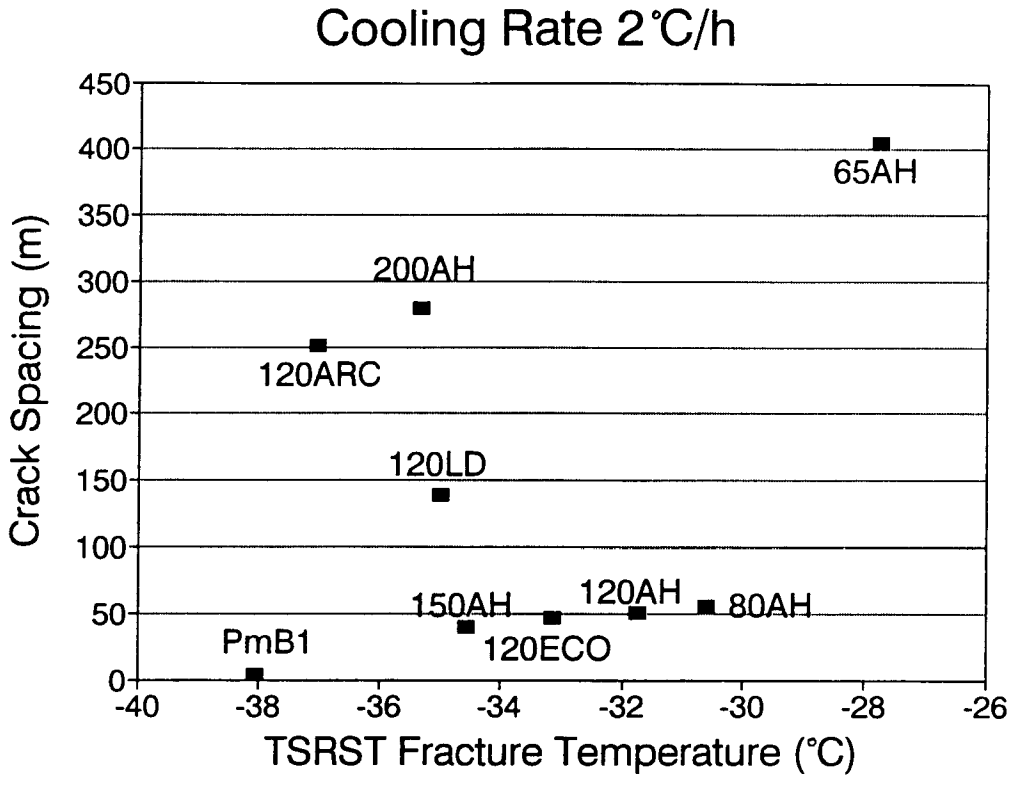

Figure 3.8 **Crack spacing versus TSRST fracture temperature for Sodankyla test sections**

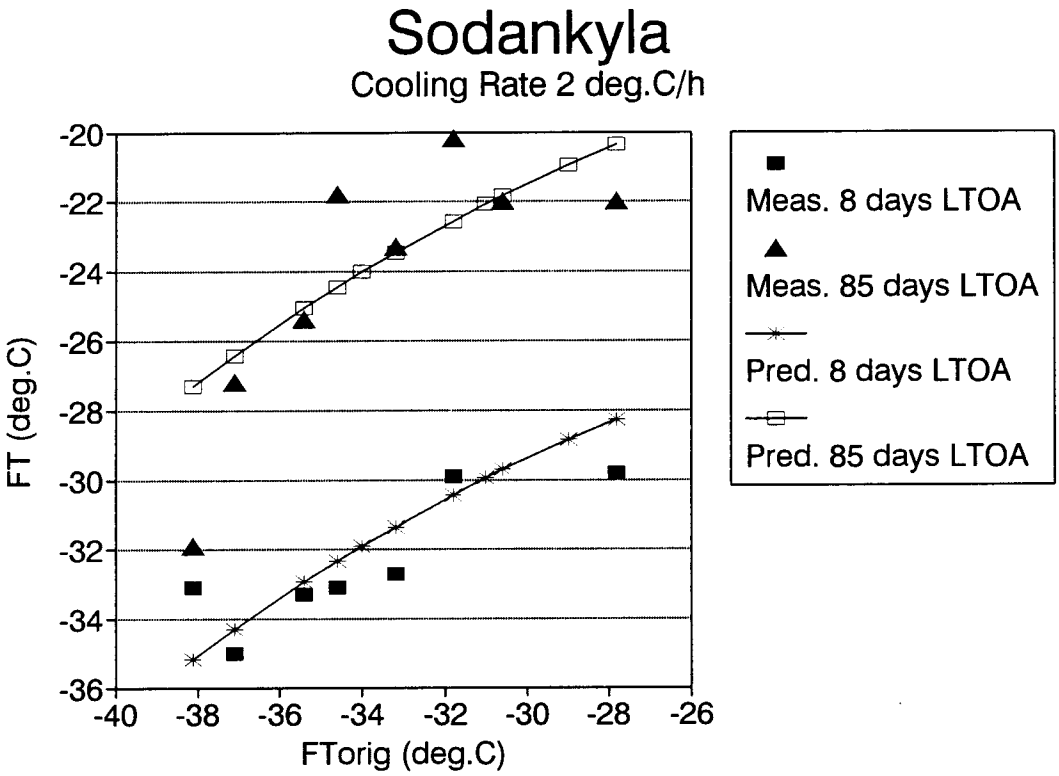

Figure 3.9 **Fracture temperature of aged specimens versus original fracture temperature with two degrees of Long Term Oven Aging for Sodankyla test sections**

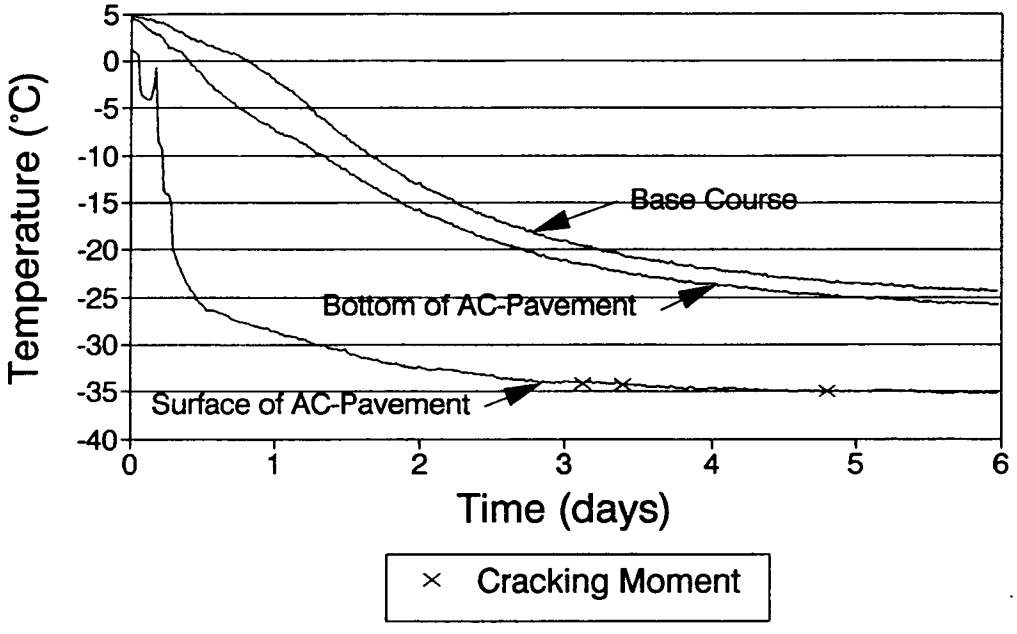

Figure 3.10 Temperature profile for USACRREL section Ib at station -11.6

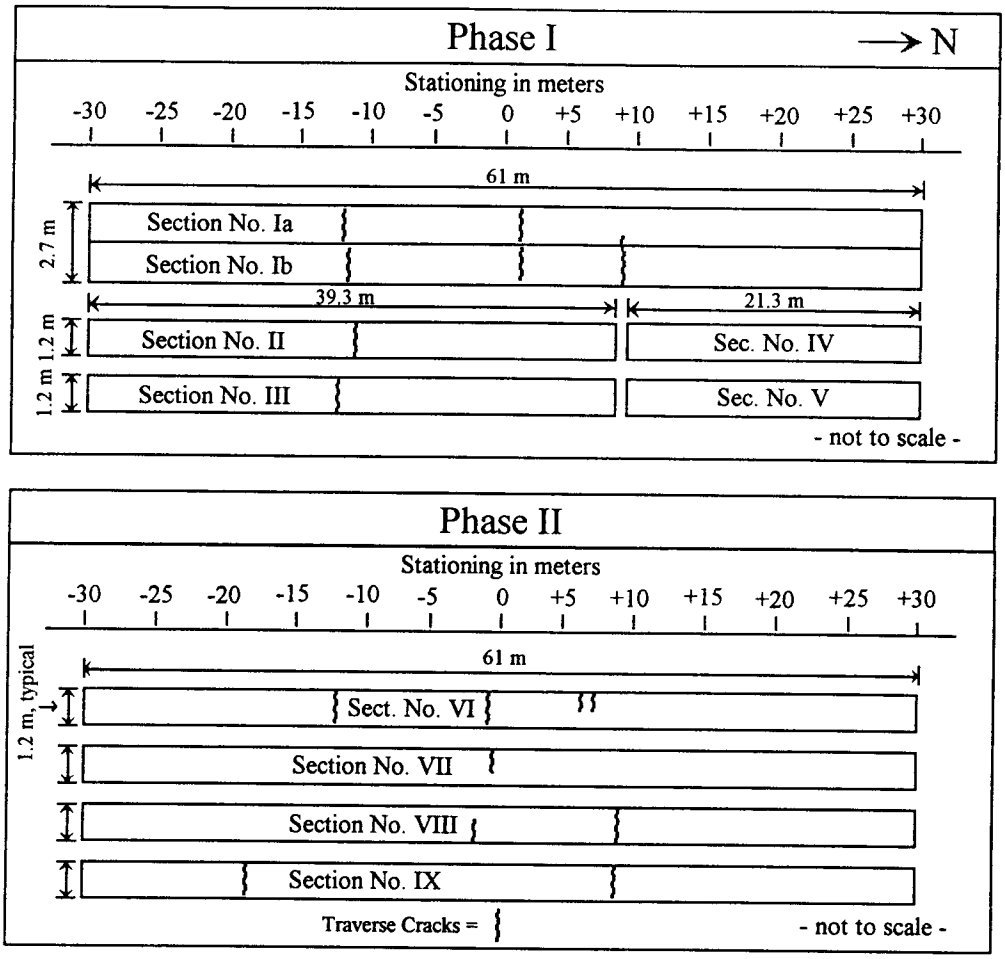

Figure 3.11 Crack map for USACRREL test sections

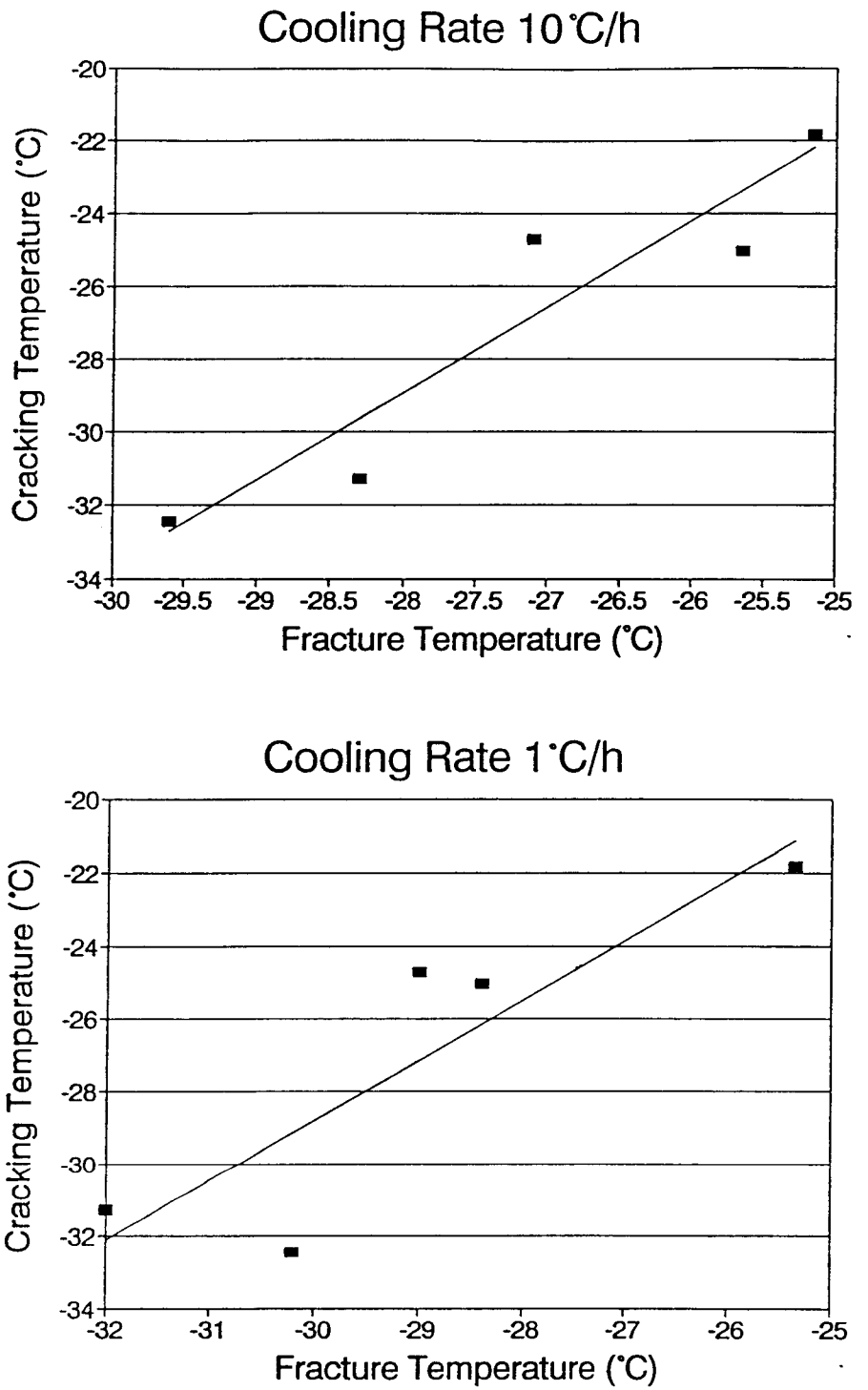

Figure 3.12 Cracking temperature versus TSRST fracture temperature for non-aged USACRREL laboratory samples

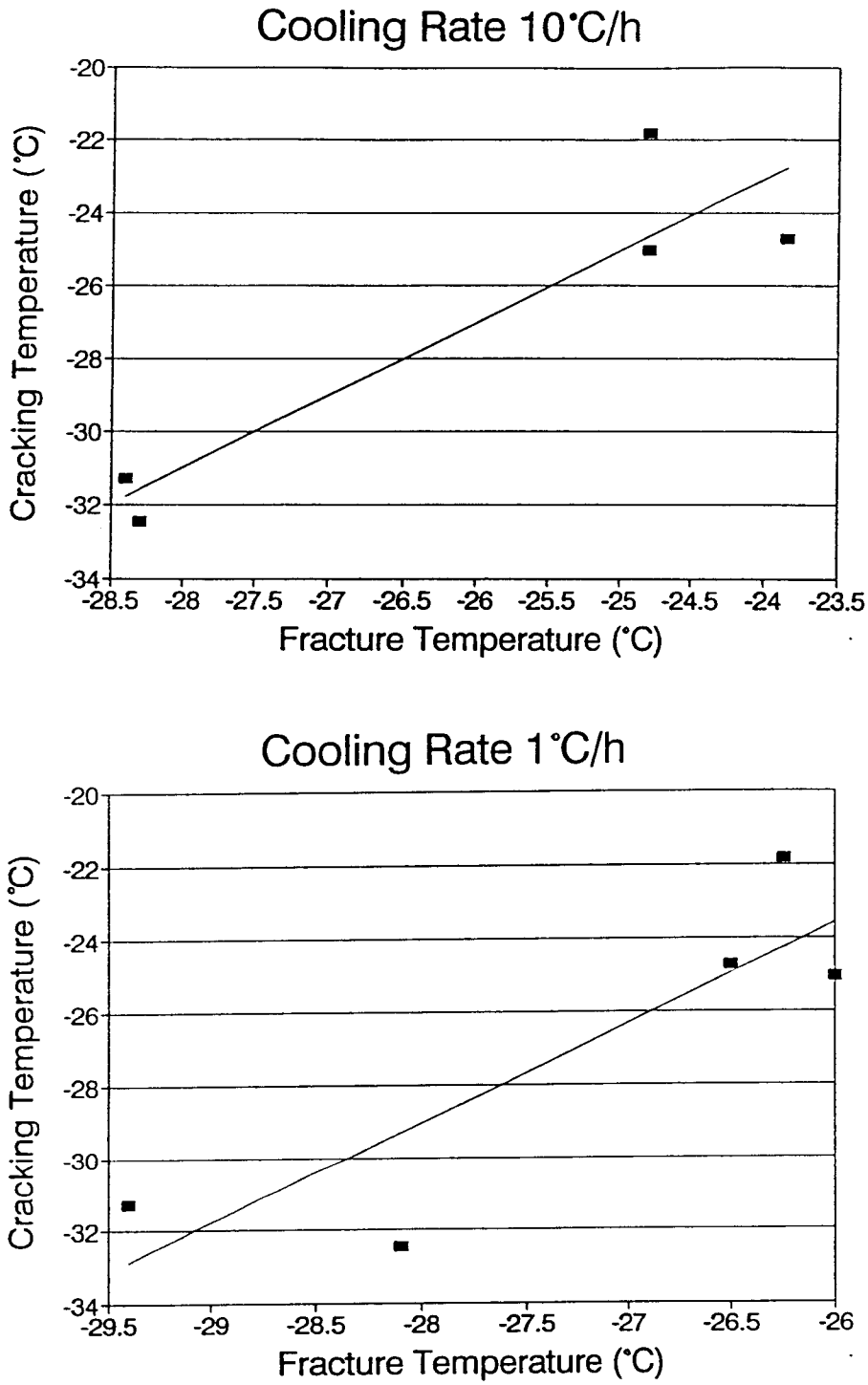

Figure 3.13 Cracking temperature versus TSRST fracture temperature for Short Term Oven Aged USACRREL laboratory samples

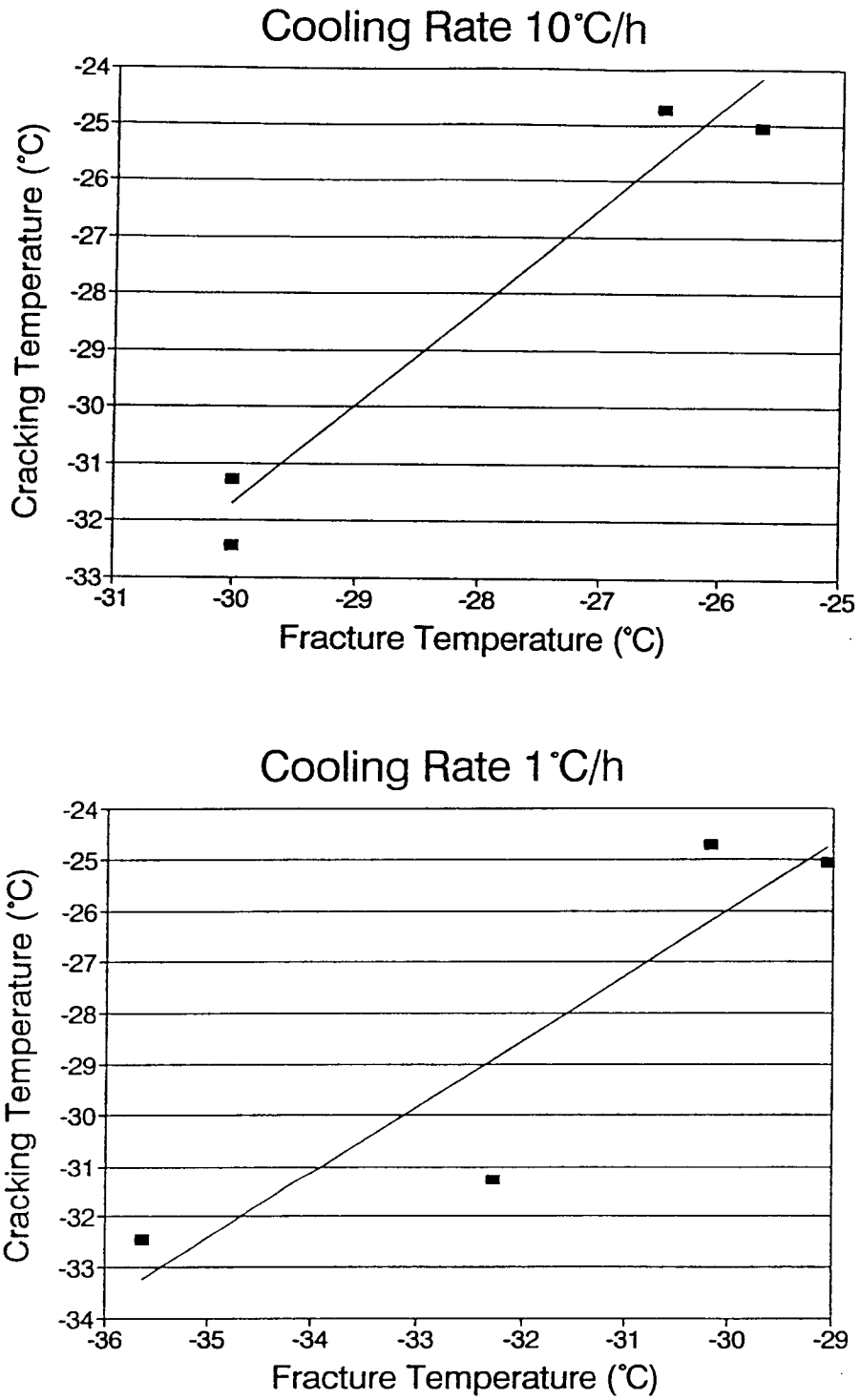

Figure 3.14 **Cracking temperature versus TSRST fracture temperature for USACRREL field samples**

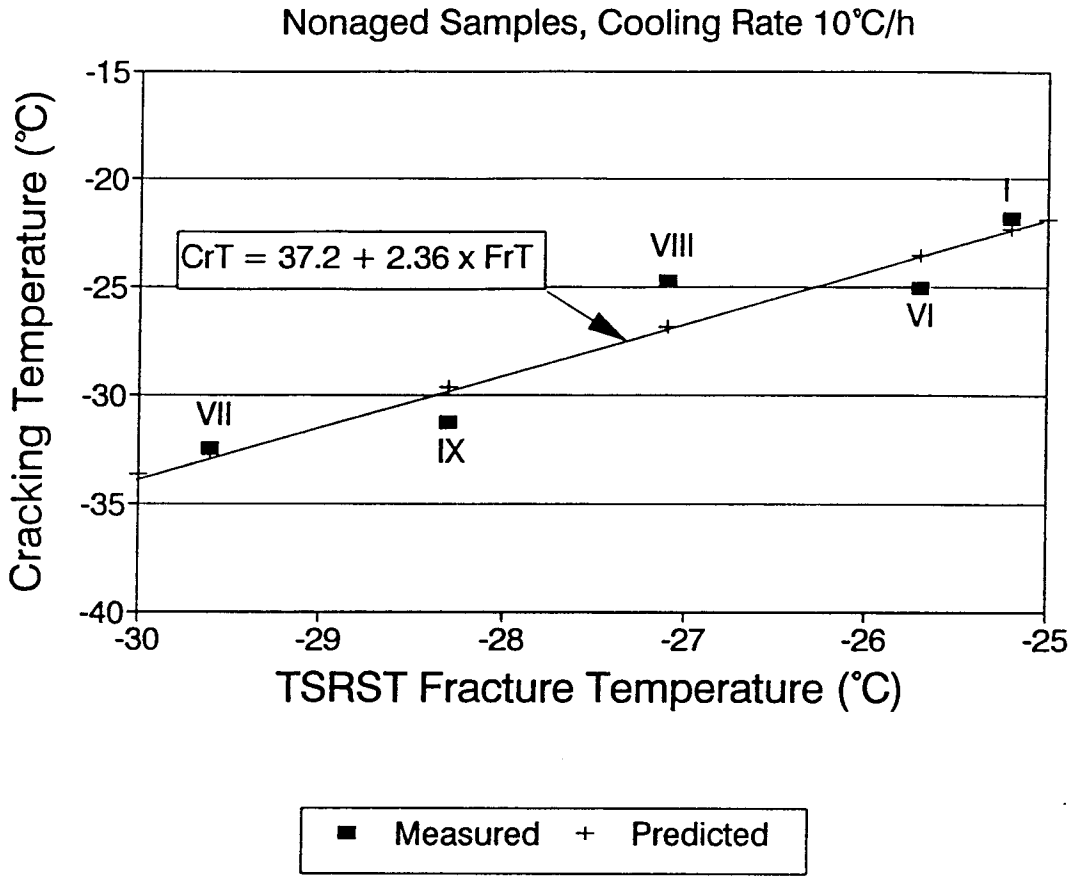

Figure 3.15 Predicted cracking temperatures for USACRREL test sections

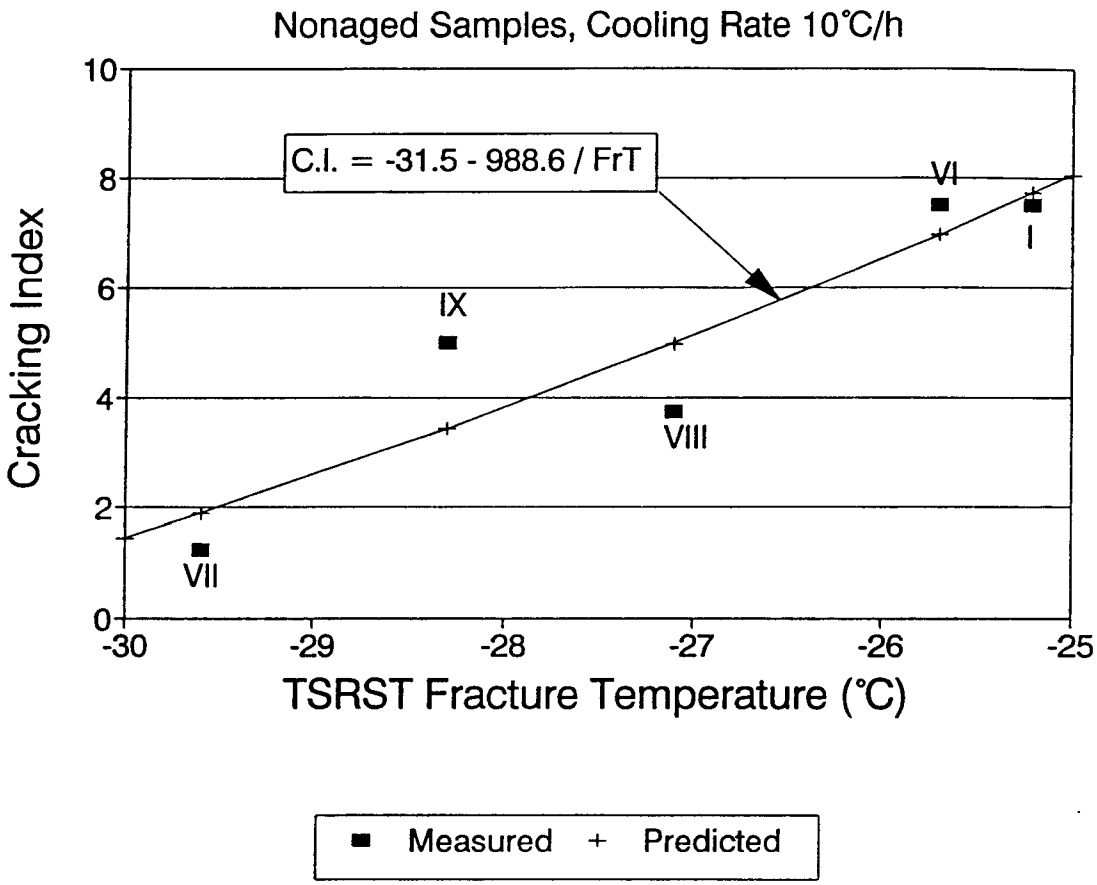

Figure 3.16 Predicted cracking index for USACRREL test sections

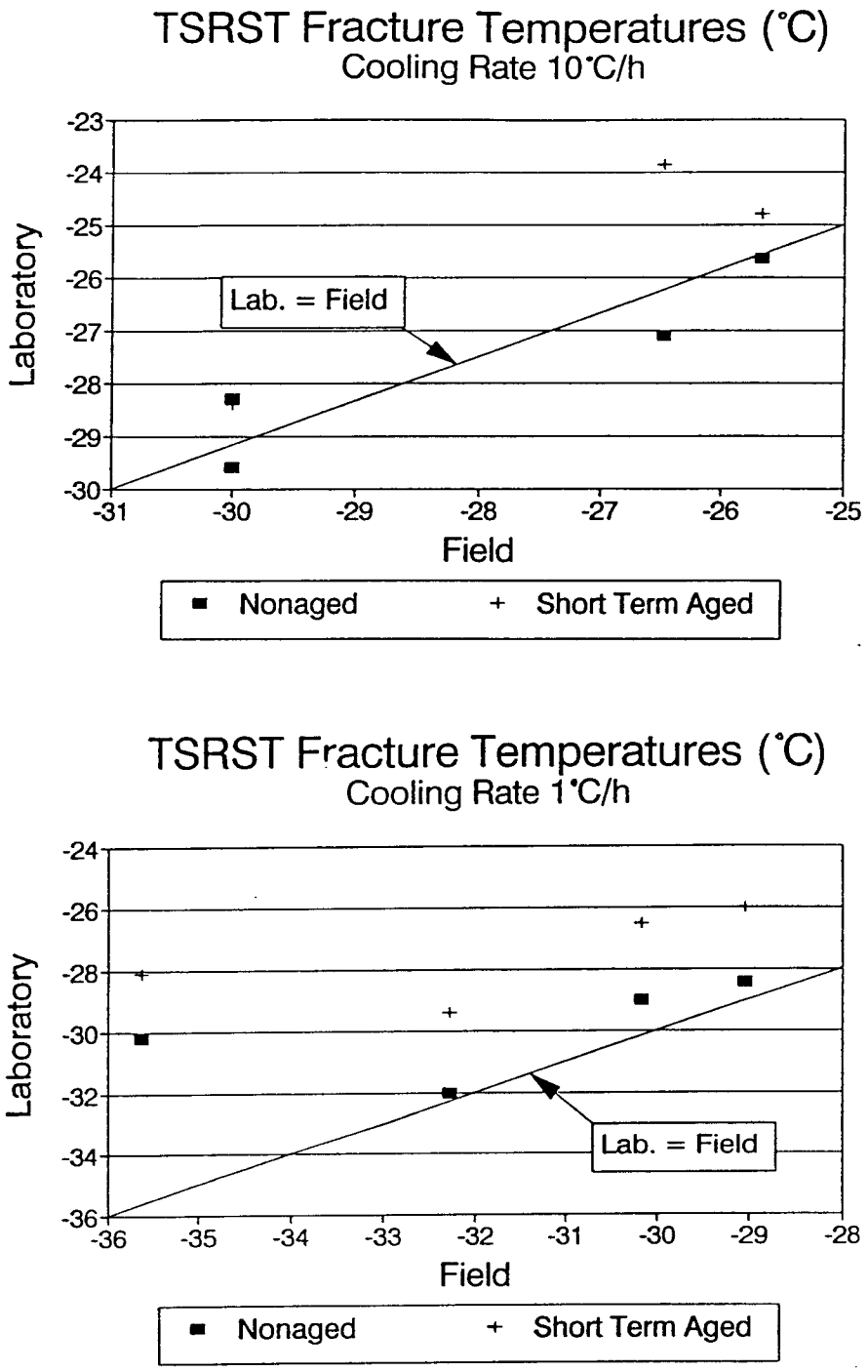

Figure 3.17 TSRST fracture temperatures of laboratory samples versus field samples for USACRREL test sections

Table 3.1 Summary of TSRST results for Alaska sections

Laboratory samples

Asphalt Cement	Mean Voids/ Std. Dev. (VPAR) (%)	Mean Fracture Stress/ Std. Dev. (kPa)	Mean Fracture Temperature/ Std. Dev. (°C)	Number of Observations
Cooling Rate 10°C/h				
AC-5	2.2/1.1	3522/500	-25.8/2.3	4
AC-2.5	3.0/0.7	3708/1231	-28.2/2.9	4
Cooling Rate 1°C/h				
AC-5	2.7/0.8	4708/147	-30.4/1.0	2
AC-2.5	2.6/0.2	4220/234	-31.1/0.1	2

Field samples

Asphalt Cement	Mean Voids/ Std. Dev. (VPAR) (%)	Mean Fracture Stress/ Std. Dev. (kPa)	Mean Fracture Temperature/ Std. Dev. (°C)	Number of Observations
Cooling Rate 1°C/h				
23rd South	4.5/0.6	2738/965	-26.7/1.4	2
23rd North	5.4/1.4	3247/133	-29.3/0.1	2
Peger Tr.	3.0/0.4	3131/260	-27.2/1.3	4
Peger Par.	2.5/0.2	3423/230	-27.4/1.5	4

Tr. = samples were taken transversely to the direction of traffic
Par. = samples were taken parallel to the direction of traffic

Table 3.2 Cracking index with time for Pennsylvania test sections

	Section I.D.					
Year	**T-1**	**T-2**	**T-3**	**T-4**	**T-5**	**T-6**
1977	51	0	0	0	38	0
1978	69	0	0	0	50	0
1979	76	-	-	-	54	-
1981	92	9	0	12	64	7

Cracking Index = (Full + 1/2 × Half + 1/4 × Partial)Cracks / 500 ft

Table 3.3 Summary of TSRST results for Pennsylvania test sections

Asphalt Cement	**Mean Voids/ Std. Dev. (VPAR) (%)**	**Mean Fracture Stress/ Std. Dev. (kPa)**	**Mean Fracture Temperature/ Std. Dev. (°C)**	**Number of Observations**
Cooling Rate 10°C/h				
T-1	1.5	3645	-19.3	1
T-2	0.4/0.5	3211/172	-22.7/0.1	2
T-3	1.4/0.7	3887/431	-24.0/1.3	2
T-4	1.9/0.1	4102/227	-25.4/0.3	2
T-5	2.8/1.1	3840/96	-19.8/0.5	2
T-6	0.7/0.2	4619/408	-26.9/0.9	2
Cooling Rate 5°C/h				
T-1	1.7	2396	-18.5	1
T-2	0.3/0.3	4689/166	-27.3/0.0	2
T-3	1.3/0.4	4462/137	-26.3/0.5	2
T-4	1.7/0.5	3673/840	-24.3/1.2	2
T-5	1.0/1.0	3942/174	-20.5/0.1	2
T-6	0.8/0.4	4655/2	-27.5/0.6	2

Table 3.4 **Summary of TSRST results for Peraseinajoki sections (adapted from Sodankyla TSRST results)**

Asphalt Cement	Mean Voids/ Std. Dev. (VPAR) (%)	Mean Fracture Stress/ Std. Dev. (kPa)	Mean Fracture Temperature/ Std. Dev. (°C)	Number of Observations
Cooling Rate 10°C/h				
BIT120AH	1.6/0.1	1962/845	-31.3/1.0	2
BIT120ECO	1.2/0.1	3607/720	-28.9/2.7	2
BIT65AH	1.6/0.2	3369/879	-28.4/1.1	2
BIT80AH	1.5/0.1	2768/33	-27.8/1.6	2
BIT200AH	2.0/0.4	4425/48	-33.9/0.2	2
PmB1	2.2/0.7	5730/300	-36.3/0.4	2
Cooling Rate 2°C/h				
BIT120AH	1.3/0.2	3499/524	-31.8/1.3	2
BIT120ECO	1.6/0.3	4015/65	-33.2/0.3	2
BIT65AH	2.0/0.5	3606/158	-27.8/0.8	2
BIT80AH	1.2	3524	-30.6	1
BIT200AH	1.4/0.1	4158/356	-35.4/0.4	2
PmB1	1.6/0.3	5566/90	-38.1/0.2	2

Table 3.5 Summary of crack observations for Sodankyla test sections

Asphalt Cement	Length of Section (m)	Number of Cracks	Crack Spacing (m)	Air Cracking Temperature (°C)	Pavement Cracking Temperature (°C)
BIT120AH	759	15	47.44	-30.0	-19.5
B120LD	1386	10	126.0	-33.0	-24.5
BIT120ECO	842	18	44.31	-25.0	-20.0
BIT120ARC	1258	5	209.7	-32.5	-22.5
BIT65AH	405	1	202.5	-20.0	-17.0
BIT80AH	394	7	49.25	-28.5	-22.5
BIT200AH	559	2	279.5	-32.5	-22.5
PmB1	400	8	44.44	-24.0	-18.0
BIT150AH	607	15	37.94	-33.0	-24.5

Cracking Temperature = Coldest observed temperature before the first crack observation.

Table 3.6 Summary of TSRST results for Sodankyla test sections

Non-aged samples

Asphalt Cement	Mean Voids/ Std. Dev. (VPAR) (%)	Mean Fracture Stress/ Std. Dev. (kPa)	Mean Fracture Temperature/ Std. Dev. (°C)	Number of Observations
Cooling Rate 10°C/h				
BIT120AH	1.6/0.1	1962/845	-31.3/1.0	2
B120LD	1.1/0.2	4009/531	-31.6/0.0.	2
BIT120ECO	1.2/0.7	3607/720	-28.9/2.7	2
BIT120ARC	-	4772/424	-35.8/0.3	2
BIT65AH	1.6/0.2	3369/880	-28.4/1.1	2
BIT80AH	1.5/0.1	2768/33	-27.8/1.6	2
BIT200AH	2.0/0.3	4425/48	-33.9/0.2	2
PmB1	2.2/0.7	5730/300	-36.3/0.4	2
BIT150AH	1.2/0.0	4125/408	-35.3/2.7	2
Cooling Rate 2°C/h				
BIT120AH	1.3/0.2	3499/524	-31.8/1.3	2
B120LD	1.6/0.3	4080/585	-35.0/1.4	2
BIT120ECO	1.6/0.1	4015/65	-33.2/0.3	2
BIT120ARC	1.1/0.0	4620/165	-37.1/0.1	2
BIT65AH	2.0/0.5	3606/158	-27.8/0.8	2
BIT80AH	1.2	3524	-30.6	1
BIT200AH	1.4/0.1	4158/356	-35.4/0.3	2
PmB1	1.6/0.3	5566/90	-38.1/0.2	2
BIT150AH	1.5/0.1	3250/1233	-34.6/2.5	2

Table 3.6 (continued) Summary of TSRST results for Sodankyla test sections

Long Term Oven Aged samples

Asphalt Cement	Mean Voids/ Std. Dev. (VPAR) (%)	Mean Fracture Stress/ Std. Dev. (kPa)	Mean Fracture Temperature/ Std. Dev. (°C)	Number of Observations
Cooling Rate 2°C/h				
8 days of LTOA				
BIT120AH	0.6/0.2	3723/52	-29.9/.4	2
B120LD	0.6	3196	-30.5	1
BIT120ECO	1.0/0.1	3254/171	-32.7/3.5	2
BIT120ARC	1.3/0.2	3676/605	-35.0/0.1	2
BIT65AH	1.6	2994	-29.8	1
BIT80AH	-	-	-	0
BIT200AH	1.1/0.3	3223/390	-33.3/1.8	2
PmB1	1.5/0.0	4124/861	-33.1/4.1	2
BIT150AH	1.2/0.0	3446/155	-33.1/1.0	2
85 days of LTOA				
BIT120AH	0.9/0.7	2690/159	-20.2/0.3	2
B120LD	0.9/0.0	2864/128	-22.3/0.7	2
BIT120ECO	1.5	2758	-23.3	1
BIT120ARC	1.0	2021	-27.2	1
BIT65AH	1.1/0.0	3300/131	-22.0/1.4	2
BIT80AH	1.4/0.4	2448/536	-22.0/1.2	2
BIT200AH	0.3/0.4	2873/697	-25.4/1.3	2
PmB1	0.5	4671	-31.9	1
BIT150AH	0.4	2306	-21.8	1

Table 3.7 Recorded crack observations for USACRREL test sections

Section I.D.	Station	Julian Day	Time	Surface Temperature (°C)	Bottom Temperature (°C)
Ia	-11.6	221	3:45	-36.6	-29.9
		220	3:15	-36.3	-27.2
Ia	+0.8	220	2:45	-35.0	-27.0
		220	11:45	-35.2	-28.2
		220	3:15	-34.8	-27.0
Ib	-11.6	220	12:00	-35.2	-22.7
		222	4:15	-36.1	-25.9
		220	18:30	-35.3	-23.5
Ib	+0.8	220	8:44	-35.9	-22.2
		220	22:30	-36.2	-23.9
		220	5:00	-35.9	-21.8
Ib	+9.1	219	2:20	-35.6	-23.9
		220	20:30	-36.2	-26.9
VI	-12.8	272	1:10	-34.6	-25.1
		272	1:10	-32.1	-25.4
VI	0	273	1:30	-33.3	-26.6
		273	10:30	-34.4	-26.6
		273	11:30	-34.3	-26.6
		274	3:45	-33.9	-26.6
		274	9:00	-34.0	-26.6
VII	+0.6	284	19:30	-32.6	-32.4
		286	1:00	-33.2	-32.7
VIII	0	293	2:10	-36.2	-31.1
		293	2:00	-36.4	-31.1
		292	20:45	-34.8	-29.6
VIII	+9.1	291	4:15	-32.7	-24.7
IX	-18.3	294	1:00	-36.4	-31.3
IX	+9.1	298	2:30	-36.6	-32.7

Table 3.8 Summary of crack observations for USACRREL test sections

Section I.D.	Asphalt Cement	Number of Cracks		Cracking Index	Cracking Temp. at Bottom (°C)	Cracking Temp. at Surface (°C)
		Full	Half			
I	United AC-20	3	0	7.50	-21.8	-35.9
VI	Viking AC-20	2	2	7.50	-25.1	-34.6
VII	Cibro AC-20	0	1	1.25	-32.4	-32.6
VIII	Petro C. AC-20	1	1	3.75	-24.7	-32.7
IX	Viking AC-10	2	0	5.00	-31.3	-36.6

Table 3.9 Summary of TSRST results for USACRREL test sections

Non-aged laboratory samples

Asphalt Cement	Mean Voids/ St.Dev. (VPAR) (%)	Mean Fracture Stress/ Std. Dev. (kPa)	Mean Fracture Temperature/ Std. Dev. (°C)	Number of Observations
Cooling Rate 10°C/h				
United AC-20	3.7/0.7	2924/166	-25.2/0.2	2
Viking AC-20	1.7/0.1	2847/521	-25.7/1.5	2
Cibro AC-20	5.9/0.8	2675/45	-29.6/0.3	2
Petro C AC-20	3.8/1.1	2628/1	-27.1/1.4	2
Viking AC-10	5.7/1.4	3034/1049	-28.3/1.7	2
Cooling Rate 1°C/h				
United AC-20	3.1/1.1	2142/264	-25.4/1.9	2
Viking AC-20	2.0/0.5	2678/136	-28.4/0.0	2
Cibro AC-20	3.8/0.1	2182/277	-30.2/0.4	2
Petro C AC-20	3.4	2798	-29.0	1
Viking AC-10	5.8/0.1	2142/190	-32.0/0.4	22

Table 3.9 (continued) **Summary of TSRST results for USACRREL test sections**

Short Term Oven Aged laboratory samples

Asphalt Cement	Mean Voids/ Std.Dev. (VPAR) (%)	Mean Fracture Stress/ Std. Dev. (kPa)	Mean Fracture Temperature/ Std. Dev. (°C)	Number of Observations
Cooling Rate 10°C/h				
United AC-20	5.9/0.9	2410/28	-24.8/0.4	2
Viking AC-20	5.0/1.0	1741/564	-24.8/0.7	2
Cibro AC-20	6.0/1.3	2063/62	-28.3/0.4	2
Petro C. AC-20	3.4/0.3	2517/58	-23.9/0.6	2
Viking AC-10	6.9/1.0	2115/156	-28.4/1.8	2
Cooling Rate 1°C/h				
United AC-20	5.8/0.5	2375/193	-26.3/0.5	2
Viking AC-20	4.6/2.3	2551/445	-26.0/1.4	2
Cibro AC-20	4.4/1.3	2054/947	-28.1/0.8	2
Petro C. AC-20	5.0/0.3	2514/12	-26.5/0.0	2
Viking AC-10	5.6/0.6	1895/265	-29.4/1.0	2

Table 3.9 (continued) **Summary of TSRST results for USACRREL test sections**

Field samples

Asphalt Cement	Mean Voids (VPAR) (%)	Mean Fracture Stress/ Std. Dev. (kPa)	Mean Fracture Temperature/ Std. Dev. (°C)	Number of Observations
Cooling Rate 10°C/h				
Viking AC-20	4.7/0.8	2709/936	-25.7/0.9	4
Cibro AC-20	5.6/0.2	2232/374	-30.0/2.3	4
Petro C. AC-20	5.2/0.3	2604/335	-26.5/1.4	4
Viking AC-10	8.2/1.0	2107/591	-30.0/1.4	3
Cooling Rate 1°C/h				
Viking AC-20	8.60/0.3	2026/291	-29.1/1.5	4
Cibro AC-20	6.3/0.2	1897/606	-35.6/2.3	3
Petro C. AC-20	5.0/1.0	1916/440	-30.2/2.0	4
Viking AC-10	7.6/0.6	1854/451	-32.3/0.8	4

Table 3.10 Results of regression analysis for USACRREL experiment

Aging	Cooling Rate (°C/h)	Origin	b_0	b_1	p-value	R^2 (%)	Std. Error of Est.
Non-aged	10	Laboratory	37.16	2.36	0.018	88	1.80
Non-aged	1	Laboratory	20.70	1.65	0.050	77	2.53
Short Term	10	Laboratory	24.20	1.97	0.026	85	2.04
Short Term	1	Laboratory	47.40	2.73	0.059	75	2.65
Non-aged	10	Field	20.50	1.74	0.023	96	1.05
Non-aged	1	Field	12.73	1.29	0.088	83	2.04

Regression Model: Mean{CT} = $b_0 + b_1$ FT

4 MODEL TO PREDICT LOW TEMPERATURE CRACKING

The severity of low temperature cracking is directly related to the spacing between the cracks. A deterministic model is developed to predict the crack spacing as a function of time. In addition, a probabilistic model is developed to *(1)* predict the crack spacing and its variation as a function of time, and, *(2)* the reliability of the design with respect to a minimum acceptable spacing criterion defined by road authorities. To predict the crack spacing, the following factors must be considered:

- the prediction of the field aging of asphalt concrete pavements based on a laboratory aging procedure,

- the effect of aging on the TSRST fracture temperature and fracture strength,

- the relationship between the TSRST fracture temperature and the cracking temperature in the field,

- the relationship between the TSRST fracture strength and the temperature dependent tensile strength of the pavement,

- the estimation of the pavement temperature with air temperature, and

- the estimation of the restraint conditions between the asphalt concrete pavement and the base course.

Following the development of the relationships listed above, the crack spacing is calculated based on the theory that the pavement slab cracks when the pavement temperature reaches the cracking temperature of the mixture and the slab is fully restrained in the vicinity of a potential crack. The approach employed in the development of the deterministic and probabilistic models is discussed in the following paragraphs.

4.1 Prediction of Field Aging with Degree of Oven Aging

Data collected by Bell et al. (1993) and Wieder et al. (1993) were used to develop a relationship between the LTOA and the field aging. A comprehensive LTOA program was performed for seven sites and, therefore, these sites were selected for the development of the model to predict the degree of field aging. The seven sites are located in Washington state and range from three to eighteen years in age. A summary of each site is given in Table 4.1.

Laboratory fabricated cylindrical samples were conditioned for at least twenty four hours in an environmental cabinet at 25°C. The resilient modulus (M_r) of each sample was determinated under repeated diametral loading according to ASTM D 4123. The same procedure was conducted for 102 mm diameter field

cores, which were obtained from the wheel paths and between the wheel paths during 1991. A detailed procedure for sample preparation and testing is given by Wieder et al. (1993).

The moduli of the laboratory fabricated samples were measured for the LTOA specimens after zero, two, four, and eight days following the 4-h STOA treatment. Moduli for the control specimens (non-aged) were also obtained.

The diametral moduli with the degree of LTOA for the laboratory specimens and the field modulus for each site are given in Table 4.2. The LTOA for zero days in Table 4.2 represents the modulus of the control specimen (non-aged). A single regression analysis was performed for each site to model the increase in the resilient modulus with the degree of LTOA. This was accomplished to determine the corresponding degree of LTOA for each site with a given field modulus. The following model was chosen to represent the relationship based on the smallest error of Y estimate for the combined data set:

$$\text{Mean}\{\text{Mod}\} = b_0 + b_1 (\text{LTOA})^{.5} \qquad (4.1)$$

in which,

Mod = diametral resilient modulus (ksi = 6894.76 kPa),

LTOA = degree of LTOA (days).

The least square estimators (b_0 and b_1), coefficient of determination (R^2) and error of Y estimate for each analysis are given in Table 4.3. The value of the field

modulus for each site was substituted into the relating equation and the time (degree of LTOA) was determined. The time is termed "equivalent days of LTOA,". It gives the number of LTOA days required to achieve the modulus in the field (for the in service aged pavement). The "equivalent days of LTOA" are given in Table 4.3. Note that all the "equivalent days of LTOA" that are greater than eight, are obtained by extrapolation. Further experimentation should be performed with longer LTOA times to confirm the relationship between the LTOA and in service aging. An example of the measured diametral resilient moduli versus the degree of LTOA with the single regression model is presented in Figure 4.1.

To investigate the relationship between the field aging and LTOA, the age of the field samples (at the moment of the modulus determination) versus the "equivalent days of LTOA" was plotted as shown in Figure 4.2. Two apparent groups of data points were observed in Figure 4.2. It was recognized, that one group consisted of sites in wet - no freeze climate and the other in dry - freeze climate. Based on this finding, two models were developed to predict the degree of field aging. A multiple regression analysis was performed to achieve the following model:

Model I

$$\text{Mean}\{AGE\} = 10.1 + 2.27\,(LTOA)^{.5} - 10.3\,(CLIMATE) \qquad (4.2)$$

S.E 0.707 0.231 0.545

p-value in two-sided t-test

0.0001 0.0001 <0.00001

R^2 = 99.1%, Error of Y Estimate = 0.71, df = 4,

in which,

AGE = degree of field aging (years),

LTOA = degree of LTOA (days), and

CLIMATE = 0 for wet - no freeze climate and 1 for dry - freeze climate.

Model I, with the measured data points, is plotted in Figure 4.3. The model is valid from three to nine days of LTOA for wet - no freeze climate and from one to twenty-three days of LTOA for dry - freeze climate. There is conclusive evidence that the degree of LTOA and the climate zone are associated with the degree of the field aging (p-values at two-sided t-test are <0.01). The decreasing effect of cold climate on aging is logical, since aging of the asphalt pavements is increased with warmer temperatures.

The model gives about 10 years of field aging corresponding to zero days of LTOA for wet - no freeze climate, which is a concern even if the model is not valid at this time range. The following model was developed to counter this problem:

Model II

$$\text{Mean}\{AGE\} = 11.3 + (3.20)\ln(LTOA) - 9.42\ (CLIMATE) \qquad (4.3)$$

S.E.	1.09	0.475	0.929
p-value in two-sided t-test			
	0.0005	0.0025	0.0005

R^2 = 97.4%, Error of Y Estimate = 1.22, df = 4

in which,

AGE = degree of field aging (years),

LTOA = degree of LTOA (days), and

CLIMATE = 0 for wet - no freeze climate and 1 for dry - freeze climate.

Model II, with the measured data points, is given in Figure 4.4. Here, too, the model is valid from three to nine days of LTOA for wet - no freeze climate and from one to twenty-three days of LTOA for dry - freeze climate. Again, there is conclusive evidence that the natural logarithm of the degree of LTOA and the climate zone are associated with the degree of the field aging (p-values at two-sided t-test are <0.01).

Based on the modeling effort to compare aging in service with LTOA the following conclusions are appropriate:

- The data for the models were collected from one state and from two climate zones. In addition, both models are influenced by the

extrapolated values for LTOA. More data are required to establish a model for nationwide use.

- There may be variables in addition to the climate zone affecting the degree of field aging.

- Model I gives a parabolic relationship between the degree of field aging and degree of LTOA. Statistically this model should be used to describe the data set based on the error of Y estimate. The model gives unreasonably high values for the degree of the field aging for LTOA less than three days.

- Model II gives a logarithmic relationship between the degree of field aging and degree of LTOA. The model gives satisfactory values for short LTOA periods but is statistically not as good as Model I based on the error of Y estimate. However, if p-values for the hypothesis that the explanatory variables are associated with the degree of field aging are considered, the model is acceptable.

- Based on these conclusions Model I is recommended for prediction of the degree of the field aging. Use of Model I is not recommended at degree of LTOA less than three days for wet - no freeze climate.

- If field aging for a degree of LTOA less than three days for a wet - no freeze climate is needed, Model II is recommended; caution must be exercised when using Model II since there are no actual data points for LTOA less than three days.

Since low temperature cracking is always associated with freezing climates, Model I will be used in the following paragraphs to predict the low temperature cracking.

4.2 Effect of Aging on TSRST Parameters

The fracture temperature becomes warmer as the mixture hardens by aging. The relationship derived in eqn. 3.6 for fracture temperature with LTOA will be used in the model:

$$FT = 1.03FT_{orig} + 1.15\sqrt{LTOA} \tag{4.4}$$

The relationship between the degree of LTOA (LTOA) and the field aging (AGE) from eqn. 4.2 (and substituting: Climate = 1) is as follows:

$$AGE = -0.19 + 2.27\sqrt{LTOA} \tag{4.5}$$

Solving for the square root of the degree of LTOA gives:

$$\sqrt{LTOA} = 0.44AGE - 0.08 \tag{4.6}$$

Substituting eqn. 4.6 into eqn. 4.4 yields the relationship between fracture temperature and the age of the pavement:

$$FT = 1.03FT_{orig} + 0.51AGE. \tag{4.7}$$

This relationship is illustrated in Figure 4.5.

As mentioned in Section 3.4.4, there is no evidence that the fracture strength is affected by aging. In the development of the model for low temperature cracking, the fracture strength is assumed to be constant with time. However, it is very important to check this assumption when more data are available.

The reason for constant fracture strength is explained by the effect of aging on both fracture temperature and strength of the mixture as shown in Figure 4.6. (The effect of aging on thermal stress was observed in the TSRST data for aged specimens, but the effect of aging on tensile strength presented in Figure 4.6 is assumed and requires further study.) Due to the hardening affect of aging, the relaxation of the thermal stress will be reduced and the thermal stress generation rate will be greater for an aged mixture than for a fresh mixture. Consequently, a higher stress will be achieved at a warmer temperature.

For a given asphalt concrete mixture, the tensile strength is dependent on loading rate and temperature. The strength increases as the temperature decreases until the "glass transition" temperature is achieved. Beyond this point the mixture becomes brittle, and the strength will decrease as the temperature decreases (re.

Figure 1.1). However, the mixture is not as temperature susceptible at temperatures colder than the glass transition point than at temperatures warmer than the glass transition point. As the mixture hardens due to aging, the glass transition point is assumed to occur at a warmer temperature. As shown in Figure 4.6, the strength will decrease at low temperatures as a result of aging, but at temperatures considerably warmer than the original glass transition point, the strength will increase.

The pavement will crack at the point where the thermal stress equals the strength of the mixture. Even if the fracture temperature is significantly increased by aging, the fracture strength may remain almost constant, since *(1)* the temperature susceptibility of the strength is small at temperatures colder than the glass transition point, *(2)* due to aging the glass transition point occurs at a warmer temperature, and *(3)* both the stress and the strength is affected by aging.

4.3 Relationship between TSRST and Field Conditions

The relationship between the TSRST fracture temperature and fracture strength and the actual cracking temperature and tensile strength in the field must be considered. The variables affecting the TSRST and the field parameters excluding aging, are restraint conditions, pavement geometry, temperature and the rate of temperature change.

The sample in the TSRST is fully restrained. If the pavement in the field is also fully restrained, the conditions could be considered equal for modeling purposes. In the laboratory, the sample is restrained at the ends whereas in the field the pavement is restrained at the bottom by the friction between the slab and the base course. If the friction force between the slab and the base course is great enough, the slab is fully restrained and the conditions can be considered equal in the TSRST and the field. This means that the thermal stress will be dependent only on mixture properties and the rate and magnitude of temperature change. If full restraint is not achieved, no cracking will occur because of the relaxation of the thermal stress due to the contraction of the pavement slab. Inadequate restraint conditions will occur near the edges of the pavement slab where the available friction force is small. The restraint conditions can, therefore, be considered equal in the TSRST and in the field, since cracking will occur only when the pavement slab is fully restrained. The restraint force can be estimated and it is possible to analyze (as shown later) if cracking will, or will not occur.

The geometry of a sample or a pavement affects the cooling of the mixture. In the TSRST, the cooling of the sample is three dimensional while the pavement in the field is cooled mainly from the top. Based on an analysis of the test results for the USACRREL experiment, cracking occurred due to the overall temperature distribution in the pavement layer and not the colder surface temperature. In addition, the asphalt pavement cracked through the entire depth of the slab. Consequently, it is assumed for the modeling effort that cracking will occur

instantly through the entire depth of the pavement (may be reasonable to the depth of 150 mm) and the cracking temperature is the average temperature of the pavement slab and, therefore, is not dependant on the number of cooled surfaces. To confirm these assumptions will require additional experiments.

Cracking and fracture temperatures are hypothesized to be equal: $H_0 = \mu_1 - \mu_2 = 0$. This hypothesis is tested with the USACRREL data. The regression model to predict the field cracking temperature (average pavement temperature at the moment of cracking) with the TSRST data for the field samples for a 1°C/h cooling rate ($CT = b_1 + b_2FT$) is as follows:

$$CT=(-36.0...20.9)+(-0.18...1.78)FT \tag{4.8}$$

the numbers in the parenthesis represent the 95% confidence limits for the least squares estimators, b_1 and b_2. By inspection, the condition that the cracking temperature equals the fracture temperature (CT = FT) is inside the confidence limits. Consequently, there is no evidence against the hypothesis. For the model, the relationship CT equals FT will be used. Then

$$CT=1.03FT_{orig}+0.51AGE. \tag{4.9}$$

It is assumed that the TSRST fracture strength equals the tensile strength of the pavement slab. The strength of asphalt concrete is dependent on temperature and loading time. However, at low temperatures, the pavement's behavior is elastic and approaches the brittle state as the temperature decreases and is less and less dependent on the loading time. At this point there is no evidence that the cracking

temperature differs from the fracture temperature; therefore, the assumption of equal strengths in the laboratory and field is reasonable.

The cooling rate of the TSRST affects fracture temperature and strength. This modeling effort is based on the TSRST for a low cooling rate of 1.5°C/h, which is considered to equal the field conditions. If faster or slower cooling rates are required, changes in the model may be necessary. If the field temperature is maintained warmer than (but close to) the transition temperature (defined in Section 1.1), the thermal stress will relax and a colder cracking temperature may be achieved. Modeling of this situation would require continuous temperature data for the future, and is impossible to conduct. Assuming monotonic cooling, conservative results will be obtained, i.e., more cracks will be predicted than will occur.

4.4 Estimation of Pavement Temperature

The "n-factor," is defined as the ratio of the surface freezing index to the air freezing index (McFadden and Bennet, 1991). Since freezing indices are calculated as yearly sums of the differences between 0°C and the daily mean temperature for the days with means below 0°C, surface temperature can be calculated by multiplying the air temperature by n-factor (assuming that the days with means below 0°C are the same for both surface and air freezing index or the error due to the difference is negligible). (Note, that the surface temperature can be estimated with this method only in Celsius degrees.) McFadden and Bennett (1991)

collected n-factors from several sources and noted a variation in values for similar conditions. A typical value of 0.9 has been used for pavements free of snow and ice undergoing freezing for pavements located north of 45°N. In West Virginia, an n-factor of 0.27 for asphalt pavement has been measured. In the areas where low temperature cracking is a problem, the n-factor varies from 0.6 to 1.0.

According to Solaimanian and Kennedy (1993), the minimum pavement surface temperature equals the air temperature at freezing temperatures. This agrees with the principle presented above, in which the average pavement surface temperature is slightly warmer than the air temperature. Solaimanian and Kennedy present an equation to estimate the pavement temperature as a function of depth from the surface of the pavement:

$$T_z = T_s + 0.051z - 6.3(10^{-5})z^2 \qquad (4.10)$$

in which,

T_z = Temperature at the depth z (°C),

T_s = Surface temperature of the pavement (°C) and

z = Depth from the surface of the pavement (mm).

The eqn. 4.10 is valid only at the top 200 mm of the pavement. An example of the temperature in the pavement layer as a function of the surface temperature calculated with eqn. 4.10 is illustrated in Figure 4.7.

For modeling low temperature cracking of asphalt pavements, the n-factor (n) of 0.9 with 10% variation is recommended. Then the pavement surface temperature is

$$PT_s=(n)Ta \tag{4.11}$$

in which,

PT_s = pavement surface temperature (°C),

n = n-factor, and

Ta = coldest daily air temperature (e.g. for a month, or other analysis interval selected by the user of the model).

The average pavement temperature, PT, is estimated as

$$PT=\int_0^D Tdz/D, \tag{4.12}$$

in which,

D = Thickness of the pavement (mm),

T = Temperature at depth z (°C) and

z = depth from the surface of the pavement (mm).

Referring to the results presented in Figure 4.7 the temperature relationship with depth is nearly linear. Consequently, the average pavement temperature is

closely approximated by the average of the coldest (surface) and warmest (base) temperature.

4.5 Estimation of Restraint Conditions between Pavement and Base

As the temperature decreases the pavement attempts to contract. However, the movement is prevented by the restraint force between the pavement and the base course. In traditional physics, the hypothesis is made that there is a linear relationship between the weight of the object to be moved (or the normal force) and friction between the object and the sliding plane. This holds true for an ideal system if two boundary conditions are satisfied. The first boundary condition is the elimination of all adhesion between the two surfaces, because adhesion is not linearly related to the nominal weight of the slab. The second boundary condition is that there are no deformations in the subbase or asphalt pavement to alter the interface profile and contribute additional resistance. If these conditions are satisfied, the shear force resisting movement is linearly dependent on the normal force, which is directly proportional to the weight of the slab. According to Wesevich et al. (1987), these boundary conditions are not met in practice for concrete pavements and, therefore, actual measurements are required to determine of the restraint forces. Wesevich et al. (1987) collected values from the literature for the friction or restraint coefficient between the concrete pavement and different base courses. Coefficients as high as 16.2 were recorded.

Zeng and Vinson (1993, unpublished) measured the restraint force between a 559 x 406 x 63 mm asphalt concrete slab and a granular base course. The lateral force was measured while the normal stress was varied from 2700 to 4600 Pa. A regression analysis was performed by the author of this report for the preliminary results of the experiment. First, a relationship of

$$RestraintForce = Adhesion + fN \tag{4.13}$$

was investigated. According to the analysis, the restraint force was not affected by the adhesion (p-value in two-sided t-test is 0.56). By omitting the adhesion from the relationship, the following results were obtained from the analysis:

- There is a linear relationship between the restraint force and normal force (p-value in two-sided t-test is < 0.00001).

- The friction coefficient was estimated as 2.07 with 95% confidence limits of 1.86 . . . 2.27.

For the modeling effort, it is assumed that there is a linear relationship between the normal force and the restraint force, and that the coefficient of friction on the granular base course is $2.0 \pm 10\%$. In addition, a rigid-plastic behavior is assumed and, consequently, that the resistance is fully mobilized with an infinite decimal strain.

4.6 Propagation of Thermal Stress and Cracks

For low temperature cracking to occur, two conditions must be satisfied: *(1)* the restraint force must be great enough to prevent the slab movement and subsequent release of the thermal stress, and *(2)* the pavement temperature must be cold enough to produce a thermal stress that equals the tensile strength of the pavement.

As the temperature decreases, the thermal stress develops gradually as shown in Figure 1.3 and is uniform along the length of an infinite slab at a given moment. For equilibrium, a restraint force in opposition to the contraction develops simultaneously. The forces in the pavement as the temperature decreases are presented in a free body diagram in Figure 4.8.

As explained in Section 4.5, the restraint force (fN) is assumed to be fully mobilized with an infinite decimal strain and to increase linearly with the normal force, i.e., from zero at the end of the pavement slab (where the normal force is zero) to a maximum value at the center of the slab of

$$(fN)_{max} = f\frac{L}{2}WD\gamma \tag{4.14}$$

in which,

W = Width of the pavement,

D = Thickness of the pavement, and

γ = Bulk density of the pavement.

A restraint stress is obtained by dividing the restraint force by the cross sectional area (A = WD) of the slab. The width and thickness cancel, and the maximum possible restraint stress as a function of longitudinal location is

$$\frac{(fN)_{max}}{A} = fx\gamma \tag{4.15}$$

in which,

x = Distance from the edge of the slab.

If the thermal stress exceeds the fully mobilized restraint stress, equilibrium is not valid and the slab is able to contract. Consequently, the thermal stress reduces to the value that equals the fully mobilized restraint stress. In practice, the thermal stress never exceeds the maximum (fully mobilized) restraint stress envelope. This situation is illustrated in Figure 4.9. The thermal stress is able to release at the vicinity of the edge of the slab and equals the restraint stress. At the center of the slab, the thermal stress is smaller than the fully mobilized restraint stress and is independent on the location. As the temperature decreases, the thermal stress increases and finally equals the fully mobilized restraint stress throughout the length of the pavement slab. The maximum value of the thermal stress at the center of the slab is

$$\sigma_{max}=f(L/2)\gamma. \qquad (4.16)$$

If this value is less than the tensile strength of the pavement (Figure 4.10), cracking will not occur. As temperature further decreases, the thermal stress is constant, while the tensile strength decreases at temperatures colder than the glass transition point (re. Figure 1.1). Consequently, cracking will occur, if the strength decreases to a value that equals the now constant thermal stress.

For the situation mentioned above, the strength as a function of temperature must be known for each mixture in order to predict low temperature cracking. To obtain the relationship that could be assumed to be linear, at least one strength measurement (including several replicates) must be conducted at a colder temperature than fracture temperature (for example at -50°C). Then two points for a line are known, (-50°C, strength at -50°C) and (fracture temperature, fracture strength), and the equation for the strength-temperature relationship could be solved. Measurements at several temperatures could be performed and a best-fit curve for strength-temperature curve used. Another method to obtain strength-temperature relationship is as follows: First, the standard TSRST is performed and the fracture temperature and strength are obtained. Then the TSRST is repeated, but this time the test is conducted so that, the thermal stress is kept constant by the feed-back system at a temperature slightly warmer than fracture temperature, while the temperature is decreased until fracture. This procedure could be repeated for several stress levels. If the mixture will not crack at the minimum available

temperature, the stress will be increased at a constant temperature until fracture. The strength is then obtained as a sum of the constant stress and the applied stress increment.

The strength-temperature relationship is affected by the aging of the mixture. If the relationship is assumed to be linear and the slope remains constant with time, the effect of aging will be contributed by the warmer cracking temperature. For example, if the strength S1 is measured at temperature T1, then the strength as a function of temperature is estimated as

$$Strength = \frac{(S1 - FS)}{(T1 - FT_{orig.})}(PT - CT) + FS. \qquad (4.17)$$

As the cracking temperature (CT) becomes warmer due aging, the strength decreases. It is necessary to verify the effect of aging on the strength-temperature relationship.

In the test program reported herein, the strength-temperature relationships for the mixtures were not obtained. Only the TSRST fracture strengths were measured for each mixture.

Cracking can only occur when the pavement temperature is cold enough to create a thermal stress that equals the tensile strength of the pavement. In Figure 4.11, the restraint stress is great enough to enable cracking, but the thermal stress is smaller than the tensile strength of the pavement, and cracking will not occur. Finally in Figure 4.12, cracking will occur, because both requirements are fulfilled; the restraint stress is high enough to allow the crack formation and the thermal

stress equals the tensile strength of the pavement at the center of the slab. Since the asphalt concrete mixture is never homogeneous, cracking will occur at the location where the slab is weakest (where the stress exceeds the strength first). The average crack spacing (L_{n+1}) will be the original slab length (L) divided by two (L_{n+1} = L/2). As a result of the cracking, the thermal stress is released at the vicinity of the crack to the value of the fully mobilized restraint stress. Depending on the length of the current slab, the remaining thermal stress at the center of the newly formed slab may still be greater than the tensile strength of the slab and further cracking will result. In Figure 4.13 two sets of cracking will occur before the remaining thermal stress is smaller than the strength of the pavement. The number of cracking incidents (N) can be solved from the relationship

$$f\gamma\frac{L}{2^{N+1}}<Strength \tag{4.18}$$

$$N>\frac{\log(f\gamma L/2Strength)}{log2} \tag{4.19}$$

Finally, N is calculated as

$$N=INTEGER[\log\frac{(f\gamma L/2Strength}{\log2}+1] \tag{4.20}$$

The average spacing is then calculated as

$$L_{n+1}=\frac{L}{2^N} \tag{4.21}$$

The condition of adequate restraint of the pavement slab for cracking to occur is included in eqn. 4.21. If the maximum restraint stress (σ = fL/2γ) is less than the tensile strength (that is assumed to equal the fracture strength, FS), N equals zero (or is negative, when a value of zero is assigned for N) and $L_{n+1} = L/2^0 = L/1 =$ L. In other words, if the thermal stress is reduced, no cracking will occur and the pavement slab length remains constant.

4.7 Deterministic Model

Based on the principles presented in the preceding paragraphs, a model was developed to predict the development of low temperature cracks with time. The deterministic model gives the crack spacing as a function of the age of the pavement using the measured TSRST results (FT and FS for non-aged specimen), coldest daily air temperature, restraint coefficient, pavement thickness and bulk density, temperature-strength relationship and original pavement slab length. This length will be compared to the criterion provided by the local authorities to determine if the mixture in question is acceptable with respect to low temperature cracking. A detailed flow chart of the model is given in Appendix B and a simplified flow chart in Figure 4.14. The following steps are performed to predict the low temperature cracking of asphalt pavements:

Step 1. The minimum daily air temperature and the number of freezing peaks to be analyzed per year is selected by the user. The pavement surface temperature is calculated with the given air temperature from eqn. 4.11. The interior pavement temperature as a function of depth from the surface of the pavement is calculated from eqn. 4.10. The average pavement temperature is estimated as

$$PT=10(\sum_{1}^{D/10} T)/D, \tag{4.22}$$

in which,

D = Thickness of the pavement (mm),

T = Temperature (°C) at the depths of 5 mm, 15 mm, 25 mm, etc. to the depth, D.

Step 2. The pavement temperature is compared to the cracking temperature. If the pavement temperature is warmer than the cracking temperature, no cracking will occur and the next time-temperature step is analyzed. If the pavement temperature is colder than the cracking temperature, Step 3 is executed.

Step 3. Cracking will occur if the restraint conditions are satisfied. The spacing (L) is calculated in meters as

$$L_{n+1} = \frac{L}{2^{INTEGER\left[\frac{\log(fL\gamma/2Strength)}{log2}+1\right]}}. \qquad (4.23)$$

in which the variables are as previously defined and the strength as a function of pavement temperature is estimated with one other strength value at colder temperature than FT as given in eqn. 4.17. Inadequate restraint conditions are taken into account in eqn. 4.23 by keeping L constant (N = 0, or if N < 0, a value of zero is assigned for N).

All given air temperatures will be read and the spacing will be calculated. The age and the spacing are printed and written into an output file and the age is increased by one year.

Step 4. The affect of aging on the cracking temperature of the pavement is computed. A new cracking temperature for each year is calculated according to eqn. 4.9. For very young pavements, eqn. 4.9 gives slightly colder cracking temperatures than the original fracture temperature. In this case (CT < FTorig), the value of the original fracture temperature is assigned for CT. The spacing for each year is calculated until the AGE reaches the analysis period.

4.8 Probabilistic Model

The variation in pavement material properties, temperatures and the uncertainties in the regression model for cracking temperature (with time) may be considered in a predictive model by determining the reliability of the system. The customary engineering definition of reliability is as follows:

> "Reliability is the probability of an object (item or system) performing its required function adequately for a specified period of time under stated conditions," (Harr, 1987).

The definition contains four essential elements:

- Reliability is expressed as a probability.
- A level of performance is expected.
- The level of performance is expected for a certain period of time.
- The level of performance is expected under specific conditions.

The concept of reliability has been introduced to highway engineers in the AASHTO guide for design of pavement structures (1986). In terms of serviceability:

> "Reliability is the probability that serviceability will be maintained at adequate levels from a users's point of view, throughout the design life of the facility" (AASHTO, 1986).

Accordingly, in a probabilistic model for low temperature cracking, the reliability that the pavement satisfies the design criterion, e.g. a minimum acceptable crack spacing for a design life, is determined.

Several methods exist to perform a reliability analysis. So called *exact methods* require that the probability distribution functions of all component variables are known initially. The unknown component distributions are usually assumed to be normal or log-normal, because of the complexity of the solution process. Numerical integration and Monte Carlo simulations are associated with this group. The advantage of these methods is that they yield complete probability distributions for the dependent random variables. The disadvantages are that the output may not be better than the assumed input and that considerable computing time is required.

The second group, *first order, second moment methods* (FOSM), simplifies the suggested functional relationship. The basis of these methods is the truncating of the Taylor series expansion of the probability distribution function. Inputs and outputs are given as expected values and standard deviations. The advantages result from simpler mathematical requirements for the FOSM (computers are not necessary) and knowledge of moments instead of complete distributions are required. The disadvantage is that the mathematical requirements, although simpler than for exact methods, are generally complicated.

The third group, *point estimate method* (PEM), was first presented in 1975 and has been widely used in engineering practice. The PEM is recommended by Harr (1987) for its simplicity and usable output. The method is based on an analogy between a probability distribution and a distributed vertical load on a horizontal rigid beam. The expected value is the analog of the point of application of the equilibrant or the center of loading, and the standard deviation is its radius of

gyration. Conceptually, the expected value and the standard deviation supply information concerning the central tendency and scatter of the variate. This information could be extracted from the beam analogy but with the rigid beam supported on two reactions, p_- acting at $x = x_-$ and p_+ acting at $x = x_+$. The reactions p_- and p_+ are said to be *two-point estimates* of the distribution of f(x),"

The PEM may be generalized for any number of random variables. For a function of three random variables $y = y(x_1, x_2, x_3)$.

$$y_{\pm\pm\pm}=y(\overline{x_1}\pm\sigma[x_1],\overline{x_2}\pm\sigma[x_2],\overline{x_3}\pm\sigma[x_3]), \tag{4.24}$$

and

$$p_{+++}=p_{---}=\frac{1}{2^3}(1+\rho_{12}+\rho_{23}+\rho_{31}) \tag{4.25}$$

$$p_{++-}=p_{--+}=\frac{1}{2^3}(1+\rho_{12}-\rho_{23}-\rho_{31})$$

$$p_{+-+}=p_{-+-}=\frac{1}{2^3}(1-\rho_{12}-\rho_{23}+\rho_{31})$$

$$p_{+--}=p_{-++}=\frac{1}{2^3}(1-\rho_{12}+\rho_{23}-\rho_{31})$$

where ρ_{ij} is the correlation coefficient of the random variables x_i and x_j. The M^{th} expectation is obtained by

$$E[y^M]=(p_{+++})(y_{+++})^M+(p_{++-})(y_{++-})^M+\ldots+(p_{---})(y_{---})^M \tag{4.26}$$

In general, for N variables there are 2^N terms and N(N - 1)/2 correlation coefficients, the latter being the number of combinations of N objects taken two at a time.

When considering the difference between the capacity (C) and demand (D) functions, a *safety margin* is defined as S = C - D (Harr, 1987). The safety margin is a random variable. The probability of failure is associated with that portion of the distribution of the safety margin which becomes negative, that is, the portion in which $S = C - D \leq 0$:

$$p(f)=P[(C-D)\leq 0]=P[S\leq 0] \tag{4.27}$$

Another measure of the adequacy of a design is the reliability index β (not the β in the beta distribution), defined as the number of h sigma units (the number of standard deviations $\sigma[S]$ between the mean value of the safety margin $E[S] = \bar{S}$ and $S = 0$, that is,

$$\beta=\bar{S}/\sigma[S] \tag{4.28}$$

The reliability is seen to be the reciprocal of the coefficient of variation of the safety margin, or

$$\beta=\frac{1}{V(S)} \tag{4.29}$$

If the variables in the C and D functions are normally distributed, then S is normally distributed, too. Then, the probability of failure is

$$p(f)=\frac{1}{2}-\psi(\beta) \tag{4.30}$$

where the function $\psi(\beta)$ is given in a normal distribution table. The coefficient of variation for the safety margin V(S) is

$$V(S)=\frac{\sigma[S]}{E[S]} \tag{4.31}$$

and the standard deviation σ[S]

$$\sigma[S]=\sqrt{E[S^2]-E[S]^2} \tag{4.32}$$

Four examples are presented to illustrate how this method is applied to the probabilistic model to predict low temperature cracking of asphalt pavements. Each example shows one step of the PEM procedure. To understand the method in its entirety, all four examples must be studied.

Example 1. *Estimate the reliability that the pavement will satisfy a minimum crack spacing design criterion, L_C (e.g. the spacing will not be less than 100 m). Assume that the strength of the mixture is not dependent on temperature.* The safety margin is S = L - L_C. Spacing (L_{n+1}) is calculated as

$$L_{n+1}=\frac{L}{2^{INTEGER[\frac{\log(fL\gamma/2FS)}{\log 2}+1]}}. \tag{4.33}$$

The probability that the spacing will satisfy the criterion is estimated with the following parameters of the variants:

Variable	*Expected Value*	*Coefficient of variation*
f	2	20%
L	2000 m	1%
γ	24 kN/m^3	3%
FS	4600 kPa	4%
L_C	100 m	

Correlation coefficient between γ and FS is 0.60 (obtained from a regression analysis with the data by Jung and Vinson, 1992). From eqn. 4.25, $p_{ijkl} = 1/16[1 + kl(0.60)] = 0.1$ for k = 1 and 0.025 otherwise. Minimum and maximum values for the variants are the following:

f_+	2.2	L_+	2020 m	γ_+ kN/m^3	24.72	FS_+	4784 kPa
f_-	1.8	L_-	1880 m	γ_- kN/m^3	23.28	FS_-	4416 kPa

First and second expectations from eqn. 4.26:

	S_{ijkl}	p_{ijkl}	$S_{ijkl}p_{ijkl}$	$S^2_{ijkl}p_{ijkl}$
S_{---}	23.75	0.1	2.375	56.406
S_{+--}	26.25	0.1	2.625	68.906
S_{-+-}	23.75	0.1	2.375	56.406
S_{++-}	26.25	0.1	2.625	68.906
S_{--+}	23.75	0.025	0.594	14.102
S_{+-+}	26.25	0.025	0.656	17.227
S_{-++}	23.75	0.025	0.594	14.102
S_{+++}	26.25	0.025	0.656	17.227
S_{---+}	147.5	0.025	3.688	543.906
S_{+--+}	152.5	0.025	3.813	581.406
S_{-+-+}	23.75	0.025	0.594	14.102
S_{++-+}	26.25	0.025	0.656	17.227
S_{--++}	23.75	0.1	2.375	56.406
S_{+-++}	26.25	0.1	2.625	68.906
S_{-+++}	23.75	0.1	2.375	56.406
S_{++++}	26.25	0.1	2.625	68.906
Sum			31.25 = E[S]	1720.547 = E[S^2]

The standard deviation is obtained from eqn. 4.32 as

$$\sigma[S]=\sqrt{1720.547-(31.25)^2}=27.276$$

Hence, the reliability index from eqn. 4.28 is

$$\beta=\frac{31.25}{27.276}=1.146$$

The probability that the design spacing criterion is satisfied is estimated as (eqn. 4.27 and 4.30)

$$p(L>L_C)=1-p(f)=1-[\frac{1}{2}-\psi(1.146)]=0.874$$

The reliability that the pavement will satisfy the given criterion of 100 m after the cracking incident is 87.4%. However, if N (eqn. 4.20) is zero, cracking will not occur. Therefore it is necessary to calculate the probability for the case that $N > 0$. The analysis will be performed identically as presented above by determining the safety margin $S = N$. Consequently, the probability $p(N>0)$ is $p = 1 - p(f)$. For the values given above, the expected value for N is $E[N] = 3.95$ and $p(N>0)$ is 1.0, i.e., cracking occurs. In addition, the expected spacing E[L] could be analyzed simultaneously by determining $L = S + L_C$. The analysis gives $E[L] = 131.25$ m with a coefficient of variation of 21%.

Example 2.

Estimate the probability that the pavement temperature (PT) is colder than the cracking temperature (CT). The cracking temperature changes as a function of the TSRST fracture temperature and oven aging (LTOA) according to

$$CT=(0.950...1.108)FT+(0.766...1.533)LTOA^{0.5} \quad (4.34)$$

The values in the parentheses represent the 95% confidence limits for the least square estimates b_0 and b_1 calculated as $b_i \pm t(0.975, n-2)S.E.(b_i)$. Similarly, the relationship between the age of the pavement (AGE) and oven aging (LTOA) is

$$AGE=(8.17...12.09)+(1.633...2.915)\sqrt{LTOA}-(8.81...11.83)Cl \quad (4.35)$$

or solving for the square root of LTOA

$$\sqrt{LTOA}=(-4.99...-2.06)+(0.272...0.437)AGE+(2.71...4.62)Cl \quad (4.36)$$

in which the Climate (*Cl*) is 1.0.

The probability of cracking is estimated with the following parameters of the variants:

Variable	*Expected Value*	*Coefficient of variation*
Ta	-30°C	10%
n	0.9	10%
FT	-27.5°C	2%
AGE	1 years	
Thickness	50 mm	

Variable	*Minimum value*	*Maximum value*
b_0	0.950	1.108
b_1	0.766	1.533
b_2	-4.987	-2.059
b_3	0.272	0.437
b_4	2.713	4.619

The correlation coefficient between the air temperature (Ta) and n-factor (n) is assumed to be -0.05.

Safety margin S = PT - CT, in which PT is the average pavement temperature and the CT is the cracking temperature. The pavement temperature as a function of depth from the surface of the pavement is calculated as

$$T_z=(n)Ta+0.051z-6.3(10^{-5})z^2 \tag{4.37}$$

The average pavement temperature PT is estimated according to Equation 4.22 (could also be averaged with the surface and the base temperature). The pavement thickness affects only the average pavement temperature. Because the variation in pavement thickness has a negligible affect on average pavement temperature, it is held constant in the analysis to reduce computation time. The cracking temperature is calculated as

$$CT=b_0FT+b_1(b_2+b_3AGE+b_4) \tag{4.38}$$

From eqn. 4.25, $p_{i\ldots q}$ = 1/256[1 + ij(-0.05)] = 0.0037 for i = j and 0.0041 otherwise. The analysis is performed identically to Example 1 and the probability for cracking to occur p(PT < CT) = 0.434.

To estimate the reliability of the design, the probability for the system to meet the design criterion will be calculated as follows:

$$p(L>L_C)=[(1-p1)+p1(1-p2)]p3+p1p2p4 \qquad (4.39)$$

in which,

p1 = probability that N > 0,

p2 = probability that (PT ≤ CT),

p3 = probability that the current spacing meets the design criterion,

p4 = probability that the spacing after the possible cracking meets the design criterion.

In other words, the design criterion will be met, if the cracking will not occur ***and*** the current slab length (spacing) meets the design criterion ***or*** cracking will occur ***and*** the new slab length will meet the criterion. Further, cracking will not occur if the restraint conditions are inadequate (N = 0) ***or*** the restraint conditions are adequate (N > 0) ***and*** the pavement temperature will not reach the cracking temperature (PT > CT). The conditions for cracking to occur are that the restraint conditions are adequate (N > 0) ***and*** the pavement temperature is smaller than or equals the cracking temperature (PT ≤ CT). The reliability of the design with respect to the low temperature crack spacing is

$$R=p(L>L_C)100\%. \tag{4.40}$$

Assume that the current spacing meets the design criterion (p3 = 1). Then with the values in Examples 1 and 2, the reliability of the design is

$$R=p(L>L_C)100\%=[[(1-1)+1(1-.434)]1+1(.434)(.874)]100\%=94.5\%$$

The probability for cracking to occur is

$$p(cracking)=p1p2=0.434 \tag{4.41}$$

Because the probability for cracking is smaller than the probability for no cracking, the slab length for the next analysis (i.e., next time step) will be the original length of 2000 m. If the probability for cracking were greater than 0.5, the new estimated length of 131.25 m would have been used.

Example 3. *Estimate the reliability of the pavement to satisfy a minimum crack spacing design criterion (L_C) by considering the effect of temperature on strength. (It was assumed in Example 1 that the strength of the pavement is not dependent on temperature.)* Here, the number of the variables increases to twelve. The following relationship is used between the strength and average pavement temperature, PT (Kanerva 1991):

$$Strength = \frac{250}{6}(PT - CT) + FS. \qquad (4.42)$$

The spacing (L) will be calculated with Equation 4.23. The pavement temperature (PT) and cracking temperature (CT) is calculated as presented in Example 2. The analysis will use the following parameters of variants:

Variable	*Expected Value*	*Coefficient of variation*
f	2	20%
L	2000 m	1%
γ	24 kN/m^3	3%
FS	4600 kPa	4%
L_C	100 m	
Ta	-30°C	10%
n	0.9	10%
FT	-27.5°C	2%
AGE	1 year	
Thickness	50 mm	
	Minimum value	*Maximum value*
b_0	0.950	1.108
b_1	0.766	1.533
b_2	-4.987	-2.059
b_3	0.272	0.437
b_4	2.713	4.619

Correlation coefficient between γ and FS is 0.60 and between n and Ta -0.05. From eqn. 4.25, $p_{ij\ldots t} = 1/4096[1 + kl(0.60) + no(-0.05)]$.

The rest of the analysis is identical to that presented in Examples 1 and 2. A total of 4096 terms is calculated for each four "safety margins" with sums up to 16384 terms per time step. As anticipated, this may require substantial

computational time and may require computer hardware not available to a highway engineer. Therefore, a simplified method is recommended as given in Example 4.

Example 4. *Estimate the reliability of the design with respect to a minimum crack spacing by assuming a fixed relationship between the cracking temperature (CT) and time as given in eqn. 4.9.* Here, the number of variants reduces to seven and 512 terms will be calculated for each time step. The probability of cracking is then estimated with the following parameters of the variants:

Variable	*Expected Value*	*Coefficient of variation*
f	2	20%
L	2000 m	1%
γ	24 kN/m^3	3%
FS	4600 kPa	4%
L_C	100 m	
Ta	-30°C	10%
n	0.9	10%
FT	-27.5°C	2%
AGE	1 year	
Thickness	50 mm	

The rest of the analysis is identical of that presented in Examples 1 to 3. A flow chart for the analysis given in this example is given in Appendix C. An example of the analysis is given in Appendix D.

The expected value for spacing will decrease with time, even if it would be constant for the deterministic model. Because the cracking temperature increases with time, the probability for cracking to occur will increase. Assume, that the

pavement will crack five times out of the total 128 possibilities for the year n. For the year n+1, the pavement will crack perhaps eight times out of 128 possibilities. The mean value for the spacing will be contributed by the cracked sections and it will decrease. To determine if this trend is correct compared to the hypothesis that the spacing remains constant, one may imagine a 12800 m long pavement consisting of 128 hundred meters long sections. In the year n, five sections out of 128 will crack and the average spacing is calculated with the new spacings. Next year, three more sections will crack, and the average spacing over the whole 12800 m will indeed be decreased.

4.9 Testing of Models

The deterministic and the probabilistic models were verified by predicting the spacing for the five test roads in Alaska, Pennsylvania, Peraseinajoki, Sodankyla and USACRREL. The models were programmed in QuickBasic 4.0 for the verification analyses. A hard copy of the input and output data is given in Appendix D. For the probabilistic model, a coefficient of variation of 2 and 4% is used for the fracture temperature and strength, respectively.

Alaska With the TSRST results for the field samples given in Table 3.1 a spacing of 78.1 m was predicted with the deterministic model for the first five years. No difference was predicted between the behavior with the mixtures

containing asphalt cement AC-5 and AC-2.5. For the laboratory fabricated samples, a spacing of 156.25 m was obtained. A minimum air temperature of -43°C, a bulk density of 24 kN/m^3, a pavement length of 10000 m, a friction coefficient of 2.0 and pavement thicknesses of 44, 57 and 102 mm were used in the analysis. The predicted spacing corresponds the value that is normally observed in the Fairbanks area (Esch, 1990). When the friction coefficient between the pavement and the base course was increased to 20, a spacing of 4.9 m was predicted, which corresponds more closely to the spacing observed.

By using the probabilistic model the following results were obtained with the field samples: A spacing of 71 m $\pm$ 20% with the reliability of 93% was predicted for the first year for the southbound lane of the 23rd Avenue. Even if the expected spacing of 71 m is greater than the criterion of 50 m, there is a 0.07 probability that the criterion is not satisfied. Respectively, a spacing of 90 m $\pm$ 31% with a reliability of 92% was predicted for the northbound lane, a spacing of 95 m $\pm$ 33% with a reliability of 92% for Peger Road for samples taken transverse to the direction of traffic and 85 m $\pm$ 27% with a reliability of 93% for Peger Road for samples taken to the direction of the traffic. The following input data were used for the prediction: a minimum air temperature of -43°C $\pm$ 10%, a bulk density of 24 kN/m^3 $\pm$ 3%, a pavement length of 10000 m $\pm$ 1%, a friction coefficient of 2.0 $\pm$ 20%, pavement thicknesses of 44, 57 and 102 mm and a minimum acceptable spacing of 50 m.

The spacings predicted for the first year by the probabilistic model were close to those predicted by the deterministic model. For example, a spacing of 78 m and 71 ± 20% was predicted for the southbound lane of the 23rd Avenue with the deterministic and probabilistic model, respectively.

Pennsylvania Prediction of the spacing for the test sections in Pennsylvania was performed with the following input data: a minimum air temperature of -29°C (± 5%), a bulk density of 23.3 kN/m^3 (± 3%), a length of pavement of 10000 m (± 1%), a friction coefficient of 2 (± 20%), a pavement thickness of 38 mm and the minimum acceptable spacing for the probabilistic model of 50 m. The numbers in the parenthesis are coefficients of variation for the variables used in the probabilistic model.

In the analysis, the sections T-2 and T-6 were not predicted to crack in the first five years. The section T-3 was predicted to crack in the fourth year with a spacing of 156.3 m according to the deterministic analysis and a spacing of 143 m ± 19% according to the probabilistic analysis. In the deterministic analysis, the sections T-1 and T-4 were estimated to crack in the first winter with a spacing of 78.1 m as was the section T-5 with a spacing of 156.3 m. The cracking intervals for these sections with time predicted by the probabilistic model are given in Table 4.4. Here too, the actual restraint force was likely greater than anticipated and, therefore, the predicted crack spacing is greater than observed.

Based on the analysis, mixtures in the sections T-2 and T-6 and possibly T-3 would have been chosen for a design, and they performed well in the field through the entire period of observation. The sections that would likely have been rejected, T1, and T-5, cracked in service in the first winter. The section T-4 that behaved poorly in the prediction, actually performed well in the field for the first three years, but after the fourth winter the crack frequency was greater than for the sections T-2, T-3 and T-6.

Peraseinajoki None of the Peraseinajoki sections were predicted to crack in the first five winters. After two winters in service, none of the sections cracked. The following input values were used in the prediction: a minimum air temperature of -20°C (± 10%), a bulk density of 24 kN/m^3 (± 3%), a length of pavement of 10000 m (± 1%), a friction coefficient of 2 (± 20%) and a pavement thickness of 50 mm.

Sodankyla As mentioned in Section 3.4.3, the interpretation of the crack spacing and the cracking temperatures in Sodankyla was extremely difficult. It was concluded that there were factors other than the mixture properties affecting the crack pattern of the pavement sections. As anticipated, the peculiar cracking behavior in Sodankyla could not be predicted. With the following input data, only the section with BIT65AH binder was predicted to crack with a spacing of 78.1 m in the deterministic prediction and 117 m ± 33% in the probabilistic prediction: a

minimum air temperature of -33°C (± 10%), a bulk density of 24 kN/m^3 (± 3%), a pavement length of 10000 m (± 1%), a friction coefficient of 2 (± 20%) and a pavement thickness of 50 mm.

USACRREL The experiment at the USACRREL was performed in a controlled environment and is in this respect ideal for the testing the deterministic and probabilistic models. However, the cooling panels were placed directly on the surface of the sections (except the section I during the first cooling, when no cracking was observed). The cooling panels increased the restraint force between the pavement and the base course due to the increased normal force; also a restraint force between the panels and the pavement was inserted. Therefore, it is not possible to analyze the system directly with the models. An effort was made, however, to make a prediction by replacing the weight of the panels by equivalent weight of the pavement (by using a longer slab length) and using a great friction coefficient between the pavement and the base (to contribute the restraint between the panels and pavement).

The following parameters were used in the prediction for one year: a minimum air temperature of -39°C (± 5%), a bulk density of 24 kN/m^3 (± 3%), a length of pavement of 25, 46 or 70 m (± 0%), a friction coefficient of 4 (± 5%) and a pavement thickness of 50 or 75 mm. The original length of the slab was given as the design criterion, and consequently the reliability gives the probability for no cracking to occur. With the TSRST results for the laboratory fabricated non-

aged specimens (Table 3.9), cracking was predicted for all sections excluding the sections IV and V. In the experiment, all sections except the sections IV and V cracked. In the beginning of the experiment, the 2.7 m wide and 61 m long section was cooled by placing the cooling panels on the supports so that an air gap remained between them and the pavement. For that test, a minimum air temperature of -33°C was measured and no cracking was observed. Using the measured air temperature (± 5%) and a friction coefficient of 2.2 (± 5%), no cracking is predicted for the section.

Similar results were obtained by using the TSRST results for the field samples (Table 3.9). The only difference in the results of the deterministic analysis was that no cracking was predicted for the section VII. In the probabilistic analysis, the expected spacing was the original length, and the probability that the expected spacing equals the original length was 0.67. In the field, one half a crack was observed in the center of the pavement.

The expected spacings are not given, because the original length of the pavement was increased by the contribution of the weight of the cooling panels. However, an average of one cracking was predicted for each section that was predicted to crack.

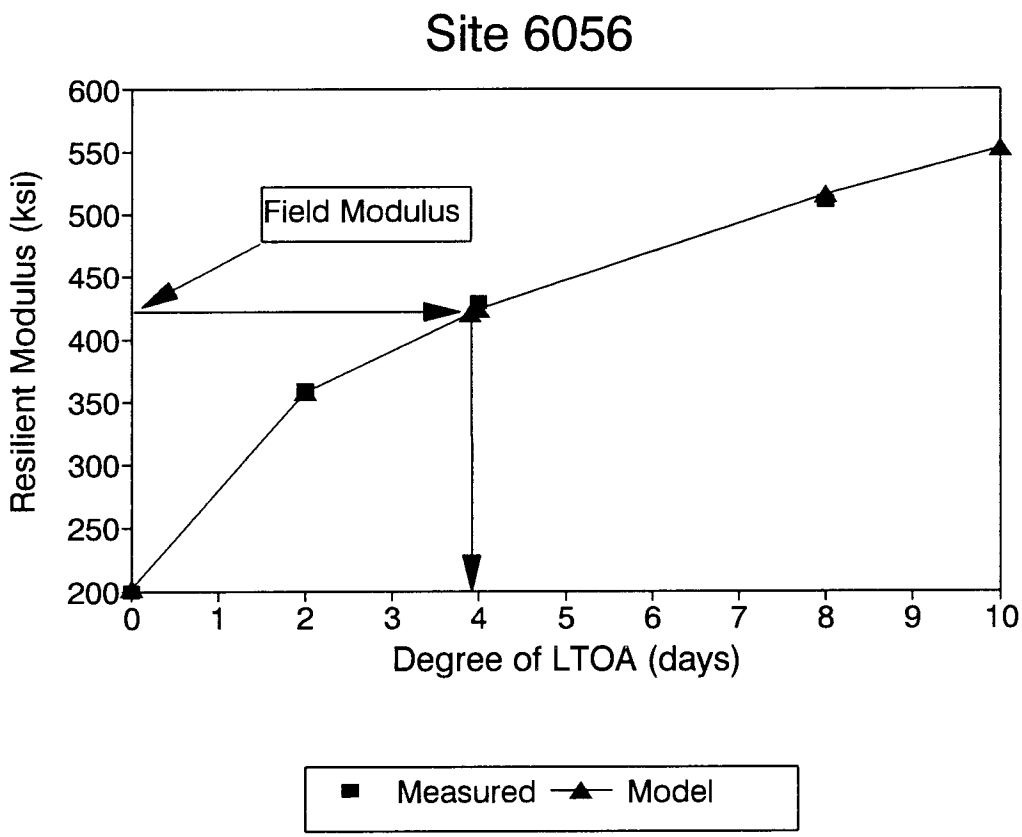

Figure 4.1 Modulus versus degree of Long Term Oven Aging for site 6056

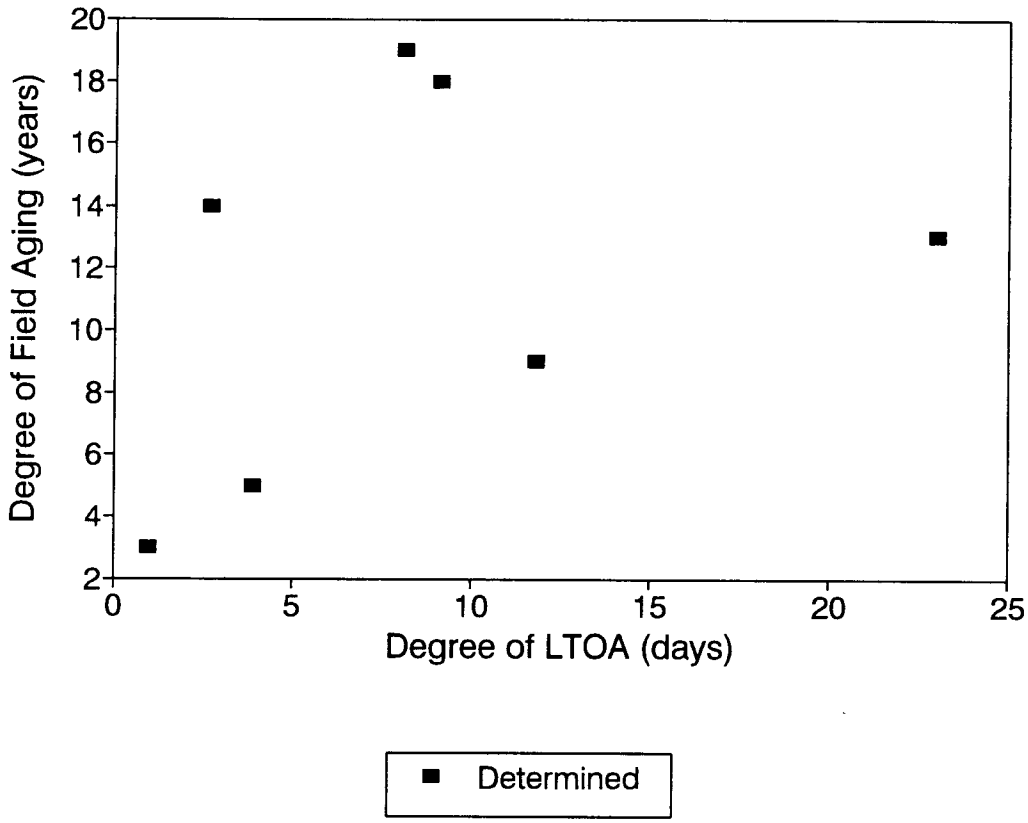

Figure 4.2 Age in field versus equivalent degree of Long Term Oven Aging

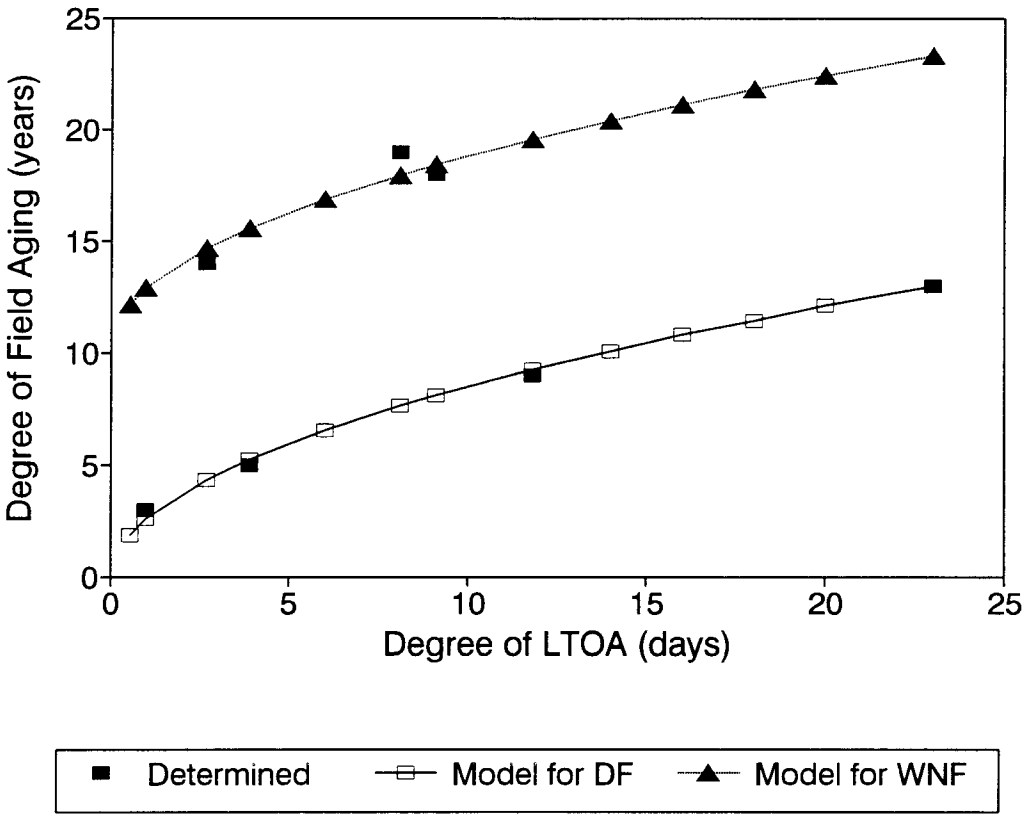

Figure 4.3 **Model I to predict degree of field aging with degree of the Long Term Oven Aging**

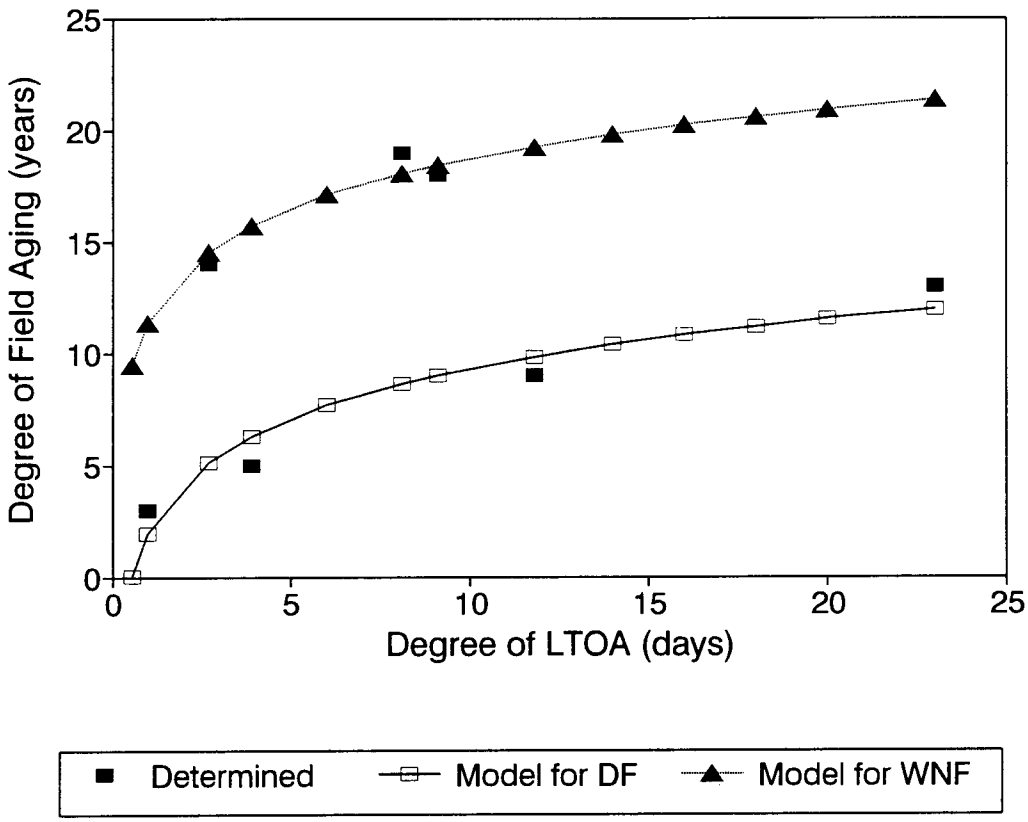

Figure 4.4 **Model II to predict degree of field aging with degree of the Long Term Oven Aging**

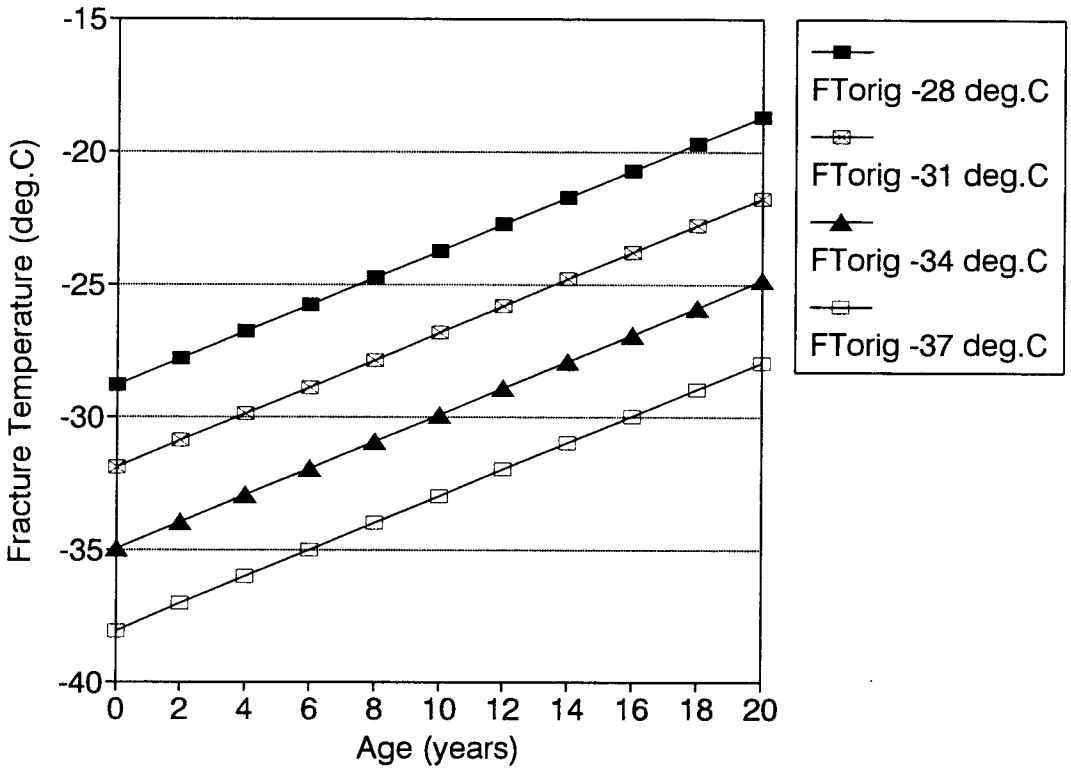

Figure 4.5 Fracture temperature versus age of pavement

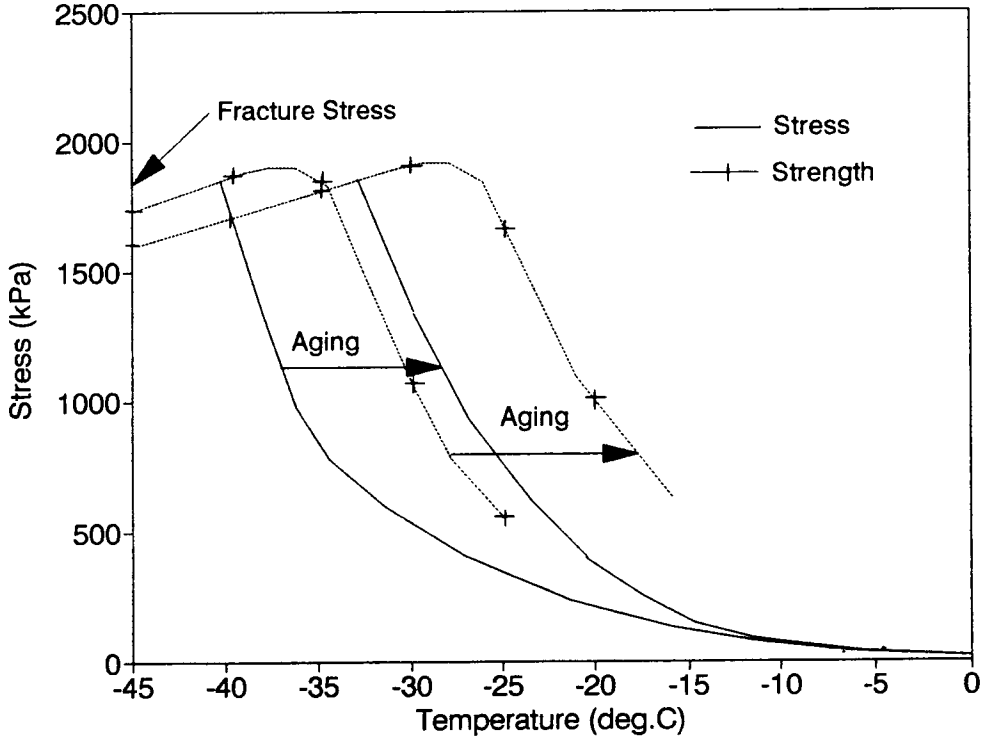

Figure 4.6 **Effect of aging on thermal stress and strength of asphalt concrete mixture**

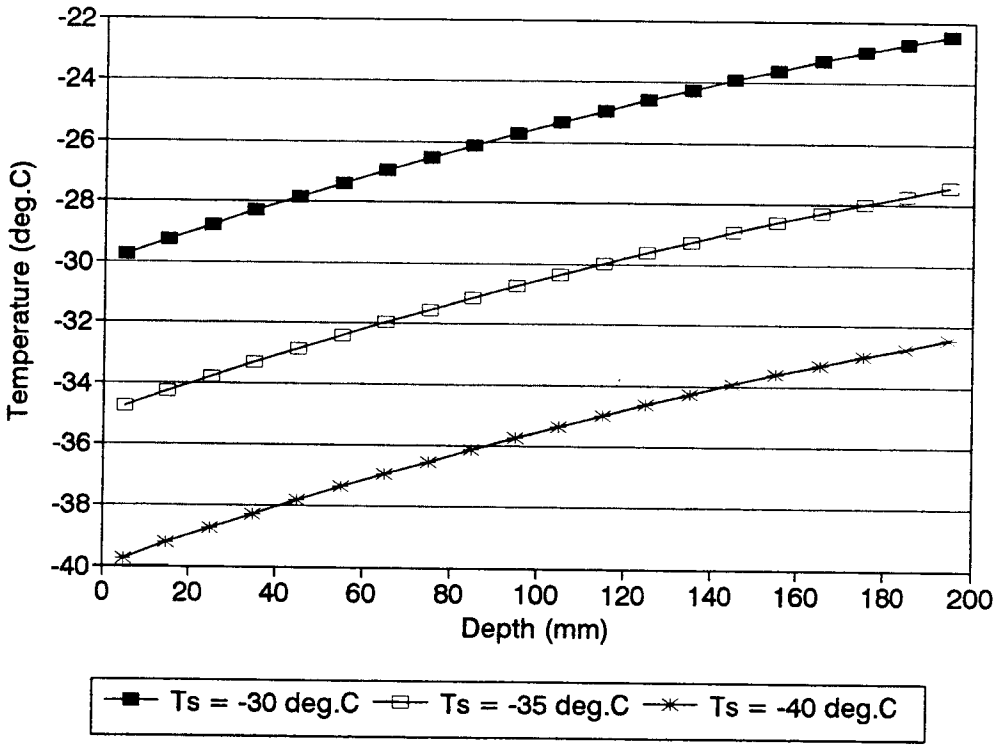

Figure 4.7 **Temperature in pavement layer as a function of surface temperature (Ts) and depth from surface**

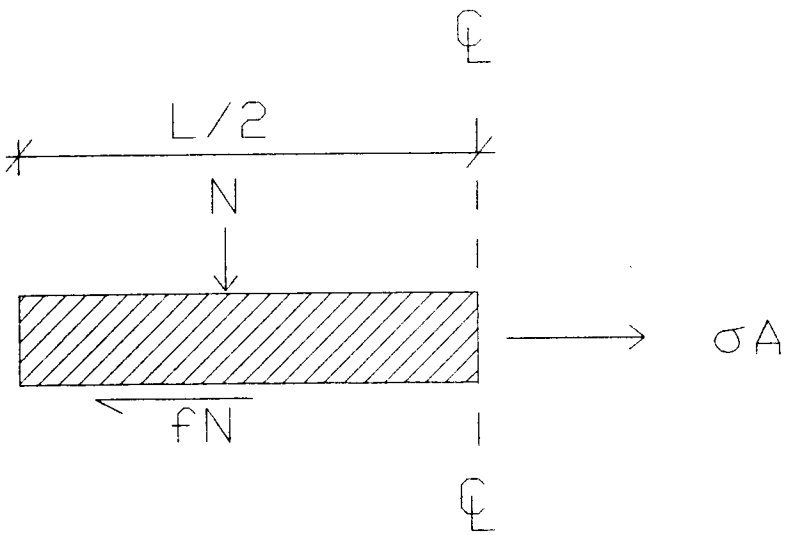

Figure 4.8 Forces in pavement slab as temperature decreases

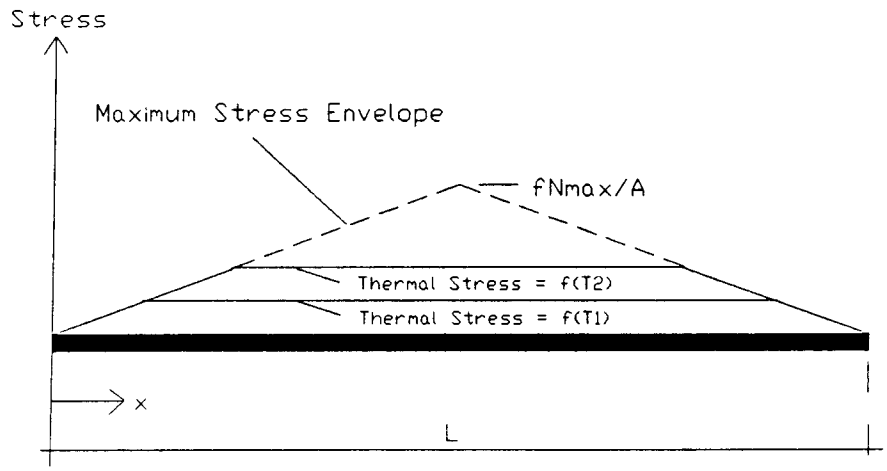

Figure 4.9 Development of thermal stress

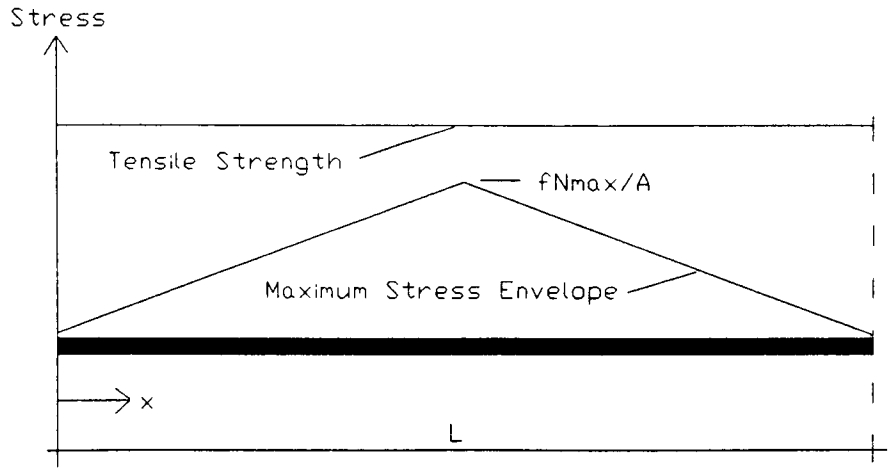

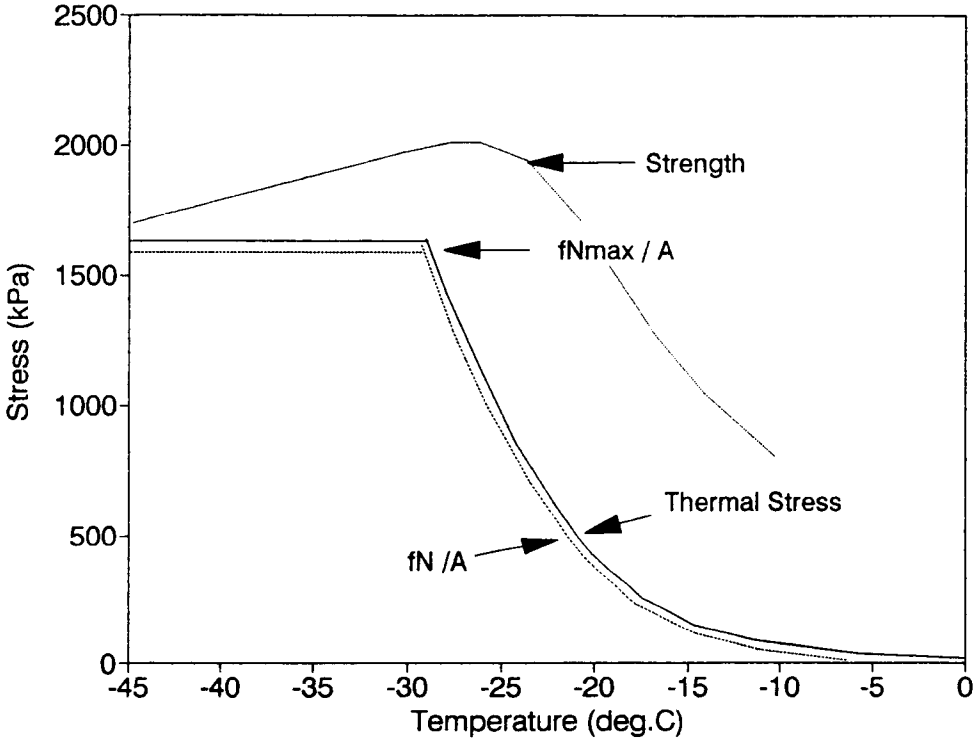

Figure 4.10 Conditions for low temperature cracking: Inadequate restraint conditions

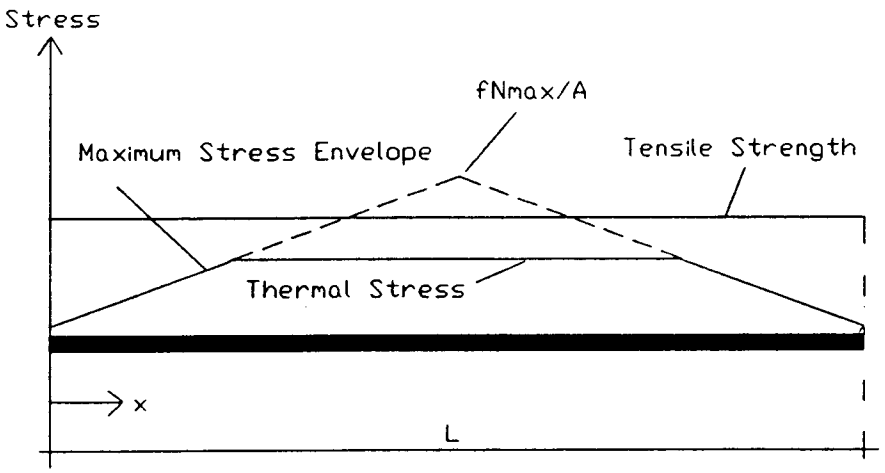

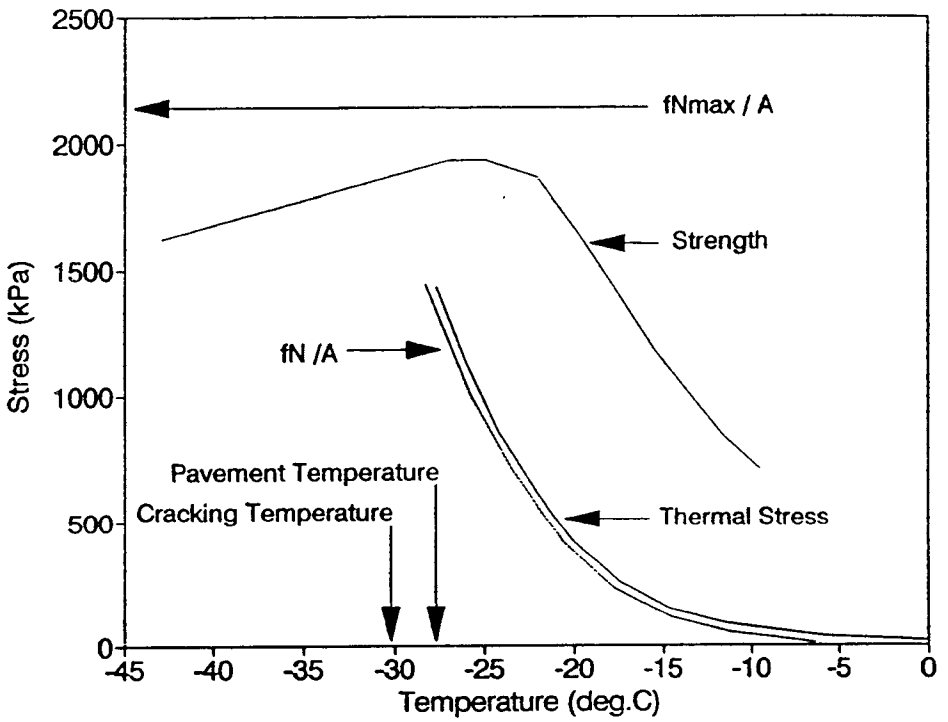

Figure 4.11 Conditions for low temperature cracking: Small thermal stress

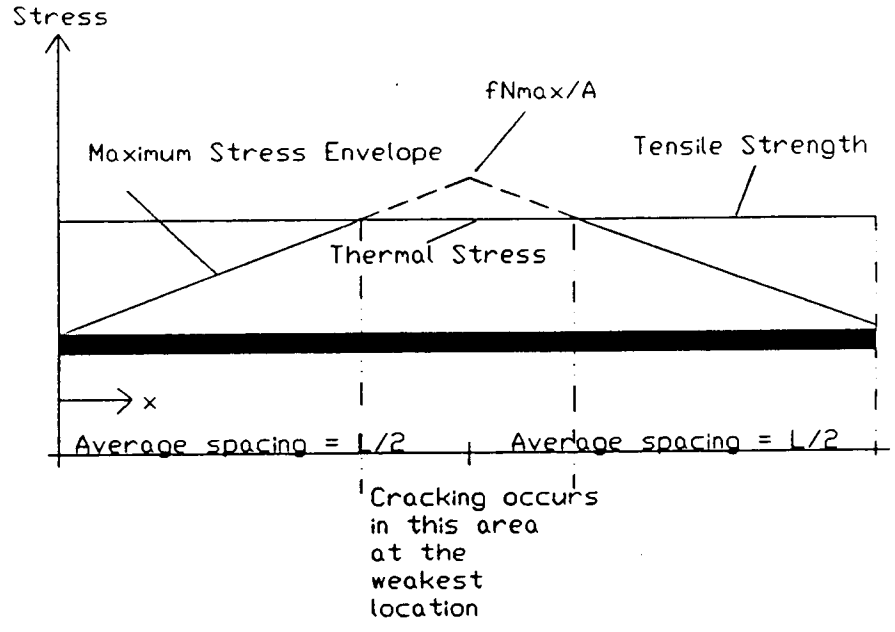

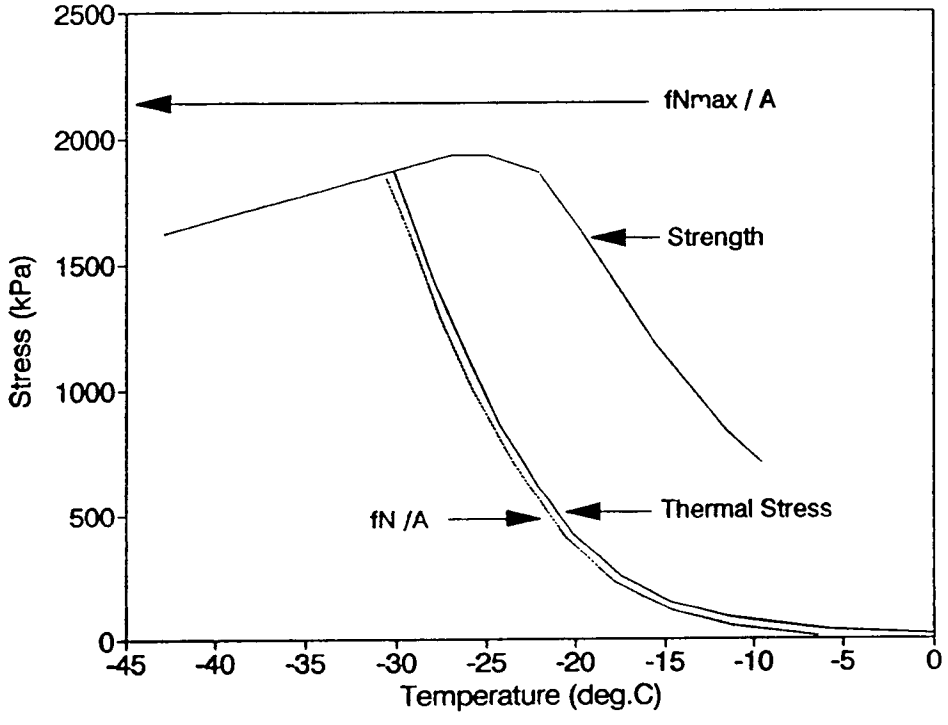

Figure 4.12 Conditions for low temperature cracking: Adequate restraint conditions and thermal stress

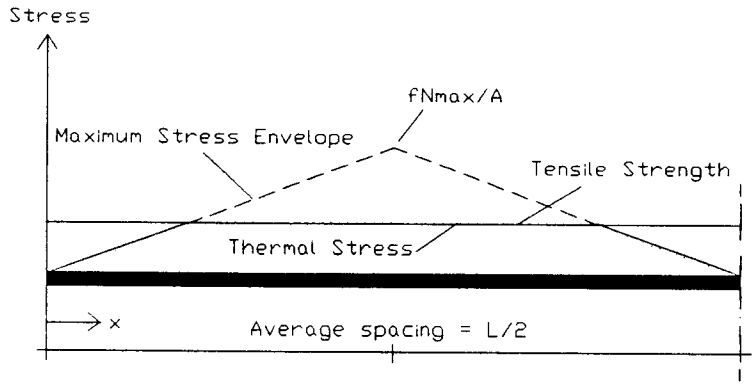

a) Thermal Stress = Tensile Strength
Further cracking

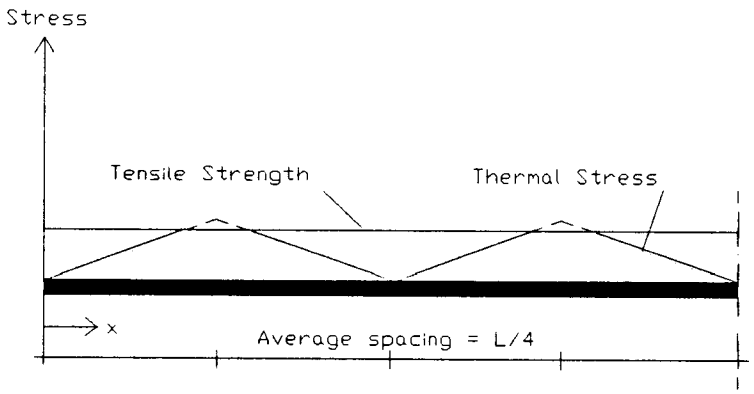

b) Thermal Stress = Tensile Strength
Further cracking

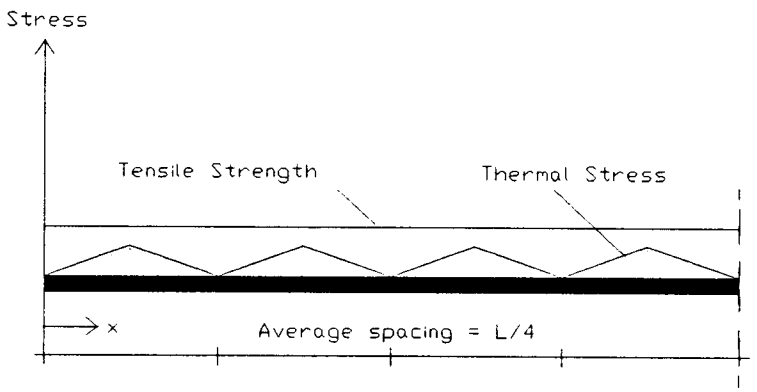

Figure 4.13 Propagation of low temperature cracking

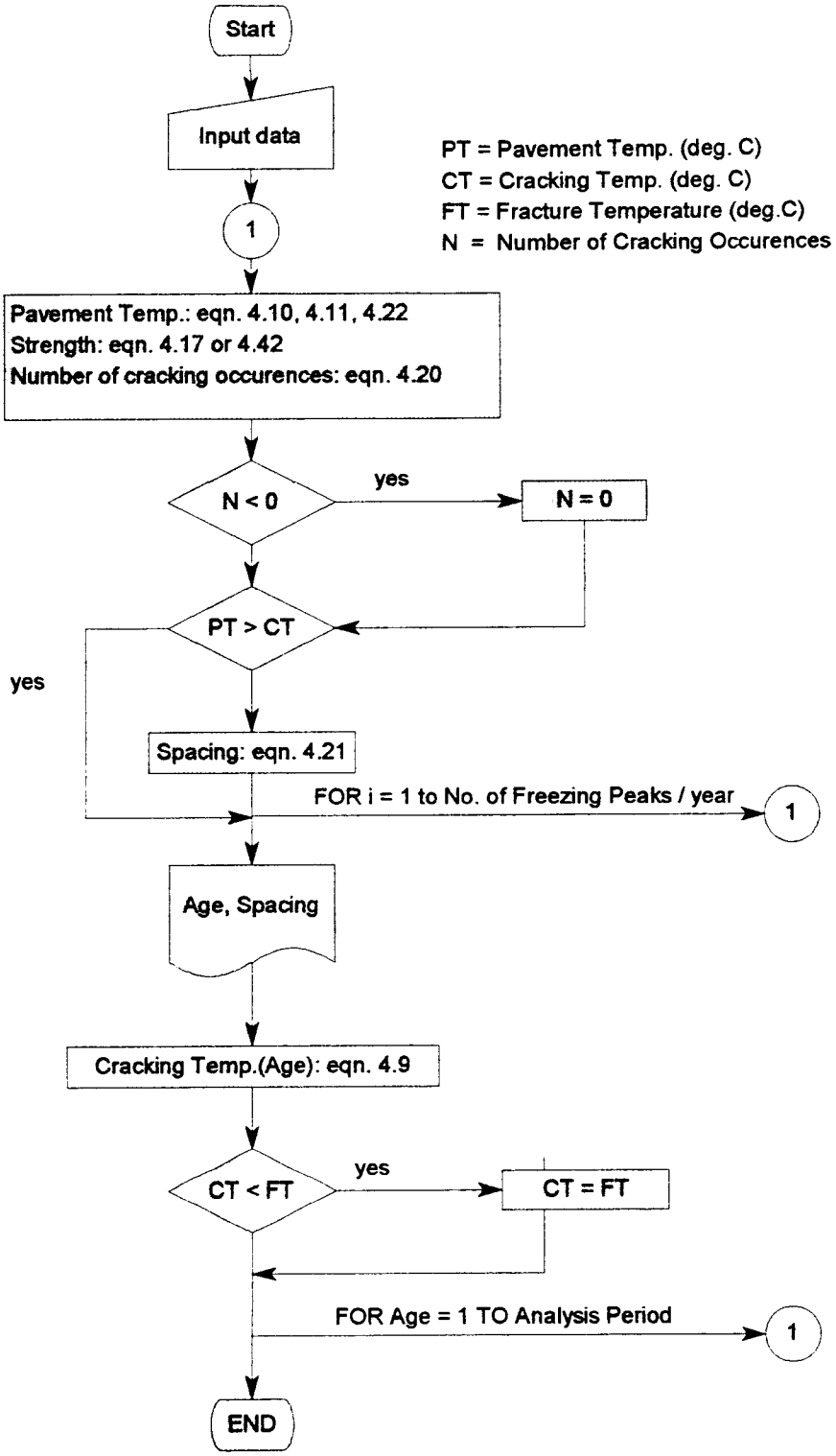

Figure 4.14 Flow chart for deterministic model to predict low temperature cracking of asphalt concrete mixtures

Table 4.1 Summary of sites for field aging study (after Wieder et al., 1993)

Site I.D.	Route Number	Vicinity	Climate Zone	Age (years)
1801	SR-14	16 km east of Vancouver, WA	wet-no freeze	18
6048	SR-522	16 km north of Seattle, WA	wet-no freeze	14
6049	SR-167	Near Kennevick, WA	wet-no freeze	19
1002	SR-12	North of Walla Walla, WA	dry-freeze	3
1006	US 97	Near Brewster, WA	dry-freeze	9
1008	US 195	16 km south of Spokane, WA	dry-freeze	13
6056	US 195	32 km north of Clarkston, WA	dry-freeze	5

Table 4.2 Diametral modulus (ksi) in field and with degree of Long Term Oven Aging (after Bell et al., 1993)

LTOA (days)	Site 1801	Site 6048	Site 6049	Site 1002	Site 1006	Site 1008	Site 6056
0	190	300	250	240	320	250	200
2	520	650	590	540	620	410	360
4	605	730	630	580	610	490	430
8	780	810	730	650	750	590	510
Field	826	639	768	418	852	825	421

Table 4.3 Regression analysis for resilient modulus versus degree of Long Term Oven Aging

Site I.D.	b_0	b_1	R^2 (%)	Error of Y Estimate	Equivalent LTOA (days)
1801	200.43	207.17	99.5	21.8	9.1
6048	335.02	184.20	95.4	59.2	2.7
6049	283.98	170.45	94.9	57.9	8.1
1002	273.30	146.86	93.6	55.9	1.0
1006	344.56	147.65	93.8	55.1	11.8
1008	246.93	120.51	99.9	6.0	23.0
6056	202.48	110.54	99.9	6.1	3.9

Mean{Modulus} = $b_0 + b_1 (LTOA)^{.5}$
Degrees of freedom = 2.

Table 4.4 Predicted crack spacing with time for Pennsylvania test sections

Year	T-1 Spacing (m)	V (%)	T-4 Spacing (m)	V (%)	T-5 Spacing (m)	V (%)
1	65	27	117	33	117	33
2	55	30	117	33	97	34
3	52	31	97	34	91	36
4	50	32	86	36	89	36
5	49	33	86	36	88	36
Reliab.		49		87		88

5 CONCLUSIONS AND RECOMMENDATIONS

5.1 Conclusions

Based on the data from the five test roads and USACRREL test sections and the prediction from the deterministic and probabilistic models developed, the following conclusions are appropriate:

- Cracking behavior could be explained with the TSRST for the test roads where mixture properties dominated low temperature cracking. It was concluded that the TSRST can be used in the prediction of low temperature cracking of asphalt-aggregate mixtures.

- A deterministic model to predict the spacing of low temperature cracking with local air temperature was developed. In addition to TSRST parameters and air temperature, field aging, restraint conditions, pavement length, thickness and bulk density contribute to low temperature cracking. Further, a probabilistic model was developed that takes account the variability of the input data.

- The deterministic and probabilistic models to predict low temperature cracking are based on several assumptions. Reasonable predictions

are obtained for typical restraint conditions. The spacing is estimated properly for the first few years with each models.

- The probabilistic method considers the variation in the minimum air temperature and other parameters; therefore, the expected average crack spacing over the pavement segment is more sensitive to changes with time than the spacing estimated by the deterministic model. In addition, the probabilistic method yields valuable information such as the variation of the spacing and the reliability of the design.

- The crack spacing from the deterministic model is not an adequate design parameter since its reliability cannot be estimated.

- The spacing of the low temperature induced cracks is greatly affected by the restraint forces between the pavement and the base course. It is concluded that when an unusually frequent cracking is observed, it is most likely caused by a substantial restraint force.

5.2 Recommendations for Implementation

It is essential that a low temperature cracking criterion be included in the mix design of asphalt concrete pavements in cold regions. A logical criterion for low temperature cracking is the crack frequency or the spacing between the cracks. Any other criterion is indirect and can only be used as a ranking system between different mixtures. For economical considerations and risk analysis, the deterministic methods are inadequate, and reliability based design methods are becoming more popular. For these reasons, it is recommended, that the probabilistic method to predict low temperature cracking presented herein be used in mix-design. The method predicts the average crack spacing of the asphalt pavement and its variability with TSRST results and a few other variables that are easily obtained. In addition, when the parameters are not known exactly (like restraint conditions between the pavement slab and base course), their expected variation can be included in the analysis. Even more important than the spacing itself, is the probability that the spacing exceeds the minimum acceptable spacing criterion. This probability, multiplied by 100%, gives the reliability of the design with respect of low temperature cracking.

5.3 Recommendations for Future Research

Several assumptions were made in the development of the model to predict the spacing of the low temperature cracks. More research is required to check the applicability of these assumptions in the following areas:

- *Relationship between laboratory aging and field aging*

  Original materials should be collected from test roads and TSRSTs should be performed for different periods of LTOA. In addition, field samples should be collected from in service pavements annually for up to twenty years, if possible. The TSRST should be conducted for the field samples to obtain a relationship between cracking temperature and strength of LTOA specimens and specimens aged in service. In addition, the effect of aging on strength of the mixture at low temperatures should be investigated. Test roads should be located in different environments and several mixture types, aggregates and binders should be used.

- *TSRST test results versus field parameters*

  Several assumptions were made to conclude that the TSRST fracture temperature and fracture strength equal cracking temperature and tensile strength of the pavement in the field. Experiments with fully

instrumented test roads should be conducted to verify these assumptions. In addition, modeling the development of the stresses in the laboratory sample and pavement slab in service with visco-elastic finite element method could provide useful information.

- *Restraint forces between the pavement slab and base course*

  The influence of different surface treatment methods, such as a prime coat, on the restraint force between the asphalt pavement and the base course is not known. Direct shear tests should be performed with several normal forces on different base courses, treated and untreated.

6 BIBLIOGRAPHY

"*AASHTO Guide for Design of Pavement Structures*," 1st ed., Vol. 1, American Association of State Highway and Transportation Officials, Washington, D.C., 1986, p. I-53.

Arand, W. "Influence of Bitumen Hardness on the Fatigue Behavior of Asphalt Pavements of Different Thickness due to Bearing Capacity of Subbase, Traffic Loading, and Temperature," *Proceedings of the 6th International Conference on Structural Behavior of Asphalt Pavements*, University of Michigan, Vol. 1, 1987.

Bell, C. A., Abwahab, Y. and Christi, M.E., "Investigation of Laboratory Aging Procedures for Asphalt-Aggregate Mixtures," presented at the January 10-14, 1991, Transportation Research Board 70th Annual Meeting, held at Washington, D.C.

Bell, C. A., Wieder, A., Fellin, M.J., "Laboratory Aging of Asphalt-Aggregate Mixtures: Field Validation," *TM-OSU-A-003A-92-23*, Strategic Highway Research Program, National Research Council, Washington, D.C. Nov., 1993.

Eaton, R. A., "Frost Effects Research Facility," presented at the July 1992 FWHA Pavement Testing Workshop held at University of Texas, Austin, Texas.

Ehrola, E., "Transverse Cracking of Asphalt Pavement in Low Temperatures and Factors affecting it," *Report 4*, Oulun Yliopisto, Tie- ja Liikennetekniikan Laboratorio, Oulu, Finland, 1986.

Esch, D. C. and Franklin, D., "Asphalt Pavement Crack Control at Fairbanks International Airfield," *Proceedings of the 5th International Conference on Cold Regions Engineering*, American Society of Civil Engineers, Vol. 1, 1989.

Esch, D. C., Letter report, October, 1990.

Fabb, T. R. J., "The Influence of Mix Composition, Binder Properties and Cooling Rate on Asphalt Cracking at Low Temperature," *Proceedings of the Association of Asphalt Paving Technologists*, Vol. 43, 1974.

Haas, R., "A Method for designing Asphalt Pavements to minimize Low temperature Shrinkage Cracking," *RR-73-1*, Asphalt Institute, 1973

Haas, R., Meyer, F., Assaf, G. and Lee H., "A Comprehensive Study of Cold Climate Airfield Pavement Cracking," *Proceedings of the Association of Asphalt Paving Technologists*, Vol. 56, 1987.

Haas, R. C. and Phang, W. A., "Relationships between Mix Characteristics and Low-temperature Pavement Cracking," *Proceedings of the Association of Asphalt Paving Technologists*, Vol. 59, 1990.

Harr, M. E., "Reliability Analysis," *Reliability-Based Design in Civil Engineering*, 1st ed., Vol. 1, McGraw-Hill Book Company, New York, 1987.

Harvey, J., "Asphalt Concrete Specimen Preparation Protocol," *TM-UCB-A-003A-90-4, Version 2*, University of California, Berkeley, California, May, 1990.

Hills, J. F. and Brien, D., "The Fracture of Bitumens and Asphalt Mixes by Temperature Induced Stresses," *Proceedings of the Association of Asphalt Paving Technologists*, Vol. 35, 1966.

Janoo, V. C., "Use of Low Viscosity Asphalts in Cold Regions," *Proceedings of the 5th International Conference on Cold Regions Engineering*, American Society of Civil Engineers, 1989.

Jung, D. H. and Vinson T. S., "Statistical Analysis of Low Temperature Thermal Stress Restrained Specimen Test Results," *Proceedings of the 37 Annual Conference of Canadian Technical Asphalt Association*, Vol. 1, 1992, pp.200-223.

Kandhal, P. S., Mellott, D. B. and Basso, H. R. Jr., "Durability Study of Viscosity Graded AC-20 Asphalts in Pennsylvania," *Research Project No. 76-12*, Commonwealth of Pennsylvania, Department of Transportation, Pennsylvania, April 1984.

Kanerva, H. K., "Sideaineen vaikutus paallysteen kylmakestavyyteen," *TR1/3*, Asfalttipaallysteiden Tutkimusohjelma ASTO, Espoo, Finland, Sept. 1991.

Kanerva, H. K., "Effect of Asphalt Properties on Low Temperature Cracking of Asphalt Mixtures," *Proceedings of the 7th International Conference on Asphalt Pavements*, Vol. 2, Aug., 1992, pp. 95-107.

Kanerva, H. K., Vinson, T.S. and Zeng, H., "Low Temperature Cracking: Field Validation of the TSRST," *TM-OSU-A-003A-92-15*, Strategic Highway Research Program, National Research Council, Washington, D.C. Nov., 1992 a.

Kanerva, H. K., Vinson, T. S., Brickman, A. M. and Janoo, V. C., "Low Temperature Cracking Experiment at USACRREL Frost Effects Research Facility," *Proceedings of the 37 Annual Conference of Canadian Technical Asphalt Association*, Vol. 1, 1992 b, pp. 289-307.

Kleemola, M. Letter report, October, 1990.

Kurki, T. Letter report, December, 1991.

McFadden, T. T. and Bennett, F.L., "Foundation Construction," *Construction in Cold Regions*, 1st ed., Vol. 1, John Wiley and Sons, Inc., New York, 1991, pp. 144-147.

McLeod, N. W., "A Four Year Survey of Low Temperature Transverse Pavement Cracking on Three Ontario Test Roads," *Proceedings of the Association of Asphalt Paving Technologists*, Vol. 41, 1972, pp. 424-493.

McLeod, N. W., "Pen-Vis Number (PVN) as a Measure of Paving Asphalt Temperature Susceptibility and its Application to Pavement Design," *Proceedings of the Paving in Cold Areas Mini Workshop*, Vol. 1, 1987, pp. 147-240.

Monismith, C. L., Secor, G. A. and Secor K. E., "Temperature Induced Stresses and Deformations in Asphalt Concrete," *Proceedings of the Association of Asphalt Paving Technologists*, Vol. 34, 1965, pp. 248-285.

Määttä, K. and Jussila S., Letter report, July, 1990.

Saarela, A. "ASTO-Koetiet 1990," Technical Research Center of Finland, Espoo, Finland, September 1991.

Scheaffer, R. L., and McClave, J. T., *Probability and Statistics for Engineers*, 3rd ed., Vol. 1, PWS Kent, Boston, 1990.

Solaimanian M. and Kennedy T. "Predicting Maximum Pavement Temperature using Maximum Air Temperature and Hourly Solar Radiation," presented at the January 10-14, 1993, Transportation Research Board 72nd Annual Meeting, held at Washington, D.C.

Tuckett, G. M., Jones, G. M. and Littlefield, G., "The Effects of Mixture Variables on Thermally Induced Stresses in Asphaltic Concrete," *Proceedings*, Association of Asphalt Paving Technologists, Vol. 39, 1970, pp. 703-744.

Wesevich, J. W., McCullough, B. F. and Burns, N. H., "Stabilized Subbase Friction Study for Concrete Pavements," *Report 459-1*, Center for Transportation Research, Bureau of Engineering Research, The University of Texas at Austin, Austin, Texas, Apr., 1987, pp. 3-10.

Wieder, A., Bell C. A., and Fellin, M. J., "Field Validation of Laboratory Aging Procedures for Asphalt-Aggregate Mixtures," presented at the January 10-14, 1993, Transportation Research Board 72nd Annual Meeting, held at Washington, D.C.

APPENDICES

Appendix A

Mix Designs and Compositions for the Test Roads

ALASKA (Esch, 1990)

23rd Avenue and Peger Road

Target Mix Composition:

Sieve Size	Passing (%)
1" (25 mm)	
3/4" (19.0 mm)	100
3/8" (9.5 mm)	77
#4 (4.75 mm)	51
#10 (2.0 mm)	37
#40 (0.425 mm)	25
#200 (0.075 mm)	6

Asphalt Content (by wt of mix): 5.4 %

Actual Mix Composition:

Sieve Size	Passing (%)
1" (25 mm)	
3/4" (19.0 mm)	100
3/8" (9.5 mm)	72
#4 (4.75 mm)	47
#10 (2.0 mm)	35
#40 (0.425 mm)	25
#200 (0.075 mm)	8

Asphalt Content (by wt of mix): 5.0 %

Marshall Design Data:

23rd Avenue:

Optim. Unit Wt (lb/ft3)	150.8
Voids Filled (%)	88
Air Voids (%)	2
Stability (lbs)	1920
Flow	9.6

Peger Road:

Optim. Unit Wt (lb/ft3)	151.3
Voids Filled (%)	88
Air Voids (%)	2
Stability (lbs)	2450
Flow	11.0

PENNSYLVANIA (Kandhal, 1984)

Mix Composition

Sieve Size	Passing (%)
1/2" (12.7 mm)	100
3/8" (9.5 mm)	93
#4 (4.75 mm)	62
#8 (2.36 mm)	45
#16 (1.18 mm)	33
#30 (0.60 mm)	22
#50 (0.30 mm)	12
#100 (0.150 mm)	9
#200 (0.075 mm)	5

Asphalt Content (by wt of mix): 7.5 %

Marshall Design Data:

Theor. Max. Spec.Gr.	2.326
Specimen Spec.Gr.	2.278
VMA (%)	18.8
Air Voids (%)	2.1
Stability (lbs)	2075
Flow	13.3

PERASEINAJOKI (Kleemola, 1990)

Mix Composition

Sieve Size	Passing (%)
3/4" (19.5mm)	96
1/2" (12.7mm)	75
3/8" (9.5mm)	62
#4 (4.75mm)	45
#8 (2.36mm)	33
#16 (1.18mm)	24
#30 (0.600mm)	20
#50 (0.300mm)	16
#200 (0.075mm)	10
Lime %	5

Asphalt Content by Weight of Mix:

BIT120AH	5.6%
BIT120ECO	5.6%
BIT65AH	5.7%
BIT80AH	5.7%
BIT200AH	5.6%
PmB1	5.8%

SODANKYLA (Maatta, Jussila, 1990)

Mix Composition

Sieve Size	Passing (%)
3/4" (19.5mm)	100
1/2" (12.7mm)	82
3/8" (9.5mm)	69.5
#4 (4.75mm)	50.3
#8 (2.36mm)	37.5
#16 (1.18mm)	27.5
#30 (0.600mm)	20
#50 (0.300mm)	14.5
#200 (0.075mm)	9.2
Lime %	6

Asphalt Content by Weight of Mix:

BIT120AH	5.5%
B120LD	5.5%
BIT120ECO	5.5%
BIT120ARC	5.4%
BIT65AH	5.7%
BIT80AH	5.7%
BIT200AH	5.6%
PmB1	5.4%
BIT150AH	5.5%

USACRREL (Kanerva et al., 1992)

Target Mix Composition:

Sieve Size	Passing (%)
1" (25.0 mm)	100
3/4" (19.0 mm)	99
1/2" (12.7 mm)	82
3/8" (9.5 mm)	68
#4 (4.75 mm)	50
#8 (2.36 mm)	39
#16 (1.18 mm)	28
#30 (0.60 mm)	20
#50 (0.30 mm)	11
#200 (0.075 mm)	3.5

Asphalt Content (by wt of mix): 4.7 %

Marshall Design Data:

Theor. Max. Spec.Gr	2.601
VMA (%)	15.2
Air Voids (%)	4
Stability (lbs)	22660
Flow	10

Actual Mix Composition:

Sections I to V:

Sieve Size	Passing (%)
1" (25.0 mm)	100
3/4" (19.0 mm)	99.7
1/2" (12.7 mm)	83.1
3/8" (9.5 mm)	70.7
#4 (4.75 mm)	50.3
#8 (2.36 mm)	37.3
#16 (1.18 mm)	27.6
#30 (0.60 mm)	18.8
#50 (0.30 mm)	9.5
#200 (0.075 mm)	3.2

Asphalt Content (by wt of mix): 5.2 %

Sections VI to IX:

Sieve Size	Passing (%)
1" (25.0 mm)	100
3/4" (19.0 mm)	99.6
1/2" (12.7 mm)	82.7
3/8" (9.5 mm)	64.6
#4 (4.75 mm)	47.1
#8 (2.36 mm)	33.8
#16 (1.18 mm)	22.3
#30 (0.60 mm)	14
#50 (0.30 mm)	7.5
#200 (0.075 mm)	3.1

Asphalt Content (by wt of mix): 5.3 %

Appendix B

Flow Chart for Deterministic Model to Predict Low Temperature Cracking

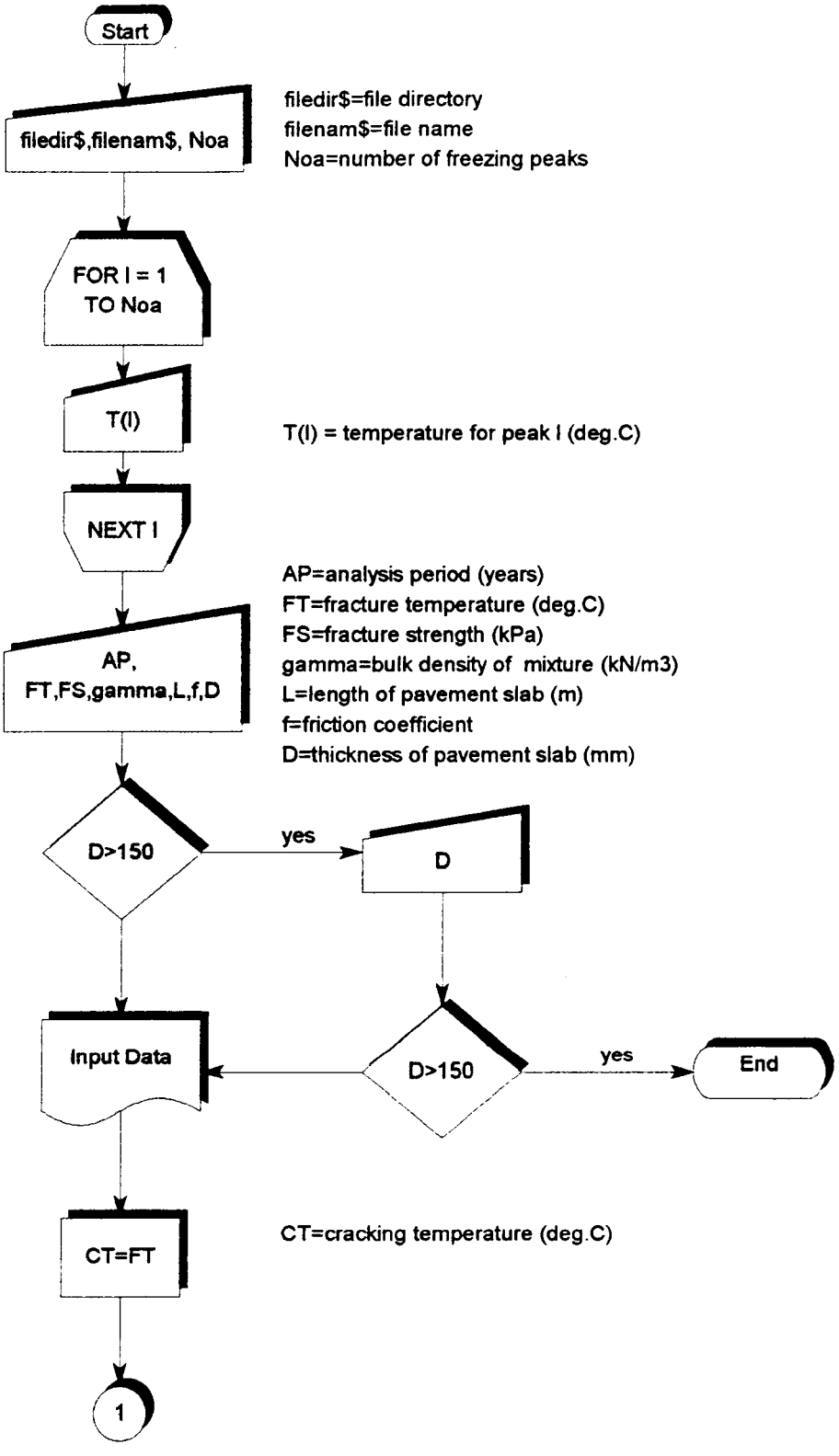
Start
filedir$,filenam$, Noa
filedir$=file directory
filenam$=file name
Noa=number of freezing peaks
FOR I = 1
TO Noa
T(I)
T(I) = temperature for peak I (deg.C)
NEXT I
AP,
FT,FS,gamma,L,f,D
AP=analysis period (years)
FT=fracture temperature (deg.C)
FS=fracture strength (kPa)
gamma=bulk density of mixture (kN/m3)
L=length of pavement slab (m)
f=friction coefficient
D=thickness of pavement slab (mm)
D>150
yes
D
Input Data
D>150
yes
End
CT=FT
CT=cracking temperature (deg.C)
1

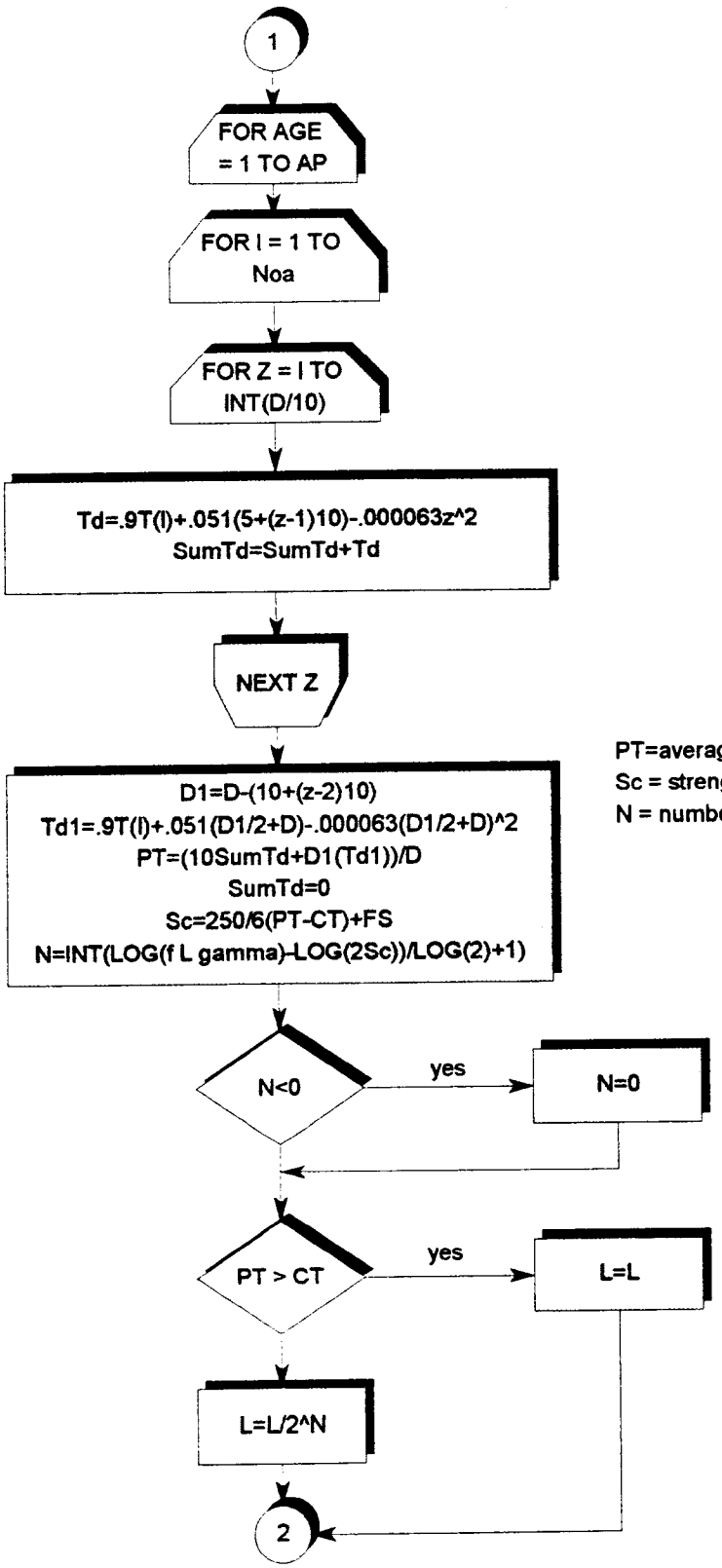

PT=average pavement temperaure (deg.C)
Sc = strength of mixture (kPa)
N = number of crackings

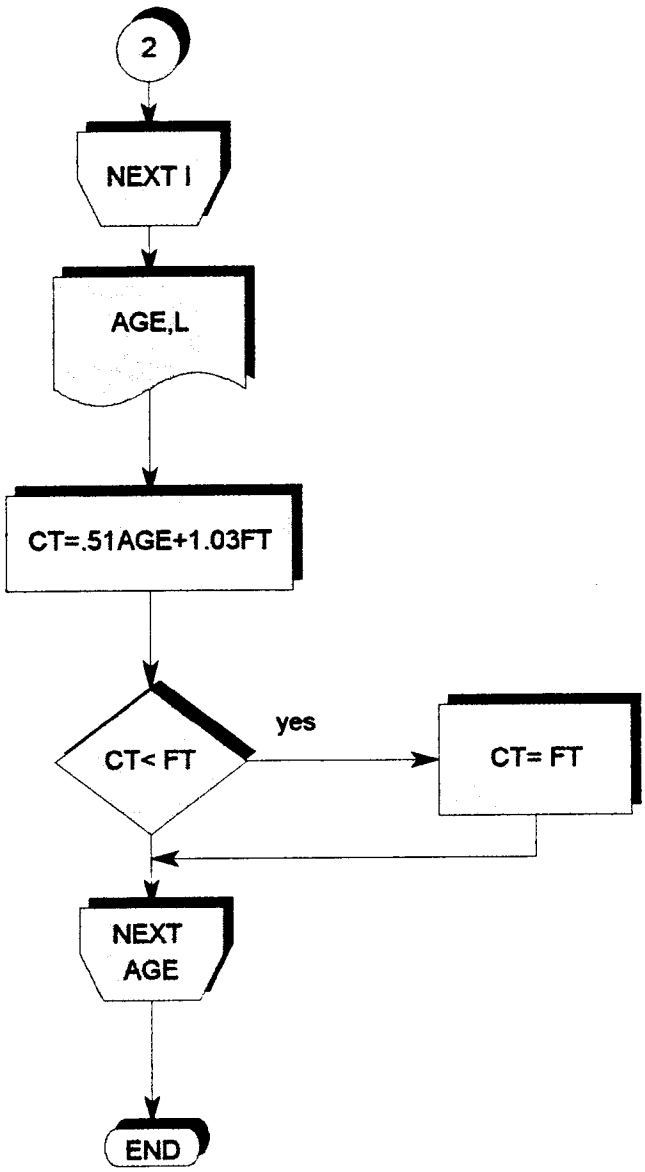
2
NEXT I
AGE,L
CT=.51AGE+1.03FT
CT< FT
yes
CT= FT
NEXT
AGE
END

Appendix C

Flow Chart for Probabilistic Model to Predict Low Temperature Cracking

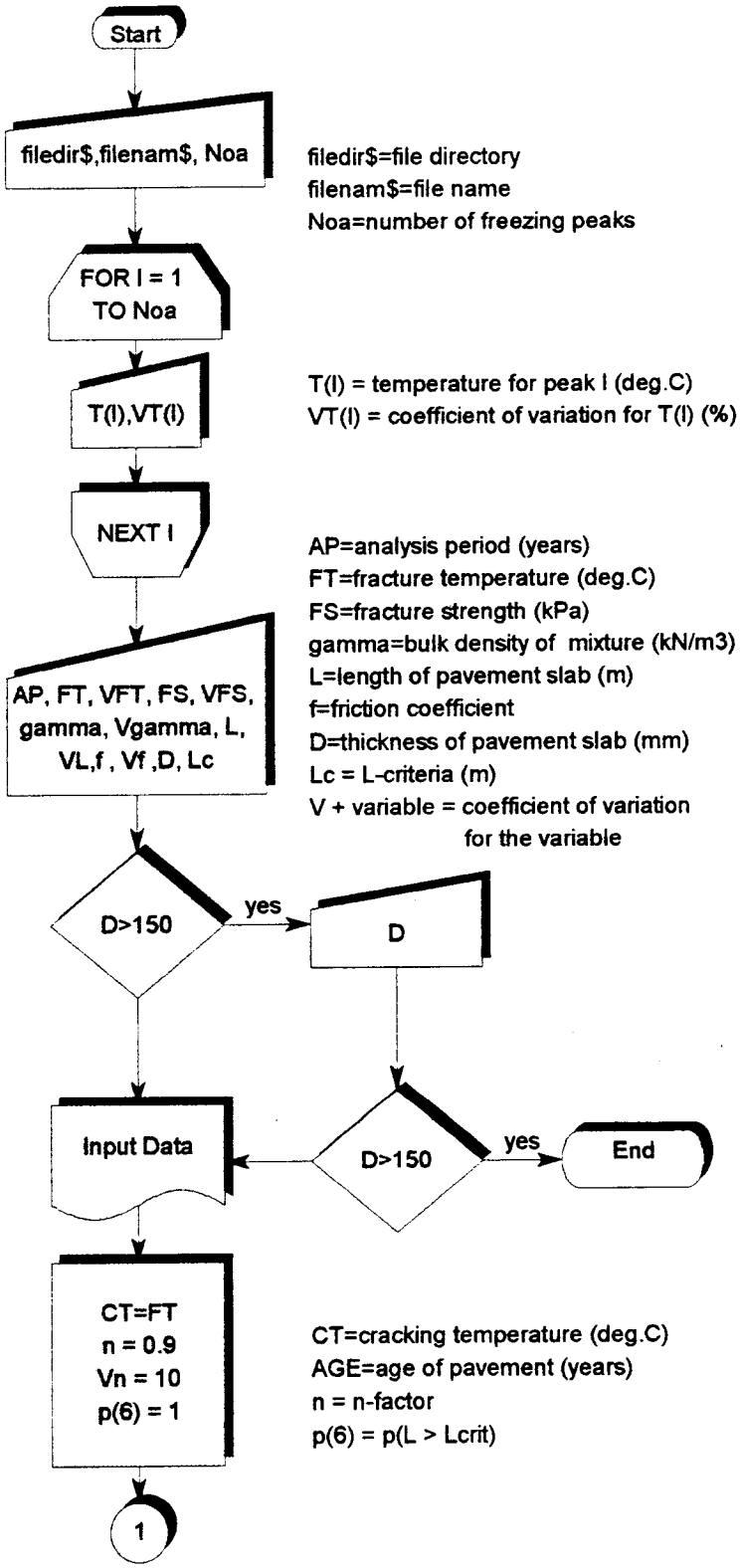
Start
filedir$,filenam$, Noa
filedir$=file directory
filenam$=file name
Noa=number of freezing peaks
FOR I = 1
TO Noa
T(I),VT(I)
T(I) = temperature for peak I (deg.C)
VT(I) = coefficient of variation for T(I) (%)
NEXT I
AP, FT, VFT, FS, VFS,
gamma, Vgamma, L,
VL,f , Vf ,D, Lc
AP=analysis period (years)
FT=fracture temperature (deg.C)
FS=fracture strength (kPa)
gamma=bulk density of mixture (kN/m3)
L=length of pavement slab (m)
f=friction coefficient
D=thickness of pavement slab (mm)
Lc = L-criteria (m)
V + variable = coefficient of variation
for the variable
D>150
yes
D
Input Data
D>150
yes
End
CT=FT
n = 0.9
Vn = 10
p(6) = 1
CT=cracking temperature (deg.C)
AGE=age of pavement (years)
n = n-factor
p(6) = p(L > Lcrit)
1

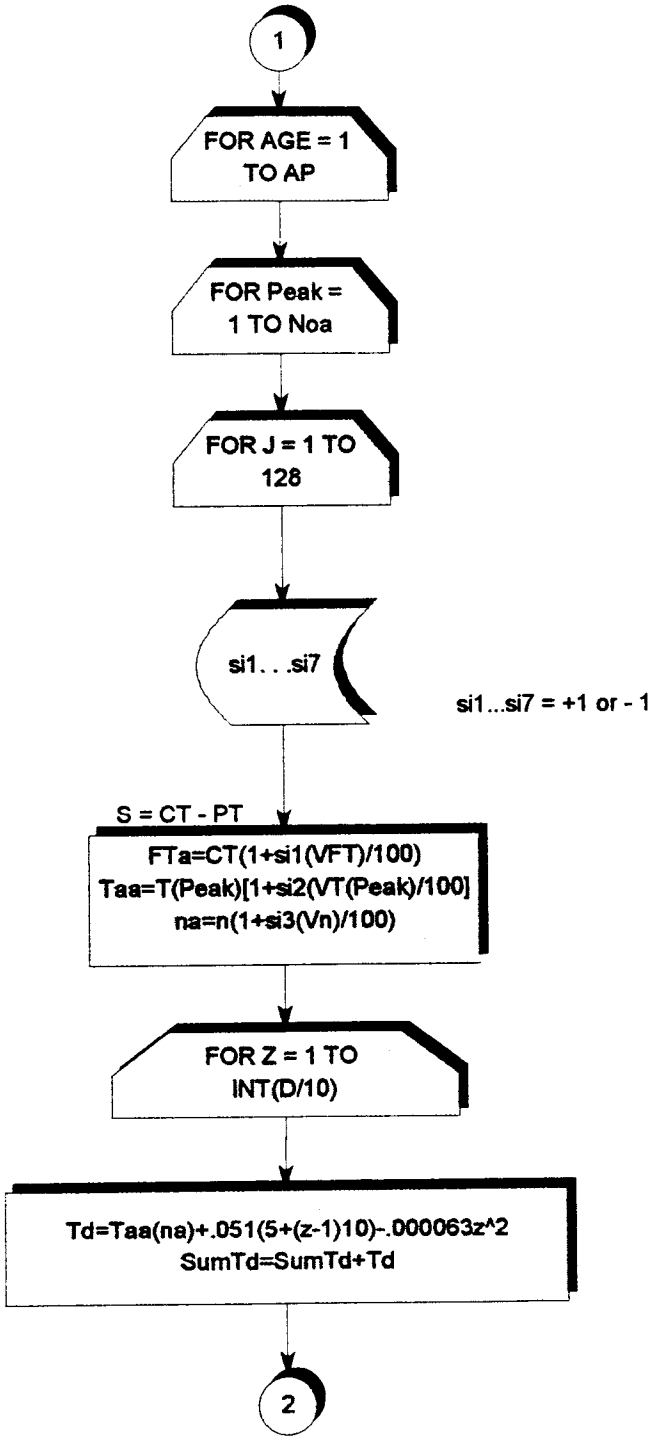
1
FOR AGE = 1
TO AP
FOR Peak =
1 TO Noa
FOR J = 1 TO
128
si1. . .si7
si1...si7 = +1 or - 1
S = CT - PT
FTa=CT(1+si1(VFT)/100)
Taa=T(Peak)[1+si2(VT(Peak)/100]
na=n(1+si3(Vn)/100)
FOR Z = 1 TO
INT(D/10)
Td=Taa(na)+.051(5+(z-1)10)-.000063z^2
SumTd=SumTd+Td
2

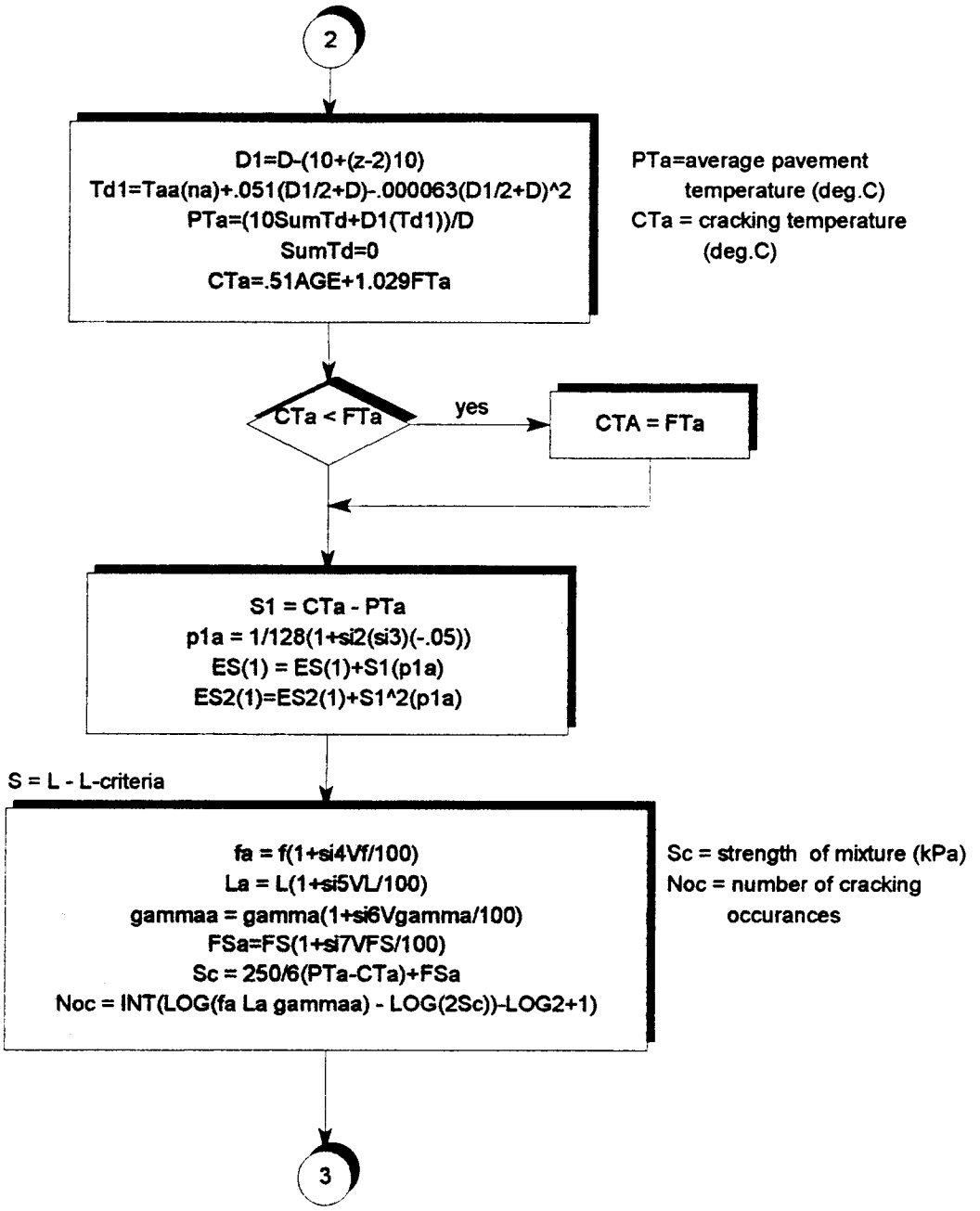
2
D1=D-(10+(z-2)10)
Td1=Taa(na)+.051(D1/2+D)-.000063(D1/2+D)^2
PTa=(10SumTd+D1(Td1))/D
SumTd=0
CTa=.51AGE+1.029FTa
PTa=average pavement temperature (deg.C)
CTa = cracking temperature (deg.C)
CTa < FTa
yes
CTA = FTa
S1 = CTa - PTa
p1a = 1/128(1+si2(si3)(-.05))
ES(1) = ES(1)+S1(p1a)
ES2(1)=ES2(1)+S1^2(p1a)
S = L - L-criteria
fa = f(1+si4Vf/100)
La = L(1+si5VL/100)
gammaa = gamma(1+si6Vgamma/100)
FSa=FS(1+si7VFS/100)
Sc = 250/6(PTa-CTa)+FSa
Noc = INT(LOG(fa La gammaa) - LOG(2Sc))-LOG2+1)
Sc = strength of mixture (kPa)
Noc = number of cracking occurances
3

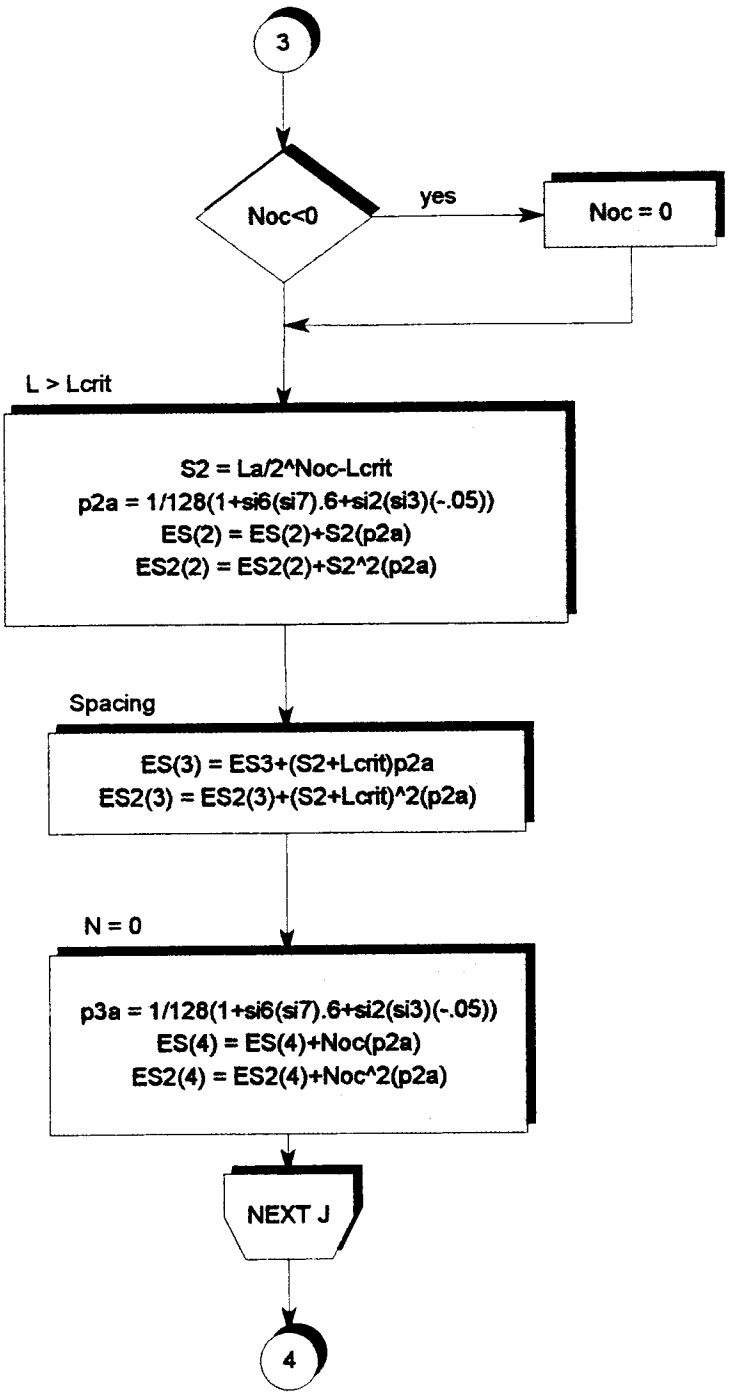
3
Noc<0
yes
Noc = 0
L > Lcrit
S2 = La/2^Noc-Lcrit
p2a = 1/128(1+si6(si7).6+si2(si3)(-.05))
ES(2) = ES(2)+S2(p2a)
ES2(2) = ES2(2)+S2^2(p2a)
Spacing
ES(3) = ES3+(S2+Lcrit)p2a
ES2(3) = ES2(3)+(S2+Lcrit)^2(p2a)
N = 0
p3a = 1/128(1+si6(si7).6+si2(si3)(-.05))
ES(4) = ES(4)+Noc(p2a)
ES2(4) = ES2(4)+Noc^2(p2a)
NEXT J
4

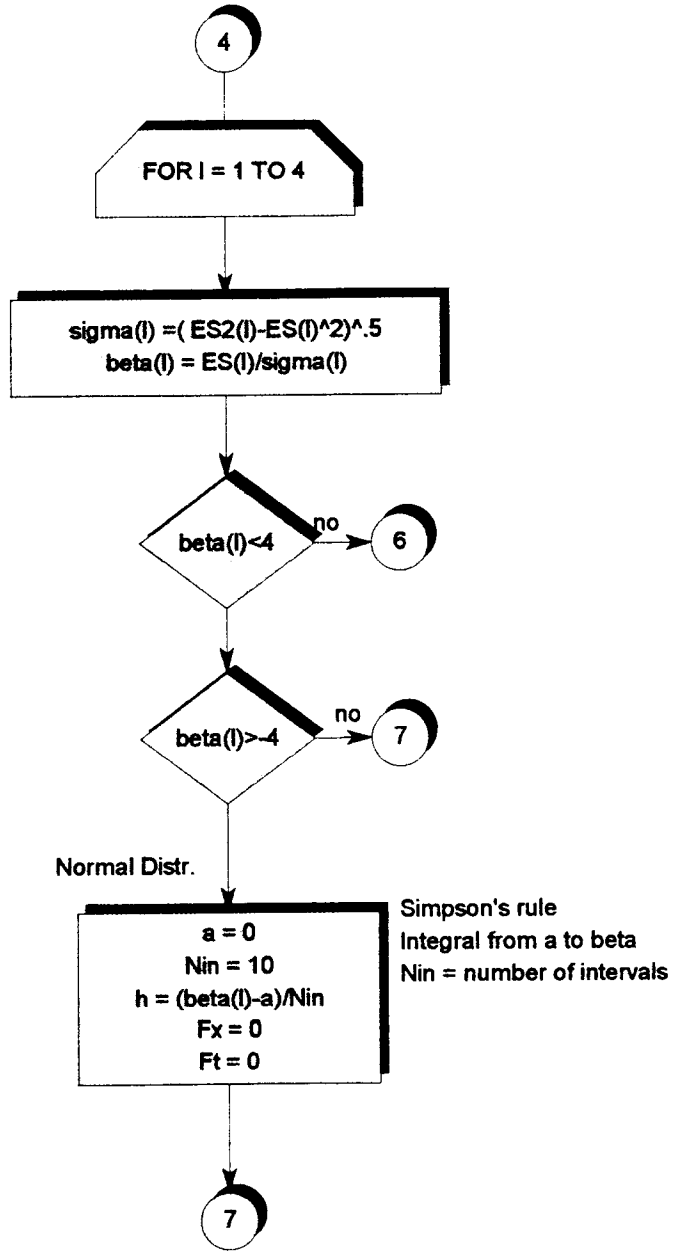
4
FOR I = 1 TO 4
sigma(I) =(ES2(I)-ES(I)^2)^.5
beta(I) = ES(I)/sigma(I)
beta(I)<4
no
6
beta(I)>-4
no
7
Normal Distr.
a = 0
Nin = 10
h = (beta(I)-a)/Nin
Fx = 0
Ft = 0
Simpson's rule
Integral from a to beta
Nin = number of intervals
7

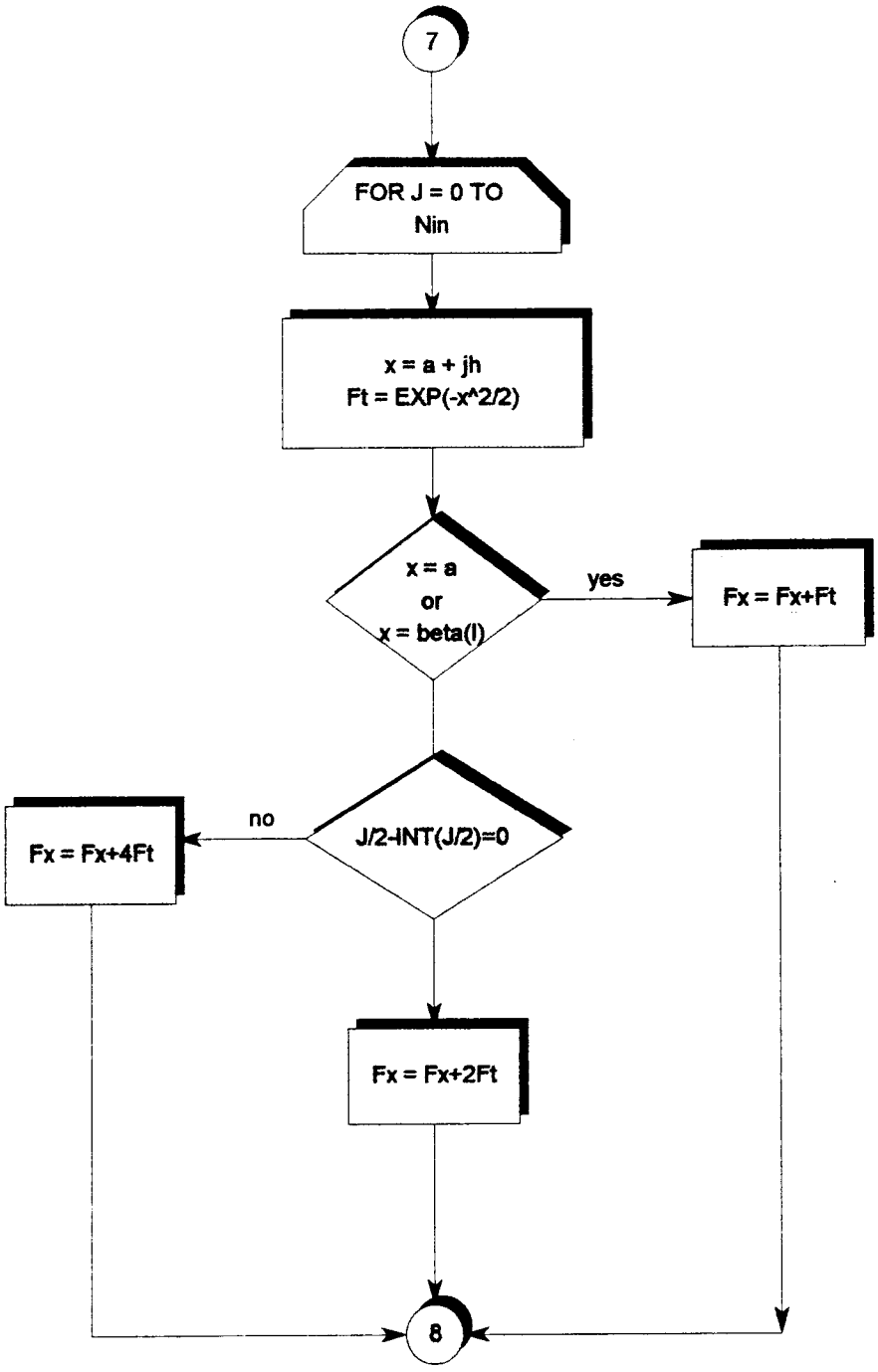
7
FOR J = 0 TO
Nin
x = a + jh
Ft = EXP(-x^2/2)
x = a
or
x = beta(I)
yes
Fx = Fx+Ft
no
J/2-INT(J/2)=0
Fx = Fx+4Ft
Fx = Fx+2Ft
8

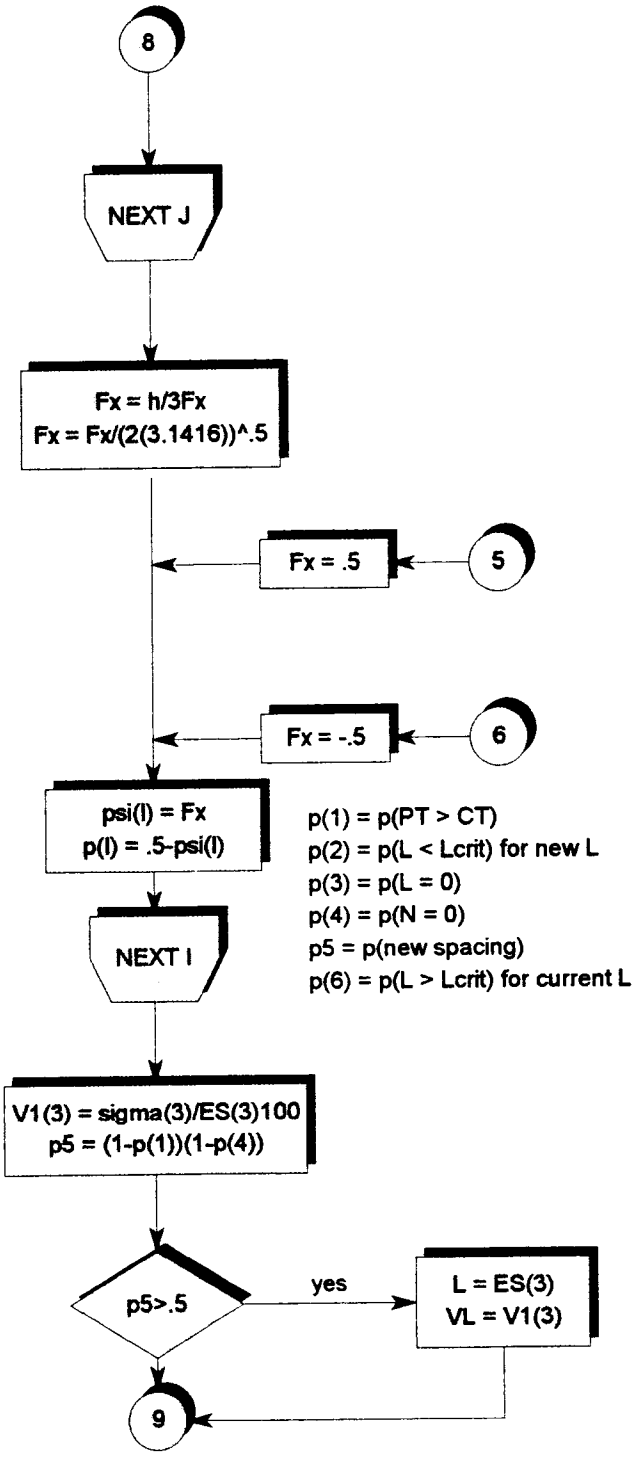
8
NEXT J
Fx = h/3Fx
Fx = Fx/(2(3.1416))^.5
Fx = .5
5
Fx = -.5
6
psi(I) = Fx
p(I) = .5-psi(I)
NEXT I
p(1) = p(PT > CT)
p(2) = p(L < Lcrit) for new L
p(3) = p(L = 0)
p(4) = p(N = 0)
p5 = p(new spacing)
p(6) = p(L > Lcrit) for current L
V1(3) = sigma(3)/ES(3)100
p5 = (1-p(1))(1-p(4))
p5>.5
yes
L = ES(3)
VL = V1(3)
9

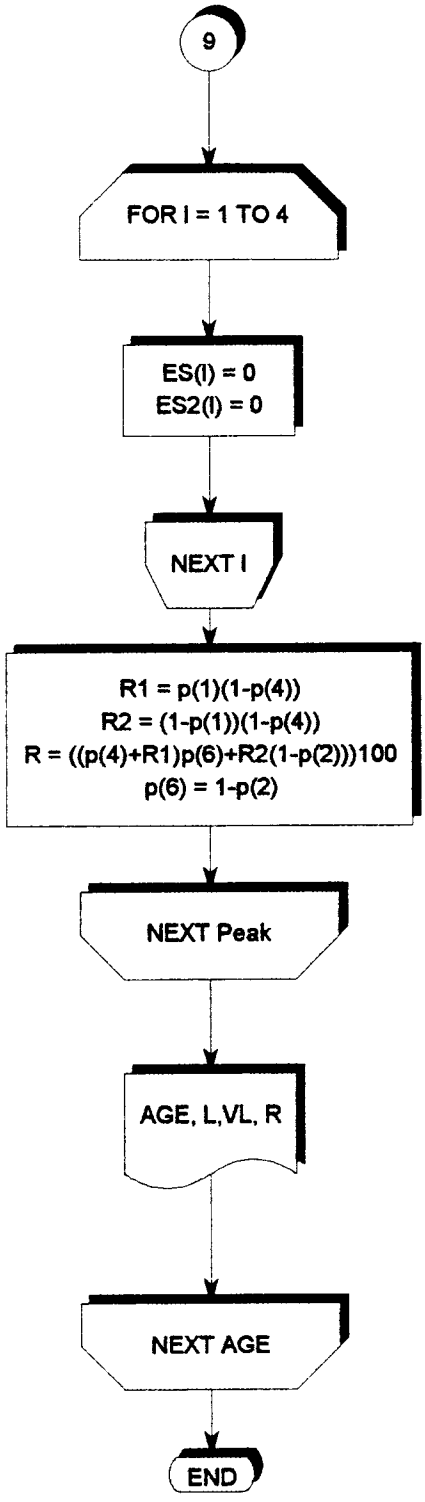
9
FOR I = 1 TO 4
ES(I) = 0
ES2(I) = 0
NEXT I
R1 = p(1)(1-p(4))
R2 = (1-p(1))(1-p(4))
R = ((p(4)+R1)p(6)+R2(1-p(2)))100
p(6) = 1-p(2)
NEXT Peak
AGE, L,VL, R
NEXT AGE
END

Appendix D

Output Files for Models to Predict Low Temperature Cracking

```
*******************************************************
*                                                     *
*   Prediction of Low-Temperature Cracking of         *
*   Asphalt Concrete Mixtures with TSRST Results      *
*              Deterministic Model                    *
*              by Hannele K. Kanerva                  *
*            Version 1.6   05/21/1993                 *
*                      19:40                          *
*                                                     *
*******************************************************
```

INPUT DATA:

File: pat1.det	
Air Temperature for Peak 1 (deg.C)	-29
Fracture Temperature (deg.C)	-18.5
Fracture Stress (kPa)	2396
Bulk Density of Pavement (kN/m3)	23.3
Length of Pavement Slab (m)	10000
Friction Coefficient between Pavement and Base	2
Pavement Thickness (mm)	38

CRACK SPACING WITH TIME:

YEAR	SPACING (m)
1	78.125
2	78.125
3	78.125
4	78.125
5	78.125

```
**********************************************************
*                                                        *
*   Prediction of Low-Temperature Cracking of            *
*   Asphalt Concrete Mixtures with TSRST Results         *
*                Probabilistic Model                     *
*              by Hannele K. Kanerva                     *
*            Version 2.2   05/21/1993                    *
*                      19:15                             *
*                                                        *
**********************************************************
```

INPUT DATA:

File:	pat1.pro
Air Temperature For Peak 1 (deg.C)	-29 ± 5 %
Fracture Temperature (deg.C)	-18.5 ± 2 %
Fracture Stress (kPa)	2396 ± 4 %
Bulk Density of Pavement (kN/m3)	23.3 ± 3 %
Length of Pavement Slab (m)	10000 ± 1 %
Friction Coefficient between Pavement and Base	2 ± 20 %
Pavement Thickness (mm)	38
Spacing Criteria (m)	50

CRACK SPACING WITH TIME:

YEAR	EXPECTED SPACING (m)	V(Spacing) (%)	R (%)
1	65	27	81
2	55	30	68
3	52	31	58
4	50	32	52
5	49	33	49

Reliability of the design is 49 %